Titre: Title:	Catalytic Design for Fructose Conversion to Speciality Chemicals
Auteur: Author:	Davide Carnevali
Date:	2018
Type:	Mémoire ou thèse / Dissertation or Thesis
Référence: Citation:	Carnevali, D. (2018). Catalytic Design for Fructose Conversion to Speciality Chemicals [Thèse de doctorat, École Polytechnique de Montréal]. PolyPublie. https://publications.polymtl.ca/3265/

UNIVERSITÉ DE MONTRÉAL

CATALYTIC DESIGN FOR FRUCTOSE CONVERSION TO SPECIALITY CHEMICALS

DAVIDE CARNEVALI
DÉPARTEMENT DE GÉNIE CHIMIQUE
ÉCOLE POLYTECHNIQUE DE MONTRÉAL

THÈSE PRÉSENTÉE EN VUE DE L'OBTENTION
DU DIPLÔME DE PHILOSOPHIÆ DOCTOR
(GÉNIE CHIMIQUE)
AOÛT 2018

UNIVERSITÉ DE MONTRÉAL

ÉCOLE POLYTECHNIQUE DE MONTRÉAL

Cette thèse intitulée :

CATALYTIC DESIGN FOR FRUCTOSE CONVERSION TO SPECIALITY CHEMICALS

présentée par : CARNEVALI Davide
en vue de l'obtention du diplôme de : Philosophiæ Doctor
a été dûment acceptée par le jury d'examen constitué de :

M. STUART Paul, Ph. D., président
M. PATIENCE Gregory S., Ph. D., membre et directeur de recherche
M. CAVANI Fabrizio, Ph. D., membre et codirecteur de recherche
Mme BOFFITO Daria Camilla, Ph. D., membre
M. VACCARI Angelo, Master, membre
Mme ROSSETTI Ilenia, Ph. D., membre

DEDICATION

Dedicated to my beloved
parents, sister, grandparents,
girlfriend and to my guardian angels ...

ACKNOWLEDGMENTS

So, I need to thank a lot of people for helping me reaching this level.

I would like to convey my sincere and heartfelt gratitude to my supervisor, Professor Gregory S. Patience for having me provided with an exceptional support and assistance in the course of this project without which no achievement would have become possible. I am honored to have had the opportunity to work as a PhD candidate under his professional supervision. I will be always grateful for his patience, enthusiasm, motivation and accurate scientific attitude. Vorrei ringraziare inoltre il Professor Fabrizio Cavani, per avermi supervisionato durante la mia permanenza all'Universitị Bologna. La ringrazio per la sua enorme gentilezza, disponibiltá ed elevata capacitá tecnica, che mi hanno permesso di imparare molto sia a livello umano che lavorativo. Ringrazio tantissimo anche la Professoressa Daria Boffito, per essere stata sempre disponibile e gentile, un incredibile punto di riferimento sin da quando sono arrivato la prima volta. Sempre sorridente e pronta ad aiutare, grazie di tutto.

I would like now to thank all the people that worked in the lab, and those who are still there.

I would like to thank Marjan, for being so kindly to be a great friend and a great boss. You taught me a lot during my first period in Montreal. Thanks also to Cristian Neagoe, one of the best scientist I ever met. Thank you for transmitting to me your passion and your knowledge.

Ringrazio anche Cristian Trevisanut, per il suo aiuto e la sua simpatia contagiosa. Grazie anche per avermi trovato una casa a Bologna, per le partite a basket e per il concerto degli ACDC.

Grazie anche a Federico Galli, per essere stato un ottimo amico, un ottimo insegnante e un grane motivatore (senza di te non sarei mai andato in palestra e non avrei mai fatto un muscle up!!!).

Grazie a Marta Stucchi, sempre super gentile e disponibile in tutto, nonché un'incredibile lavoratrice. Grazie mille per le chiacchierate e per l'incredibile aiuto per la scrittura dell'articolo.

Grazie mille a Marco, persona fantastica ed ottimo amico. Sempre pronto a dare il consiglio giusto ed ad aiutare nel momento del bisogno. Ti auguro il meglio in tutti i campi della tua vita. Grazie mille di tutto.

Grazie mille a Gianluca. Grazie per la tua simpatia, i caffé e le fantastiche cene. Sono sicuro che sarai la nuova punta di diamante del gruppo.

Un grande grazie anche a Stefano, per i bellissimi pranzi e cene, e per le partite a Dota.

Un grand merci à Adrien. Vous êtes un bon ami et un bon travailleur. Je suis sûr que vous réussirez votre thèse. Merci pour votre aide pendant ces mois. Cela aurait été dur sans toi.

Merci á Olivier Pombert, un bon ami et celui qui m'a amené áma premiére course Spartan. Merci pour cette expérience incroyable.

Thanks to Song, for being a good friend and to forcing me to go to the gym. At least I won't arrive at the defense fat.

Thanks to Oliveir Guévremont, for helping me in the lab and for the first article.

I would like to thank all the people that work in prof. Patience's group. Thanks to Ma Zhenni and Li He, for letting me discover China also in Canada, and Jaber, for showing me the best and the worst part of Iran :) I would like to thank also Guillermo, Jemika and Ibrahim, for helping me during the first phase of my project.

Thanks to Faehez and Maryam, excellent friends, always smiling and fantastic people. Thanks for all the nice chats and the great advices.

Vorrei ringraziare tutti i ragazzi del laboratorio di Bologna, per la vostra simpatia e per avermi accolto nel vostro gruppo.

Grazie anche agli amici della casa di Bologna, per la vostra ospitalitá e simpatia.

Grazie anche a Riccardo, per avermi accolto nella sua umile dimora, e per essermi sempre stato vicino durante i mesi passati a Bologna.

Grazie a Manuela e Fabio, per la loro gentilezza e disponibiltá. Grazie per avermi accolto ed ospitato a casa vostra durante i ritorni da Bologna.

Un grazie di cuore a mia mamma, mio papá, mia sorella, mia nonna e mio nonno. Siete la mia colonna portante, mi siete sempre stati accanto e mi avete supportato dutante tutto il mio percorso. Un infinito grazie di cuore.

Grazie a Sara, per essere ció che mi manca. Grazie mille per essermi stata accanto, per avermi supportato e sopportato in tutti questi anni. La nostra vita insieme sta per iniziare.

Infine, un grazie ai miei due nonni che dall'alto mi proteggono e mi spingono ad andare avanti sempre. Siete i miei angeli custodi.

RÉSUMÉ

La biomasse va devenir le nouveau pétrole en raison de son abondance et du ratio oxygène/carbone élevée, ce qui en fait une excellente alternative aux composées à haute valeur ajoutée. Le marché de la production d'électricité à partir de la biomasse ne cesse d'augmenter et atteindra environ 50 Milliards USD d'ici 2022 Market Research Reports Search Engine (2015). Les processus bio-catalytiques, chimio-catalytique et les modifications chimiques des biopolymères sont les trois principales conversions de la biomasse Gallezot (2012). La fermentation vers le bioéthanol est la valorisation de sucres la plus propagée, représentant plus de 60 % de la production mondiale Business insider (2018). Cette voie majeure de conversion découle de son application de biocarburant. En effet, le bioéthanol présente un plus faible coût de production et un nombre d'octane plus élevé comparé à l'essence. La fermentation présente deux limitations principales : un rendement molaire théorique maximal de 50 % et une faible valeur marchande. L'équation chimique inclue une formation de CO_2 par molécule de sucre ayant réagi. La marge du bénéficie nette du bioéthanol est faible, et est déterminée par la différence entre les prix des matières premières et ceux du produit final. Le sucre blanc coûte environ 300 USD/t International Sugar Organization (2018), alors que le prix du bioéthanol est approximativement de 450 USD/t S & P Global Platts (2018). Le fructose représente une matière première a haut potentiel pour la transformation en 5-hydroxymethylfurfural (HMF), 2,5-furandicarboxylique acide (FDCA), acide lévulinique, furfural (FUR), dimethylfurfural, dimethyltetrahydrofurane et acide lactique.

Le processus de déshydration des hexoses en HMF joue un rôle clef dans la valorisation du sucre, dû à l'importance des produits chimiques et biocarburants de moyenne à haute valeur ajoutée. La synthèse est enrayée par la polymérisation d'HMF en produits insolubles - appelés humins - et la réhydratation de l'HMF, qui sépare la molécule en acide lévulinique et formique. Les solvants organiques et ioniques, les réacteurs multiphasiques et les systèmes d'extraction minimisent les étapes de dégradation.

Nous avons abordé la conception catalytique de la conversion du fructose en molécules spécifiques à partir de deux points de vue. La première était de développer une technologie alternative pour convertir le fructose en molécules présentant une plus haute valeur marchande que l'éthanol. Nous avons désigné un μ-réacteur à lit fluidisé (15 mm ID), ou un atomiseur pulvérisait une solution aqueuse de sucre directement dans le lit catalytique. Cette partie du projet s'est déroulée à l'École Polytechnique de Montréal. La seconde étape s'est focalisée sur la valorisation de l'acide lévulinique, un co-produit de la deshydratation de l'HMF.

Nous avons developpé une nouvelle voie catalytique pour oxyder le substrat en acide succinique, en combinant de l'acide tungstique et du peroxyde d'hydrogène pour la conversion de Baeyer-Villiger. Ce projet a été conclu à l'Université de Bologne.

Nous avons identifié l'injection du liquide dans le μ-réacteur a lit fluidisé (FBR) comme une alternative pour convertir le sucre en molécules à haute valeur ajoutée. La conception du système est basé sur une vitesse de réaction plus élevée en biomolécules que la dégradation en humins ou en coke. Le lit fluidisé a réduit le temps de contact à une fraction de secondes, minimisant les réactions parallèles. Le réacteur travaille dans la gamme de 300 °C to 400 °C et à pression atmosphérique. Nous avons synthétisé et caractérisé quatre catalyseurs hétérogènes composés de différentes concentrations d'oxyde de tungstène déposées sur TiO_2. La synthèse a été spécifiquement conçue pour accomplir toutes les exigences spécifiques pour les particules dans un FBR - tailles de particules, vitesse de fluidisation minimale, résistance à l'attrition, densité apparente.

Nous avons optimisé le chargement de tungstène, la concentration en oxygène pour la fluidisation et la température pour la décarbonylation du fructose en furfural. Nous avons obtenu un maximum de 22 % pour le furfural à 200 °C, avec 5 % de WO_3 et un ratio molaire O_2 :fructose de 20. Nous avons détecté et quantifié des concentrations en acide acétique et diformylfuran (DFF) pour chaque heure des 6 h expérimentales. Ces résultats démontrent la création d'une nouvelle voie pour la conversion du sucre C-6 en phase gazeuse dans un FBR, conduisant à la publication d'un article scientifique et la poursuite d'un brevet.

La mise en œuvre du processus passe par l'optimisation du système FBR, du catalyseur et des variables du processus pour maintenir les 6 atomes de carbones dans la solution de fructose et ainsi augmenter l'efficacité du carbone. Nous avons alors ciblé l'oxyde-deshydratation du fructose en FDCA. Nous avons ajouté du Pt sur la surface du catalyseur, et avons identifié puis optimisé les paramètres de la réaction. Un faible temps de contact et la plus faible concentration en platine ont favorisé la deshydratation du fructose en HMF. Les analyses de la réaction en HMF ont démontré un pouvoir oxydant relativement haut en platine pour convertir le groupement alcool en aldéhyde - HMF en DFF -, mais pas assez pour oxyder l'aldéhyde en acide carboxylique - DFF en FDCA. Une sélectivité maximum en HMF égale à 12 % est obtenue après 6h en utilisant le fructose comme réactif initial. Cependant, injecter l'HMF comme un substrat, nous a permis d'obtenir un maximum en sélectivité de 43 % en DFF avec 1.5 g de catalyseur à 250 °C. Augmenter la température a favorisé l'oxydation mais aussi la vitesse de dégradation du l'HMF.

L'un des principales avantages démontré par cette nouvelle technologie est la grande polyvalence, qui permet l'adaptation à de nombreuses réactions différentes.

Dans la troisième partie de cette thèse, nous avons identifié et développé une réaction verte pour convertir l'acide lévulinique — le produit de l'hydrolyse de l'HMF. Dans un réacteur BATCH, nous avons développé l'oxydation de Baeyer-Villiger par du peroxyde d'hydrogène et de l'acide tungstique comme catalyseur de l'acide succinique.

Une concentration plus élevée en H_2O_2 et le temps ont augmenté la conversion de l'acide lévulinique. Augmenter la charge de H_2WO_4 a produit plus d'acide succinique, atteignant une sélectivité maximale de 75 % avec un ratio molaire initial d'acide lévulinique :catalyseur de 50 et un ratio H_2O_2 :acide lévulinique égale à 5 après 3 h. L'oxydation de Baeyer-Villiger passe par deux voies réactives, formant de l'acide succinique ou de l'acide 3-hydroxypropionique (HPA). H_2WO_4 a formé un abduct avec le substrat durant l'oxydation ; augmentant la charge catalytique, l'interaction module le ratio des produits, déplaçant la sélectivité du HPA à l'acide succinique. Nous avons récupéré jusqu'à 70 % en masse du catalyseur. Les essais de recyclage du H_2WO_4 ont démontré une activité similaire du catalyseur.

ABSTRACT

Biomass will become the new petroleum because of its abundancy and higher oxygen/carbon ratio that make it an excellent alternative feedstock to value-added compounds. The biomass power generation market is continuously increasing, and it will reach approximately 50 billion USD by 2022 Market Research Reports Search Engine (2015). Bio-catalytic processes, chemo-catalytic processes and chemical modifications of biopolymers are the three main biomass conversions Gallezot (2012). Fermentation to bio-ethanol is the most diffused sugars upgrading, accounting to more than 60 % of the global production Business insider (2018). This major conversion pathway derives from its application as bio-fuel. In fact, bio-ethanol presents lower production cost and higher octane number compared to gasoline. Fermentation has two main limitations: maximum theoretical molar yield of 50 % and low market value. The chemical equation includes the formation of a molecule of CO_2 per sugar molecule reacted. The bio-ethanol net profit margin is low, and it is determined by the difference between feedstock and product market price. White sugar costs around 300 USD/t International Sugar Organization (2018), while bio-ethanol is approximately 450 USD/t S & P Global Platts (2018). Fructose represents a high potential feedstock to 5-hydroxymethyl furfural (HMF), 2,5-furandicarboxylic acid (FDCA), levulinic acid (LEV), furfural (FUR), dimethyl furfural, dimethyl tetrahydrofuran and lactic acid.

The hexoses to HMF dehydration process is acquiring a key role in the sugar valorization, due to its importance as intermediate to high value chemicals and bio-fuels. The synthesis is hindered by the polymerization of carbohydrates and HMF to insoluble products — humins —, and the water rehydration of HMF, that cleaves the molecule to levulinic and formic acids. Organic solvents and ionic liquids, coupled with multi-phasic reactors and extraction systems, minimize the degradation steps.

We approached the catalytic design of fructose conversion to speciality chemicals by two points of view. The first was developing an alternative technology to convert fructose to value-added chemicals, which present higher market value than ethanol. We designed a μ-fluidized bed reactor (15 mm ID), where an atomizer sprayed the aqueous sugar solution directly into the catalytic bed. This part of the project was carried out at Polytechnique Montreal. The second step focused on the valorization of levulinic acid, the dehydration by-product of HMF. We developed a new catalytic route to oxidize the substrate to succinic acid, combining tungstic acid and hydrogen peroxide for the Baeyer-Villiger conversion. This part of the project was carried out during the period at University of Bologna.

We identified the liquid injection in a μ-fluidized bed reactor (FBR) as alternative technology to convert sugars into value-added chemicals. The concept of the system was based on the higher reaction rate to bio-chemicals than the degradation to humins or coke. Fluidized bed reduced the contact time to fractions of second, minimizing the side reactions. The reactor operated in the range of 300 °C to 400 °C and at atmospheric pressure. We synthesized and characterized four tungsten oxide loading on TiO_2 as heterogeneous catalyst. The synthesis was specifically tailored to accomplish all the specific requirements for particles in a FBR: particle size distribution, minimum fluidization velocity, attrition resistance and bulk density. We optimized tungsten loading, oxygen concentration in the fluidization gases and temperature for the fructose decarbonylation to furfural. We achieved a maximum of 22 % of furfural at 200 °C, with 5 % WO_3 and a molar ratio O_2:fructose of 20. We detected and quantified also the concentration of acetic acid and diformylfuran (DFF) every 60 min, for a total of 6 h reaction. The system demonstrated the creation of a new pathway for the conversion of C-6 sugars in gas phase in a FBR, leading to a scientific article and a continuation of a patent.

Implementation of the process included the optimization of the FBR system, the catalyst and the process variables to maintain the six atoms of carbon of the feed and consequently to increase the carbon efficiency. We targeted the oxidehydration of fructose to FDCA. We added Pt on the surface of the catalyst, and we identified and optimized the reaction variables. Lower contact time and higher amount of platinum favored the dehydration reaction to HMF. Analysis of the HMF reactivity demonstrated relatively high oxidation power of Pt to convert the alcohol functional group to aldehyde — HMF to DFF —, but not enough strength to further oxidize the aldehyde to carboxylic acid — DFF to FDCA. Fructose as starting material showed a maximum selectivity to HMF of 12 % after 6 h. Differently, injecting HMF as substrate, we reached a maximum of 42 % selectivity to DFF with 1.5 g catalyst at 250 °C. Increasing the temperature favored the HMF degradation rate.

One of the main advantage of this new technology is the great versatility, that can be tailored to a variety of reactions.

In the third part of the thesis we identified and developed a green reaction to convert levulinic acid — the HMF hydrolysis product. In a batch reactor, we developed the Baeyer-Villiger oxidation by hydrogen peroxide and tungstic acid as catalyst to succinic acid. Higher H_2O_2 concentration and time increased the levulinic acid conversion. Increasing H_2WO_4 loading produced more succinic acid, reaching a maximum selectivity of 75 % with a levulinic acid: catalyst molar ratio of 50, and H_2O_2:levulinic acid of 5 after 3 h. The Baeyer-Villiger oxidation passes through two possible attack of the oxygen, forming in prevalence more succinic acid or more 3-hydroxypropionic acid (HPA), based on the reaction conditions and the type of

catalyst. H_2WO_4 formed an abduct with the substrate during the oxidation; increasing the catalyst loading, the interaction modulates the product ratio, shifting the selectivity from the HPA to the succinic acid. We recovered up to 70 % in mass of catalyst. Recycle tests of the H_2WO_4 demonstrated similar activity of the fresh catalyst.

TABLE OF CONTENTS

LIST OF TABLES

LIST OF FIGURES

LIST OF ACRONYMS AND ABBREVIATIONS

FRU	Fructose
HMF	5-hydroxymethyl furfural
LEV	Levulinic acid
FUR	Furfural
FDCA	2,5-furandicarboxylic acid
DFF	2,5 - diformyl furan
FBR	Fluidized bed reactor
HPLC	High performance liquid chromatography
GC	Gas chromatography
MS	Mass spectroscopy
ID	Internal diameter
SSF	Saccharification and fermentation
FBR	Fluidized bed reactor

LIST OF ANNEXES

CHAPTER 1 INTRODUCTION

1.1 Background and problem identification

Hexoses represent the majority of carbohydrates, and a fundamental resource to bio-chemicals. Glucose and fructose are the two most abundant sugars in nature. The extraction by acid hydrolysis of cellulose or sucrose produces high purity glucose or a 50 : 50 mixture of glucose and fructose, respectively. Bio-ethanol is the main sugar transformation. The fermentation process requires acidic/basic catalysts or enzymes. The final yield, which is largely influenced by the starting materials and the process technology, can almost be the maximum theoretical molar conversion of 50 % Sánchez and Cardona (2008). Its synthesis increased exponentially since the application of bio-ethanol as bio-fuel. USA — 16 000 million gallons — and Brazil — 7 million gallons are the two main world producers Statista (2017a). In addition to the stoichiometry limitation, this alcohol presents lower market value than others sugars bio-chemicals. Fructose is an extremely interesting bio-feedstock, and a substitute to various petroleum based chemicals. Mainly found bonded with glucose — sucrose —, the molecule has six atoms of carbon and oxygen. Fructofuranose, a fructose conformation, has a furanic structure, which favors the synthesis of bio-chemicals such as 5-hydroxymethyl furfural (HMF) Tang et al. (2018); Hou et al. (2018), 2,5-furandicarboxylic acid (FDCA) Gawade et al. (2018); Albonetti et al. (2015), furfural Cui et al. (2016); Karinen et al. (2011) and dimethyl furan Kazi et al. (2011); Román-Leshkov et al. (2007).

HMF is one of the most promising bio intermediates for a large variety of bio-chemicals and bio-fuels ; hydrogenation produces dimethyl furan, a bio-fuel with 40 % more energy density than ethanol Guerrero Peña et al. (2018), while the oxidation forms diformyl furan (DFF) and consequently FDCA, the furanic substitute of terephthalic acid to plastics Avantium (2018). Transition metals demonstrate high yields in the FDCA synthesis from HMF Yang et al. (2016); Albonetti et al. (2012).

Compared to glucose, fructose shows faster reaction rate and higher yield for the dehydration to HMF. The reason is the similarity in the spatial conformation — fructofuranose versus glucofuranose — and the faster enolisation reaction Tan-Soetedjo et al. (2017). Aqueous systems with homogeneous catalysts dehydrate fructose to HMF with high yield.

The reaction suffers from the product rehydration, which cleaves the molecule to levulinic acid Son et al. (2012); Victor et al. (2014) and formic acid Sairanen et al. (2014). Furthermore, in presence of acidic catalyst, fructose and HMF polymerize to insoluble compounds called

humins. To increase the carbon efficiency and the final yield, the main approach is to develop multi-phasic reactors or ionic liquid systems, that continuously extract the HMF or suppress the degradation/rehydration reaction. The main drawbacks are the higher production final costs and the increase of the safety/environmental risks. Furthermore, higher temperature increases the products reaction rate, but also triggers the caramelization and the degradation of the materials.

To overcome those limitations, we identified as suitable alternative to multi-phasic systems the liquid injection into a micro-fluidized bed reactor. A sprayer atomized the aqueous sugar solution into the catalytic bed, where rapidly evaporated and reacted, minimizing the caramelization process. In fact, this technology ensures :

— Elevate heat and mass transfer
— No hot spots
— Avoid organic solvents
— Extremely fast kinetic and contact time (order of fractions of second)
— Fast feed atomization and elevate reaction rate with the catalyst, minimizing the caramelization/degradation process

Developing a new catalytic system is one route to improve the carbon efficiency of a reaction, and reduce at the same time the wastes production. Another pathway is to identify or investigate new reactions to valorize the by-products.

Levulinic acid, the HMF rehydration product, is a bio building block to value-added biochemicals such as γ-valero lactone, methyltetrahydro furan, succinic acid and α-angelica lactone. Bozell and Petersen (2010) listed succinic acid and levulinic acid as top 10 bio-based products from carbohydrates. Acidic hydrolysis of biomass dehydrates firstly to HMF and consequently cleaves the molecule to levulinic acid and formic acid. Oxidation of levulinic acid forms succinic acid, but a carbon atom is lost during the transformation. Succinic acid is a potential intermediate to a variety of bio-chemicals, and the precursor for the polymerization of polyesters and the starting material of 1,4-butanediol. In nature, it is the intermediate in the citric acid cycle, the series of chemical reactions that convert carbohydrates into energy. Industrially, hydrogenation of maleic acid, carbonylation of ethylen glycol or enzymatic transformation of glucose are the main succinic acid synthesis. Its market value is in continuous expansion, and by 2021 it will reach 700 millionUSD Markets & Markets (2018a). Its derivatives are divided into four class, based on the industrial application : acyclic O-containing, acyclic O,N-containing, cyclic O-containing and cyclic O,N-containing Bechthold et al. (2008). Converting levulinic acid to succinic will reduce the conversion of the C4-fraction of crude oil necessary for the synthesis, obtaining a more environmental friendly

process.

1.2 Objectives

The main objective of this project is the catalytic design for the fructose conversion to value-added molecules, and the upgrade of levulinic acid to succinic acid. To achieve the main goals, we divided the project into three specific objectives, that produced three articles published or to be submitted to peer-reviewed scientific journals, and a continuation of a previous patent.

The specific objectives of this work and their milestones are :

1. Demonstrate the gas-phase conversion of fructose in a μ-fluidized bed reactor to value added molecules. The results of this objective are described in chapter 4, and published as scientific article in **ACS Sustainable Chemistry and Engineering (I.F. 6.0)**. Furthermore, the work produced a continuation of the patent US9598343B2 — **Oxidation of C5 and C6 sugar feedstocks to carboxylic acids, ethers and ketones** (Appendix A).
   - — Design a process to atomize the sugar solution into a fluidized bed reactor
   - — Prepare and characterize 4 WO_3 loading on TiO_2 support
   - — Determine the effects of temperature, tungsten content and O_2 concentration on furfural selectivity
   - — Investigate the steady-state and the effects of coke on the selectivity to furfural and by-products
2. Develop the fluidized bed system, targeting the oxidehydration of fructose. Results will be submitted as scientific article in **Bioresource Technology (I.F. 6.1)**
   - — Prepare and characterize Pt-WO_3/TiO_2 for the fructose to HMF dehydration reaction
   - — Screen 6 parameters that can affect the reaction
   - — Develop an analytical method for the quantification of furanic products
   - — Develop a design of experiments to optimize temperature, oxygen concentration and mass of catalyst to dehydrate fructose to HMF
   - — Optimize the oxidation of HMF to DFF
3. Establish the levulinic acid upgrade to succinic acid through organic solvent-free Baeyer-Villiger oxidation with hydrogen peroxide. Results are published in **Applied Catalysis A : General (I.F. 4.4)**
   - — Determine the effects of catalyst loading, time and hydrogen peroxide on the levulinic acid conversion and products selectivity

— Identify the reaction pathway through intermediate reactivity
— Propose an interaction mechanism with the catalyst to modulate the regioselectivity of the reaction

The first two specific objectives were achieved at Polytechnique Montreal, while the third at University of Bologna (Italy).

CHAPTER 2 COHERENCE OF THE ARTICLES

A brief description of the chapters and the coherence between them :

Chapter 1 : this first section highlights the potential of sugars conversion to value-added chemicals and bio-fuels. After a rapid summary of the importance of the lignocellulosic material transformation, we will define the fructose dehydration methodologies to HMF and the further oxidation to FDCA, indicating advantages and drawbacks. We will propose an alternative technology for the valorization of fructose, highlighting the major advantages. A second part will focus on the levulinic acid oxidation to succinic acid, describing the market value and the potential of the two molecules. To achieve the main goal of the thesis, we propose three specific objectives, underlying the major milestones of each one.

Chapter 2 : a brief description of the chapters of this manuscript, and the main links between them.

Chapter 3 : this section covers the state of the art of the oxidehydration of hexoses and the oxidation of levulinic acid to succinic acid. Conversion of sugars in a μ-fluidized bed reactor, operating in the gas-phase, is a breakthrough technology, and based on our knowledge only few articles or patent describe similar work. To explore the state of the art, the section will mostly delineate the liquid phase dehydration and oxidation of hexoses, and will illustrate few application of liquid injection into a fluidized bed reactor. The second part of the section will describe the importance of levulinic acid as bio-feedstock to value-added chemicals, and the potential of one derivative, the succinic acid. We will define the main valorization processes for the synthesis of the two compounds, outlying the Baeyer-Villiger oxidation to convert levulinic acid to succinic acid.

Chapter 4 : according with the first specific objective, this chapter describes an alternative methodology for the conversion of fructose, through the liquid injection of the feed into a fluidized bed reactor. The results are published in **ACS Sustainable Chemistry & Engineering** and are the basis for the patent continuation **Oxidation of C5 and C6 sugar feedstocks to carboxylic acids, ethers and ketones**. To demonstrate the sustainability of the system on the conversion of sugar in the gas phase, we synthesized and characterized four tungsten oxide loadings on the TiO_2 inert support. We developed and improved the atomizer, able to continuously inject the feed for 19 h. The sparger injected the sugar aqueous solution directly into the fluid bed, where formed an aerosol that reacted with the catalyst. We analyzed the influence of temperature, tungsten loading and O_2 :fructose molar ratio on the furfural selectivity. A GC-MS measured the liquid products concentration, while an online

MS monitored the non-condensable gases during the reaction. Acetic acid and diformyl furan were the two main by-products. During the reaction, coke built up on the surface, increasing the selectivity to furfural and decreasing the acetic acid.

Chapter 5 : the main limitation described in the article of chapter 4 is the low carbon efficiency, due to the decarbonylation of the fructose to furfural. We targeted the dehydration of fructose to HMF, investigating the effects of six reaction variables and synthesizing a Pt-WO_3/TiO_2 catalyst. Furthermore, we established the relationship between platinum content, temperature, oxygen concentration and catalyst loading on the furanic selectivity. Addition of Pt increased the oxidative power of the catalyst, but demonstrated the inefficiency to convert HMF directly to FDCA. We investigated the oxidation of HMF to DFF.

Chapter 6 : fructose dehydration has as by-product levulinic acid. This molecule is an important intermediate to bio-chemicals and bio-fuels. This section describes the oxidation of levulinic acid to succinic acid. This process is an interesting route to increase its market value and at the same time valorize the undesired products. We developed the green oxidation with H_2O_2 in a batch reactor, catalyzed by H_2WO_4. We estimated the influence of the reaction time, catalyst loading and reagent concentration on the products selectivity and on the LEV conversion. For a deep understanding of the reaction pathway, we investigated the reactivity of the main intermediates and proposed a reaction network. Furthermore, we explained how the interaction mechanism between catalyst and reagent modulates the selectivity of two competitive reaction kinetics. Results are published as scientific article on **Applied Catalysis A : General**.

Chapter 7 : general discussion of the work and summary of the results achieved.

Chapter 8 : summary of the project, focusing on the main hurdles and the limitations, providing recommendations for future work.

CHAPTER 3 LITERATURE REVIEW

Biomass is the main resources for fuels and bio-chemicals. Worldwide, biomass and wastes grant 10 % of the global energy demand Jahirul et al. (2012). In 2017, Canada produced more than 2000 MW of energy from solid biomass and renewable wastes Statista (2017b). Petroleum refinement establish 7 main building blocks, as base of the main industrial chemical processes Boisen et al. (2009). Shifting from crude oil to renewable feedstock will reduce the fossil fuels dependence and diminish the CO_2 emission.

This chapter, divided in five main sections. Initially, after a brief description of biomass and sugars, a section will explain the extraction and hydrolysis of hexoses from lignocellulosic materials, and further the fermentation process to obtain bio-ethanol. A second section will focus on the fructose potentialities and the corresponding applications. The next part will discuss one of the most important reaction of fructose, the dehydration to 5-hydroxymethyl furfural and the further oxidation to 2,5-furandicarboxylic acid. The fourth section clarifies the benefits of fluidized bed reactors, the advantages of micro systems and the liquid injection directly into the catalytic bed. The last part will evaluate the importance of levulinic acid — the by-product from the fructose dehydration — and its valorization to succinic acid. The section includes the Baeyer-Villiger oxidation mechanism, as interesting reaction to oxidize levulinic acid to succinic acid.

3.1 Biomass and sugars

Biomass is organic matter, which can be converted to bio-fuels and bio-chemicals. Based on the origin, Vassilev et al. (2010) classifies it in : woody, herbaceous and agricultural, aquatic, animal and human wastes, contaminated and industrial wastes (semi-biomass) and a mixtures of the previous. Thermal (to produce heat), thermo-chemical (to gas, liquid and solid bio-combustibles) and bio/chemical (to speciality chemicals) are the three main valorization routes. Dry lignocellulose contains around 55 % to 75 % carbohydrates Mosier et al. (2005). Around 80 % in weight of lignocellulosic material can be transformed into chemicals and fuels Alonso et al. (2017). Cellulose, hemicellulose and lignin forms the majority of lignocellulosic material, the most value and abundant group of biomass. The three components proportion varies with materials. Lignin is an organic cross-linked polymer, where the high-molecular units are bonded to create a complex amorphous structure. Polysaccharides, and especially glucose, mannose, xylose and arabinose, composes hemicellulose. Cellulose is a polymer, consisting of *D*-glucopyranose units linked by (1→4) β-glycosidic bonds. Hemicellu-

lose differs from cellulose by the insertion of xylose and C5 monosaccharides in the polymeric matrix.

High oxygen/carbon ratio and the low cost extraction give to sugars a huge potential as substrate to speciality chemicals. The US chemical market value is approximately 2 trillion USD each year, while the speciality chemicals value is around 400 billion USD Markets & Markets (2018b).

3.1.1 Extraction and hydrolysis

Glucose and fructose are the most abundant sugars in nature, formed by six carbon and six oxygen atoms. Hydrolysis of cellulose cleaves the polymeric bonds, producing monomeric glucose, while sucrose — molecule deriving by the bonding of glucose and fructose, the sweet component of fruit and vegetables — hydrolysis breaks the disaccharide bond forming a 50 :50 mixture of both hexoses.

Monosaccharides industrial production includes two steps : the lignocellulosic material pre-treatments and the polysaccharides hydrolysis. The first approach removes lignin and hemicellulose, reducing the sugar degradation and the by-products formation, resulting in higher hydrolysis yields Kan et al. (2016). In fact, reducing the crystallinity contributes to facilitate the interaction between the enzymes or the catalysts with cellulose. Pre-treatments include physical Shuping et al. (2010), thermal Isaksson et al. (2013), chemical Carrier et al. (2011); Kilambi and Kadam (2015); Camarero Espinosa et al. (2013) and biological Fu et al. (2011) processes. Industrially, the prevalent treatment is the steam explosion ; the material is high-pressure saturated by a steam (160 °C to 260 °C with a pressure of 0.69 MPa to 4.83 MPa), then exposed to atmospheric pressure, causing an explosive decompression. The approach thermally degrades the hemicellulose and transform the lignin Kumar et al. (2009), which presence drastically reduces the hydrolysis efficiency Rahikainen et al. (2013).

The second step is the polysaccharides hydrolysis, which cleaves the polymeric bonds to form mainly monomeric hexoses from cellulose and a combination of hexoses and pentoses from hemicellulose. Industrial processes rely on homogeneous, heterogeneous and enzymatic catalysts. The number of Brønsted acid sites, affinity with the substrate and catalyst stability are the most influence variables for the lignocellulosic hydrolysis Huang and Fu (2013). Concentrated acids (H_2SO_4 and HCl) demonstrate higher activity then heterogeneous catalysts, but suffer for high environmental impact, high system corrosion and require complex recovery steps von Sivers and Zacchi (1995). Diluted acids, combined with higher temperature (above 130 °C) reduce the toxicity and improve the operational range of the process Lenihan et al. (2010). Heterogeneous catalysts present easier separation steps, higher recyclability and lo-

wer system corrosion, but lower yield. Addition of W to mesoporous transition-metal oxides — like Nb — demonstrates higher activity than other traditional solid acidic catalyst, such as Amberlyst-15 or pure Nb_2O_5. Tagusagawa et al. (2010) describe the glucose production of $12\,\mathrm{mmol\,g^{-1}\,h^{-1}}$, with a turnover frequency of $40\,\mathrm{h^{-1}}$. Heteropolyacids present high acidic density, which reflects the higher activity compared to mineral acids and H-zeolites Huang and Fu (2013) ; $H_5BW_{12}O_{40}$ demonstrates a maximum glucose yield of 77 % at 60 °C.

Enzymatic hydrolysis is the prevalent methodology for glucose production, due to the low toxicity, costs and reactor corrosion compared to acidic hydrolysis. Type of substrate, *cellulase* activity and reaction conditions affect the hydrolysis efficiency. Each type of substrate requires a specific type of *cellulase* enzyme. The optimal conditions range between 40 °C to 50 °C and 4 pH to 5 pH Neves et al. (2007). Increasing the cellulose concentration increments the reaction rate Cheung and Anderson (1997), but an excessive amount of substrate inhibits the reaction Penner and Liaw (1994).

b-fructofuranosidase shows an almost complete cleavage of sucrose at 50 °C Akgöl et al. (2001). Glucose inhibits the enzymatic cleavage. Coupling the fermentation process with the cellulose hydrolysis reduces the hexose concentration and improve the ethanol production Sun and Cheng (2002).

3.1.2 Fermentation to ethanol

Despite numerous energy forms, liquid fuels are the main type of energy transportation. Currently, the transportation sector is responsible of 20 % of global CO_2 emissions The Royal Society (2008). Blending gasoline with bio-fuels will limit the increment of the net carbon dioxide production. In USA, around 85 % of gasoline is now blended with ethanol from biomass Demirbaş (2005). The current fermentation technology still requires improvement on processing the lignocellulosic materials — pre-treatments — and developing new methodologies to reduce the total costs — like adding a mixture of micro organisms.

Fermentation of sugars proceeds with the formation of two molecules of ethanol and two of carbon dioxide (equation 3.1). The maximum molar theoretical yield of 50 %, combined with the lower market value versus bio chemical, highly limits the potential of the sugars valorization.

$$C_6H_{12}O_6 \rightarrow 2C_2H_6O + 2CO_2 \tag{3.1}$$

Industrially, the process passes through two steps : the broth fermentation and the distillation. After the pre-treatments, the starting material is mixed with micro organisms to ferment.

This step is limited by the lack of efficient enzymes able to simultaneously convert hexoses and pentoses, which requires purification of the starting materials. Furthermore, most of enzymes lose activity or are completely inhibited at higher concentration of glucose (saccharification). Wyman and Yang (2009) report a maximum yield of 90 % of the theoretical from glucose, adding *Saccharomyces yeast*. Mixing micro organisms to the fermentation broth favors the conversion to ethanol and reduces the decline of activity. This process is called simultaneous saccharification and fermentation (SSF).

The advantages are Sun and Cheng (2002) :

— higher hydrolysis rate
— lower minimum enzymes concentration
— enhance ethanol yield
— reduce the sterile conditions, due to the instantaneous removal of glucose
— lower process time
— lower reactor volume

The second step is the separation of ethanol from the fermentation broth with distillation. This technique ensures the separation of the product from the solid residue, such as lignin, unreacted cellulose and hemicellulose, ash and enzymes, which will be further burned to supply energy to the system Wooley et al. (1999). Periodical distillation, coupled with batch fermentation, produces 92 % of theoretical yield and an ethanol concentration of $10\,\mathrm{g\,L^{-1}}$ to $80\,\mathrm{g\,L^{-1}}$ Kishimoto et al. (1997).

Based on the fructose and ethanol market price, and the limitation of the fermentation reaction, the potential of this substrate is not fully exploited. Fructose is an high value feedstock with a wide range of applications.

3.2 Fructose valorization

3.2.1 Applications

Fructose is an hexose (6 carbon and 6 oxygen atoms), and the structural isomer of glucose. Sugar cane and sugar beets are the main sources, from which is extracted as mixture with glucose, and commercialized as *high-fructose corn syrup*. In the food industry, it is largely added as sweetener, due to low cost and the highest sweetness among all the carbohydrates. One of the carbohydrates limitation is the caramelization process, which is a non-enzymatic browning of sugars, caused by excessive temperature. During the caramelization, various reactions occur, such as condensation, dehydration, intra-molecular bonding, formation of unsaturated polymer and isomerization. In the food industry, sugar browning is largely used

to give colour and in the cooking process. The thermal limit value depends on the type of saccharide, and for the most common sugars varies between 110 °C to 180 °C. The fructose threshold is 110 °C.

In the chemical industry, fructose is one of the main bio-feedstock, thanks to its furanic ring, that makes it suitable for the synthesis of a variety of chemicals and bio-fuels. Its importance is highlighted by the presence of 7 molecule on the list of the top 10 bio-based products from carbohydrates, which are directly associated to fructose Bozell and Petersen (2010).

As already mentioned, fermentation to ethanol is the largest fructose conversion, but various reactions can exploit the sugar potential to bio-chemicals and bio-fuels. Figure 3.1 shows the main trasformation of fructose. The reforming process cleaves the molecule to H_2 and CO, which is further injected into a Fisher-Tropsch reactor to produce hydrocarbons Michailos et al. (2017). The hydrogenation process forms sorbitol and mannitol, the corresponding alcohols. Even if their sweetness is lower compared to sucrose — 50 % to 60 % less —, they are largely added as sugar substitute to prevent caries, due to the low fermentation rate of oral bacteria Livestrong (2018). Catalytic hydrogenation over CuO-ZnO produced from 60 % to 68 % mannitol, at 35 bar to 65 bar and 90 °C to 130 °C Kuusisto et al. (2005). The retro-aldol reaction, the opposite of the aldolic reaction between two carbonyl groups, cleaves the molecule into an aldehyde and a ketone. In the case of fructose, the breakage produces glycol aldehyde and erythrose.

Another important reaction is the isomerization to glucose. Acidic catalyst, basic catalyst or enzymes are able to convert one sugar into the corresponding isomer. Industrially, *D-glucose / xylose isomerase XI* (GI, EC 5.3.1.5) isomerize the glucose to high-fructose corn syrup. The main drawbacks are the loss of activity at temperature higher than 60 °C, a small pH work capability, necessity of high amount of catalyst and a deactivation after few cycles Bhosale et al. (1996). Glucose oxidation forms firstly gluconic acid and further glucaric acid. Gold supported on activated carbon demonstrates an high oxidation power in liquid phase. Changing operative conditions modulate the oxidation Megías-Sayago et al. (2018); Önal et al. (2004); An et al. (2012). Gluconic acid is mainly applied in the medical field and in the food industry as additive. Glucaric acid is added as detergent builder, due to its property to suspend calcium and magnesium ions in water, reducing the hard deposits. A further dehydration and hydrogenation of glucaric acid gives adipic acid Boussie et al. (2010). This monomer, is also the precursor to synthesize nylon.

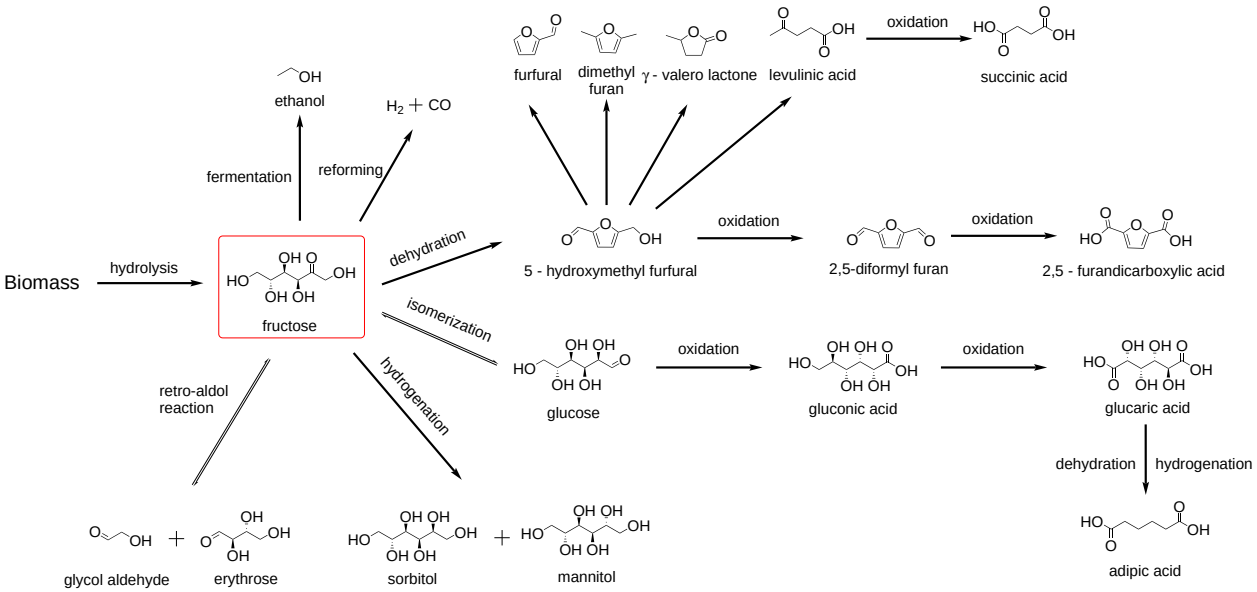

Figure 3.1 Fructose conversion to bio-chemicals and bio-fuels

3.2.2 Furfural and pyrolysis

The US Department of Energy listed furfural as one of the "top 10 biobased products" Werpy and Petersen (2004). Industrially is found mainly as extraction solvent. Reduction by hydrogen Ying Hao et al. (2005) or enzymes Diaz De Villegas et al. (1992) produces furfuryl alcohol, a monomer to furan resins. Pentoses — like xylose — from hemicellulose are the industrial starting materials to furfural. The reaction includes the loss of three molecules of water, and requires the presence of acid catalyst. Industrially, the batch process of QUAKER OATS produces furfural in presence of sulfuric acid at 153 °C for 5 h Zeitsch (2000). The main limitations are the multiple passages of a steam through the reactor, long contact time, toxicity and corrosive catalysts and formation of acidic wastes Bu et al. (2011).

Solvents modifies the reaction mechanism : alcohols stabilize the intermediates formation, and promotes the furfural production. Iso-propanol and 2-butanol converts directly xylose to the corresponding levulinic ester, while ketones inhibit the dehydration to furfural. Esters as solvent — such as methyl formate — at 150 °C promote the dehydration (yield 70 %) and produces formates, highly volatile molecules that can be easily separated from furfural Hu et al. (2014).

The main drawbacks of furfural production is the limitation to C5 carbohydrates as starting material. Furthermore, the presence of this molecule in the fermentation broth inhibits the transformation of hexoses, and glucose in particular, to bio-ethanol Taherzadeh et al. (1999).

Identify new route to simultaneously convert hexoses and pentoses will make the lignocellulosic processes more accessible to various starting materials. C5 sugars generally dehydrate to furfural, while C6 carbohydrates form HMF. However, fast pyrolysis of sugars decarbonylates hexoses. This technique consists of a rapid increase of the temperature (more than $500\,^{\circ}\mathrm{C\,s^{-1}}$) up to 400 °C to 600 °C, to mainly produce bio-oils or bio-fuels. Carlson et al. (2010) report the synthesis of furfural from glucose via fast pyrolysis (1000 °C with H-ZSM-5 up to 20 % in the molar ratio to glucose ratio of 1.5. Decreasing the pore size distribution increases the oxygenated products and reduces the coke formation. ZK-5 (zeolite with SiO_2/Al_2O_3 of 5.5) produces 40 % of the oxygenated products Jae et al. (2011).

As well as fast pyrolysis, combination of heterogeneous catalysts with organic solvents decarbonylate glucose to furfural. H-mordenite in γ-valero lactone reaches a 80 % furfural yield from hemicellulose and 37 % from glucose Gürbüz et al. (2013). Zhang et al. (2017) report 69 % yield from glucose at 180 °C after 33 min, with Sn-Beta zeolite.

Among all the solvents tested, γ-valero lactone or γ-butyrolactone are the two main solvents that demonstrated higher yields during the decarbonylation of glucose.

3.3 5-hydroxymethyl furfural

3.3.1 Dehydration to HMF

5-hydroxymethyl furfural (HMF) encases a huge potential as bio-intermediate to a wide range of bio-chemicals and bio-fuels. In nature is found in various food, produced by the thermal decomposition of carbohydrates. The molecule has medical properties : it increases the blood circulation, behaves as antioxidant and against the sickle-cell disease.

Due to the lower concentration of acyclic conformation of glucose than fructose, aldoses are less reactive than ketoses for the dehydration reaction Kuster (1990). The six atoms ring of

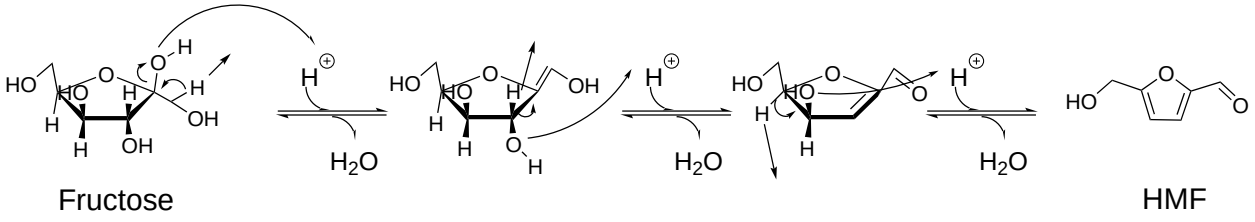

Figure 3.2 The triple dehydration of fructose to HMF starts with the loss of a water molecule in position 2, and the formation of a cyclic intermediate.

glucose is more stable and less reactive than the furanic ring. Furthermore, only 1 % of glucose is in the furanose form, while fructose reaches 21.5 % as fructofuranose Chao Wang et al. (2017). Enolisation is the reaction limiting step, resulting in higher fructose reactivity than glucose. The dehydration mechanism of C6 sugars is still under investigation. Two pathways describe the reaction : the formation of acyclic intermediates or the creation of closed ring intermediates (Figure 3.2). Recently, ^{13}C NMR in DMS demonstrated the presence of cyclic molecules in the dehydration mechanism Akien et al. (2012).

The first HMF synthesis was described by pressurizing a solution of inulin — a polysaccharide — and oxalic acid Düll (1895). Commercially, high-fructose corn syrup is the starting material for the HMF production Kläusli (2014). During the years, the dehydration process was largely improved, testing and comparing type of reactors, solvents, type of catalysts and product isolation methodologies.

The two main hurdle of the process are :

— Polymerization of HMF/hexoses to insoluble brown materials, called humins
— Rehydration of the HMF, that cleaves to formic acid and levulinic acid

Brønsted acid sites on the catalyst surface favors the dehydration reaction. Mineral acids, such as HCl and H_2SO_4 (Table 3.1, entry 1 and 2), are the most applied catalysts, but at high fructose concentration, the HMF yield decreases due to the elevate polymerization rate to humins. Switching to organic acid, like acetic acid and lactic acid (Table 3.1, entry 3 and 4), decreases the environmental and process risks. Excessive corrosion, high level of toxicity and necessity to recycle the catalyst induced to shift to heterogeneous catalysts. Coupling solid particles with organic solvents are a viable solution to extract HMF from the aqueous phase and avoid the side products (Table 3.1, entry 5 to 7).

The main advantages are :

— Shift the equilibrium through the products, continuously removing the HMF formed
— Decrease the by-products formation
— Reduce the polymerization to humins
— Increase conversion and selectivity

Methyl isobutyl ketone (MIBK), dichloromethane (DCM), ethyl acetate, dimethylether (DME), tetrahydrofuran (THF) and dimethyl sulfoxide (DMSO) are the most common organic media. Fructose in presence of DMSO at 150 °C dehydrates without catalysts Musau and Munavu (1987). Two main sections compose biphasic and triphasic reactor : the aqueous phase, where the dehydration process occurs, and the organic phase, where HMF migrates due to the low solubility in water (Figure 3.3). Further purification of the organic media isolates the products. Combination of organic phase and heterogeneous catalyst shows easier separation,

Table 3.1 Fructose dehydration to HMF. [BMIM][Cl^-] : 1-ethyl-3-methylimidazolium chloride ; MW : microwave assisted ; (ho) : homogeneous catalyst ; (he) : heterogeneous catalyst ; X : conversion ; S : selectivity

Entry	**Solvent**	**Catalyst**	**T,** °C	**Time** min	X, %	S_{HMF}, %	**Ref.**
1	H_2O	HCl (ho)	185	1	71	75	Tuercke et al. (2009)
2	Ethylen glycol, DME	H_2SO_4 (ho)	200	210	100	70	Chen et al. (1991)
3	H_2O	Acetic acid 10 % wt (ho)	150	120	38	76	de Souza et al. (2012)
4	H_2O	Lactic acid 50 % wt (ho)	150	120	95	67	de Souza et al. (2012)
5	1 :5 H_2O : DMSO/ MIBK - 2-butanol	HCl (ho)	185	1	98	81	Tuercke et al. (2009)
6	5 :5 H_2O-DMSO/ 7 :3 MIBK :2-butanol	HCl (ho)	170	4	95	89	Chheda et al. (2007)
7	Saturated H_2O with CsCl - 1-butanol	HCl (ho)	180	15	92	80	Román-Leshkov and Dumesic (2009)
8	DMSO	Amberlyst15 (he)	120	120	100	100	Shimizu et al. (2009)
9	DMSO	$FePW_{12}O_{40}$ (he)	120	120	100	97	Shimizu et al. (2009)
10	Acetone-DMSO	Dowex-type (he) ion-exchange resin	150 (MW)	20	99	84	Qi et al. (2012)
11	subcritical H_2O	H_3PO_4 (ho)	240	2	—	65	Asghari and Yoshida (2006)
12	90 :10 supercritical acetone - H_2O	H_2SO_4 (ho)	180	2	—	77	Bicker et al. (2003)
13	[BMIM] [Cl^-]	Amberlyst 15 (he)	80	10	99	83	Qi et al. (2010)

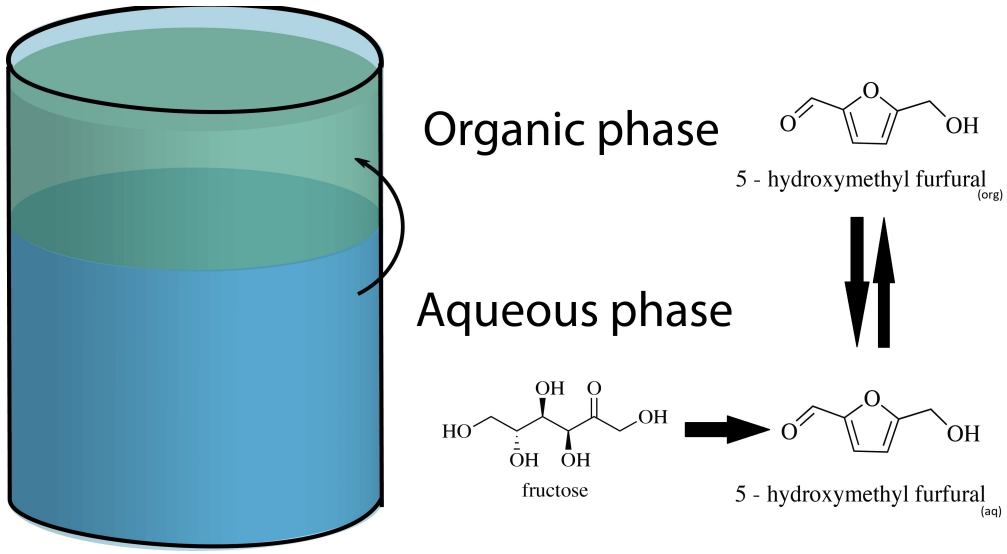

Figure 3.3 The dehydration of fructose occurs in the aqueous phase of the biphasic reactor. HMF migrates into the organic phase, reducing the rehydration to levulinic acid and formic acid, and the polymerization to humins

lower corrosion, and a possible recycling of the solid particles (Table 3.1, entry 8 to 10). Recently, liquids in supercritical and subcritical state improve the final products separation step (Table 3.1 entry 11 and 12).

Ionic liquids are largely applied as solvents. They can dissolve more concentrated carbohydrates respect to organic solvents, and can be easily recycled. Furthermore, they demonstrated higher yields than heterogeneous catalysts Zhao et al. (2007). A combination of acidic solid catalyst and ionic liquids ensure high yields with low contact time —10 min (Table 3.1 entry 13). The main limitations are the higher costs, the low biodegradability (may be toxic to micro-organisms) and are potentially toxic (especially the so-called first generation).

3.3.2 HMF valorization

HMF is the intermediate to various furanic-based bio-chemicals and bio-fuels. Figure 3.4 shows the main products from HMF. Lewkowski (2005) classifies the conversion to value-added molecules based on the type of reaction and the functional group involved in the process :

— Reaction with the hydroxymethyl group ; includes formation of esters, ethers, halides and oxidation to aldehydes and acids
— Reaction with the formyl group ; reduction to alcohol, condensation and oxidation
— Reaction with the furan ring

— Polymerization
— Electrochemical conversion

Etherification of the hydroxymethyl moiety forms to 5-alkoxymethyl furfural. In particular, methylation produces methoxymethyl furfural, which is the key part on the oxidation to 2,5-furandicarboxylic acid (FDCA) from HMF in the Avantium YXY technology. Commercially it is applied as antifungal, while in the tobacco industry, addition of alkoxymethyl furfural enhanced the sweet flavor of the smoke Hind et al. (1963). The hydrogenation of both functional groups forms 2,5-dimethyl furan (DMF), a potential bio-fuel. Compared to ethanol, it possesses higher energy content, higher boiling point and octane number, with a reduced oxygen content. Furthermore, its miscibility with gasoline is higher than ethanol, while it is immiscible with water Román-Leshkov et al. (2007). Pt/rGO (reduced graphene oxides) hydrogenates HMF to DMF, with 73 % yield at 3 MPa of H_2 after 2 h reaction Shi et al. (2016). Partial reduction forms 2,5-bishydroxymethyl furan, a component to fabric resins, polymers and artificial fibers Lewkowski (2005). Water hydrolyses HMF to formic acid and levulinic acid, which can further dehydrate to α-angelica lactone in presence of acidic catalyst. This molecule is added in oral care formulation to increase the mint and the coffee flavor. Decarbonylation of HMF produces furfural, which in nature spontaneously occurs at high temperature.

One of the most important and famous reaction is the oxidation to 2,5-furandicarboxylic acid, the furanic substitute of terephthalic acid to plastics.

Partial oxidation to DFF and HMFCA

HMF oxidation follows two pathways, depending on the fastest moiety that reacts (Figure 3.5). Type of metal and solvents modulate the selectivity of the two-competitive kinetics. Transition metals demonstrate high catalytic activity in the oxidation. Ru/C in toluene, with 2 MPa O_2, efficiently produces DFF with a yield of 96 % at 110 °C Nie et al.. Hydroxyapatite as support for ruthenium nanoparticles increases the oxidation power, converting HMF to FDCA with 99.6 % yield at 120 °C and with 1 MPa oxygen Gao et al. (2018). Magnesium/cerium oxides selectively oxidized HMF to DFF in water with O_2 and without any other additives. The same amount of acidic and basic sites establish the maximum yield of 98 % Ventura et al. (2018).

One-pot conversion of DFF from fructose requires acidic sites for the dehydration step, and transition metal oxides for the further oxidation. Sulphonated MoO_3-ZrO_2 oxides converted directly fructose to DFF with a yield of 74 % Zhao et al. (2018a). Combining MoO_3 with nitrogen-doped carbon (Mo-HNC) produces 77 % DFF after 9 h at 150 °C Zhao et al. (2018b).

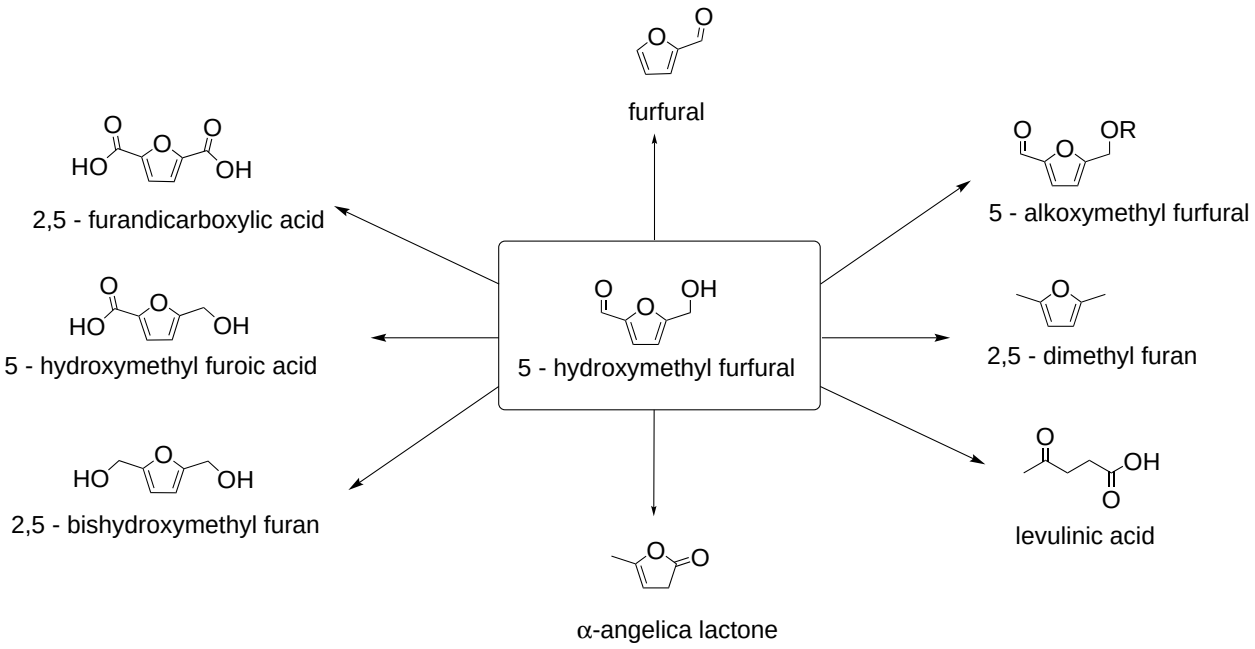

Figure 3.4 Conversion of HMF to value added molecules

Formation of HMFCA requires a faster oxidation step for the formyl moiety than the hydroxyl group. Like for DFF, transition metals demonstrated high selectivity toward the oxidation of HMF. Cs-substituted tungstophosphate-supported ruthenium particles converted HMF to HMFCA with a yield of 72.9 % after 12 h at 130 °C, with molecular oxygen flowing at 20 mL min^{-1}. Addition of aromatic solvents enhanced the yield, but the catalyst suffered from instability and loss of activity during the recycling experiments Wang and Zhang (2017). Molybdenum acetylacetonate complex, immobilized on montmorillonite K-10 clay, shows a selective oxidation to HMFCA with 87 % yield after 3 h in toluene, without any significant loss in activity after several recycles Zhang et al. (2014). HMFCA is quite unstable, and easily oxidize to FDCA.

3.3.3 Oxidation to FDCA

2,5-furandicarboxylic acid is one of the most promising monomer to replace terephthalic acid to green plastics. Polymerization with ethylen glycol forms poly(ethylene furanoate) (PEF). This material possesses superior chemical and physical properties than poly(ethylene terephthalate) (PET), such as higher O_2 (X 9 Burgess et al. (2014a)), CO_2 (X 11 Burgess et al. (2015)) and H_2O vapors (X 2 Burgess et al. (2014b)) barriers, higher glass transition temperature, lower melting point and higher modulus Burgess et al. (2014c). Furthermore,

PEF is recyclable and can be included up to 5 % into PET recycle stream without affecting its performance Gotro (2013). The main application regards bottles, fibers and films.

The Coca Cola Company, Avantium, Danone and ALPLA are working together to commercialize PEF bottles. Avantium developed the YXY technology, where methanol or ethanol etherificates 5-hydroxymethyl furfural, which is further oxidized by O_2 to FDCA Avantium (2018). The process demonstrated more than 96 % yield, but requires a catalytic hydrogenation purification step Janka et al. (2013). In 2016, the joint venture with BASF, Synvina, aimed to built a reference plant with a capacity up to 50000 metric tons per year BASF (2016), but the commercial facility was delayed by 2023 - 2024, due to process inefficiency in the pilot plan Scott (2018).

The oxidation of HMF to FDCA passes through two ways : the conversion of the hydroxymethyl moiety to the corresponding aldehyde, or the formation of an acidic functional group from the formyl moiety. The first leads to diformyl furan, while the second to 5-hydroxymethyl-2-furancarboxylic acid (HMFCA). HMF to 5-hydroxymethyl-2-furancarboxylic acid (HMFCA) is thermodynamically more inclined to oxidation, but type of catalyst and reaction conditions modulate the kinetic. A further oxidation gives 5-formyl-2-furancarboxylic acid (FFCA) and finally FDCA (Figure 3.5).

The are many hindrances in the FDCA synthesis :

- Reagents and intermediates degrade in acidic conditions, cleaving to smaller by-products or polymerize to humins
- Furanic compounds generally demonstrate poor solubility in water. Organic solvents, like dimethylsulfoxide (DMSO) or γ-valero lactone (GVL), dissolves reagents and products, but are not environmental friendly
- Polymerization to PEF requires high purity of the final product. In fact, intermediates

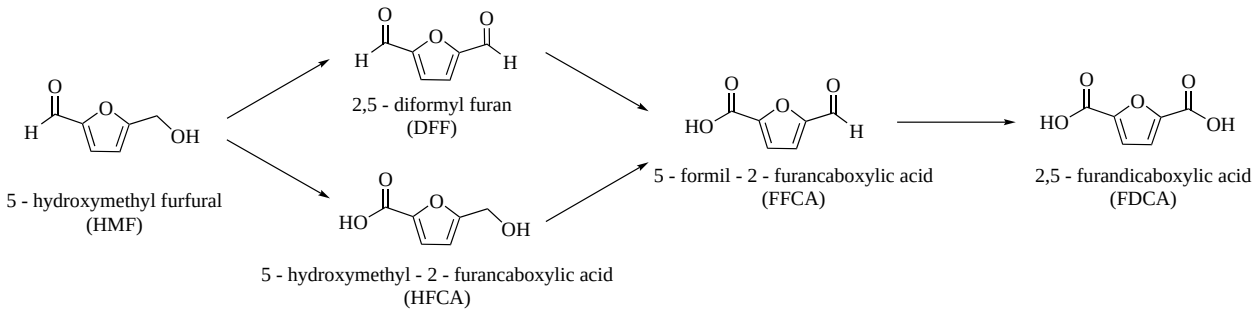

Figure 3.5 Catalysts and solvents define the HMF oxidation pathway : through the conversion of the hydroxymethyl group to aldehyde, or the formyl group to acid.

and by-products like HMF, furfural and DFF modify the colour, which will shifted to yellowish tones

— Glucose is less reactive than fructose, and requires an isomerization step to increase the yield

Enzymatic oxidation of HMF to FDCA requires engineered micro-organisms able to convert both alcohol and aldehyde moieties. Furthermore, the process needs a purification step to recover the products or separate the enzymes from the broth. *Raoultella ornithinolytica BF60* shows an HMF conversion of 93.6 %,with a maximum concentration of 93.6 mM FDCA production Yuan et al. (2018). Koopman et al. (2010) demonstrate that *Cupriavidus basilensis HMF 14* achieve 97 % yield, and propose a purification step to obtain 99.4 % pure dry FDCA from the fermentation broth, with a maximum concentration of 190 mM.

The three major limitations for the bio-oxidation are the narrow experimental conditions, the high enzymatic concentration required and the low reusability. A great step forward is the immobilization over a material, which overcomes the majority of the drawbacks. A magnetic *laccase* catalyst, with (2,2,6,6-tetramethyl-piperidin-1-yl)oxyl (TEMPO) as solvent, produces 90 % yield FDCA after 96 h reaction, maintaining 84.8 % of its activity Wang et al. (2018).

Supported noble metals drastically reduce the reaction rate, but require harsher conditions. Furthermore, most of them need the addition of a base, to attack the HMF aldehyde moiety. In aqueous condition, Pd/CC converts HMF to FDCA with 85 % yield. The reaction requires addition of O_2 at 140 °C for 30 h. The same catalyst demonstrates also the two-step conversion from fructose with a yield of 64 % Rathod and Jadhav (2018). Deposition of 4.9 % Pt over carbon nanotubes in aqueous media and with 0.5 MPa of molecular oxygen oxidizes HMF with a yield of 98 % to FDCA and 1.5 % to FFCA at 95 °C. The carbon support presents some carbonyl/ quinone groups that accelerate the hydrogen transfer from the Pt sites and favor the reaction Zhou et al. (2015).

As for the fructose dehydration to HMF, biphasic or multiphasic reactors ensure the oxidation of HMF to FDCA, minimizing the by-products, and also allow the two-step conversion directly from fructose. Leshkov et al. (2006) developed a multiphasic reactor with methyl-isobutyl ketone and 2-butanol as organic phase ; in the aqueous solution, fructose dehydrates to HMF, while the organic phase extracts it and further oxidizes to FDCA. Pt/C oxidehydrates fructose to FDCA in γ-valero lactone and H_2O Motagamwala et al. (2018). Yi et al. (2015) developed a tri-phasic system to convert sugars to FDCA. In the first phase (tetraethylammonium bromide (TEAB) or water), Amberlyst-15 dehydrates fructose to HMF, which is extracted and transported by a bridge (methyl isobutyl ketone) to another phase (water), where Au_8Pd_2/HT catalyst and Na_2CO_3 oxidize HMF to FDCA. After 20 h, FDCA reached

a maximum yield of 78 % at 95 °C.

Recently, a combination of ionic liquids and non-noble metals avoid the organic phase and directly converted fructose to FDCA Yan et al. (2018).

3.4 Fluidized bed reactor

Kunii and Levenspiel (1991a) describe fluidization as *operation by which fine solids are transformed into fluidlike state through contact with a gas or liquid*. Fluidized bed reactors were invented in 1920 by Fritz Winkler for the powdered coal gasification. Air and steam were injected from the bottom of a reactor (22 m high) loaded with coal. The gas, passing through a distributor, suspended the solid. This technology was extensively applied for the Thermal Catalytic Cracking (TCC), and further to implement another process, the Fluid Catalytic Cracking (FCC) Kunii and Levenspiel (1991b). Recent applications involve metallurgic and thermochemical processes (combustion, gasification and pyrolysis). The main examples are the synthesis of isobutene, naphta cracking and acetone recovery, FCC, methanol to olefins (Exxon process) and Fisher-Tropsch synthesis. Particle size distribution Sun (1991) and inter particle forces Shabanian and Chaouki (2015) largely affect the hydrodynamic properties. The fluidization regime is dictated by experimental conditions, diameter and density of the particles, and density and velocity of the fluidGeldart (1973). Increasing the fluid velocity, the particles will behave as : fixed bed, minimum fluidization, particulate fluidization, bubbling, slugging, and finally as lean phase fluidization with pneumatic transport Kunii and Levenspiel (1991a) . The main advantages of fluidized bed are :

— Particle homogeneity in the catalytic bed
— Continuous process
— Short contact time
— Elevate mass and heat transfer
— Easy handling and transport of solids
— Excellent gas-solid contact
— Avoid formation of hot spots

Biomass and wastes fluidized bed gasification are relatively easy to scale-up and avoid some limitations of fixed bed reactors, such as the formation of hot spots Kurkela et al. (2004). The main drawbacks are the non-uniformity of the particles, which makes the fluidization more complex Cui and Grace (2007). Hydropyrolysis of biomass involves the reaction of the starting material with hydrogen at high temperature and pressure. The great advantage, compared to thermal pyrolysis, it the maximization of the process carbon efficiency. In fact, for catalytic fast pyrolysis in fluidized bed reactor, the product's yield is generally lower than

20 %, while the coke formation can exceed 40 % Carlson et al. (2011).

3.4.1 μ-fluidized bed

The concept of micro-fluidized bed reactor was introduced in 2005, and includes reactors with a diameter from millimeters to few centimeters Potic et al. (2005). The operability benefits of this system are the on-line pulse feeding of the reagents, the fast heating, the on-line monitoring of the gases exiting the reactor and the minimization of the intra-particle diffusion Yu et al. (2011, 2010). Furthermore, due to the small geometry, the system demonstrates various benefits ; the initial and the operational costs are drastically decreased, leading to easier and more accessible study of reactions that involves expensive reagents or catalysts. Those reactors are easier to control, making them suitable for a intensive hydrodynamic and kinetic studies Chen et al. (2017a); Li et al. (2018). A great advantage of the system is also the combination of low energy required to heat the system and the excellent heat transfer inside the catalytic bed, which increase the safety of the operation. The main disadvantage is the strong walls effect on the fluidization, which modify the hydrodynamic and can determine the formation of a slug when particles aggregate Liu et al. (2008). In the biomass pyrolysis, μ-fluidized bed reactors allows a deeper understanding of the reaction kinetics, compared to thermogravimetric analysis Guo et al. (2015). Furthermore, the design allows the fast release of the volatile compounds. Biomass gasification is largely investigated in micro-fluidized bed reactor. Gao et al. (2017) report the conversion at 700 °C to 1000 °C, demonstrating the strong dependency of the activation energies with the particle size of the bed.

3.4.2 Liquid injection in FBR

Feed injection is crucial in the fluidized bed process, and affects the contact between the feed and the solid and consequently the reaction rate. Industrially, liquid spray is largely developed for a variety of applications. In the petroleum sector, crude oil is injected to produce gasoline by FCC Patel et al. (2013). Compared to gas injection, liquid feed evaporates directly into the fluidized bed, reducing the external costs for heat exchangers, and minimize the hot-spots near the nozzle, due to the latent heat necessary for the evaporation Bruhns and Werther (2005). Furthermore, atomization benefits from a rapid and uniform distribution of the feed in the catalytic bed, reducing the formation of agglomerates, resulting in higher yields. Applications and conditions determine the injector structure. In a dual-fluid nozzle, generally the gas pushes and sprays the liquid feed. The zone of mixing of the two fluids differentiate the spray types : internal mixing and external mixing. In the first conformation, the liquid and the gas enter in contact directly into the injector. This system requires less

atomization gas and demonstrates a deeper interaction between the fluids. In the second conformation, the gas and the liquid are carried separately until the orifice, and the mixing occur only at the exit of the nozzle, due to the difference of pressure between them.

Droplets size affects the interaction between the solid catalyst and the liquid feed. Gas-to-liquid ratio, orifice diameter, and physical feed properties are the most affecting parameters that affects the atomization quality Juslin et al. (1995); Portoghese et al. (2010).

One of the simplest method to spray a liquid feed through a single orifice is increasing the pressure of the feed, producing a liquid jet at the exit of the nozzle. Outside the sparger, the liquid feed fragments, due to the drastic pressure variation and to the shear of the surrounding gas. Consequently, the fluid forms ligaments, which also break down into smaller droplets (Figure 3.6). Decreasing the drop size enhance the feed evaporation and improve the solid-liquid contact.

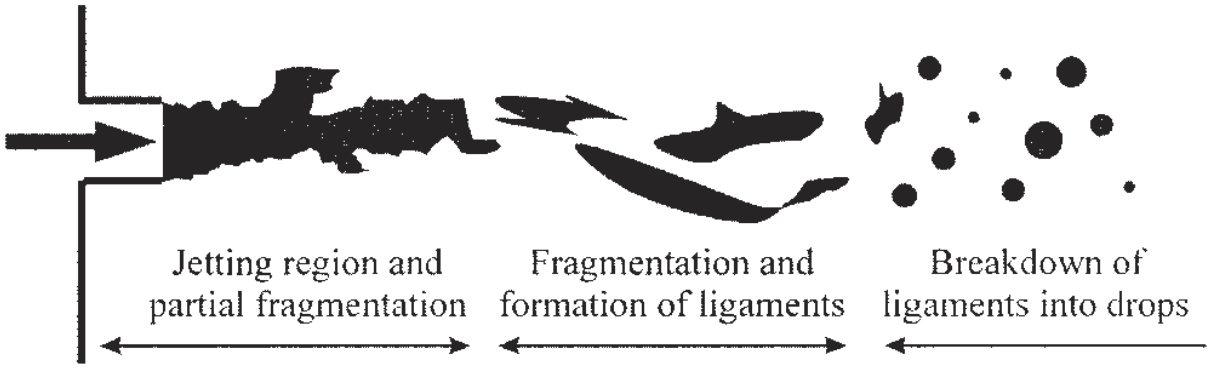

Figure 3.6 Fragmentation of the liquid leads to small droplets Bruhns and Werther (2005).

Modeling liquid injection into fluidized bed improves the understanding of the interaction between the catalytic bed and the feed, and help to develop new atomization system. Initially, Theologos and Markatos (1993) assumed that the liquid instantaneously evaporates at the orifice and the liquid feed was treated as a gas stream entering the bed. Successively, the model was developed, including the formation of continuous droplets that vaporize inside the gas phase and then interacts with the solid phase Gao et al. (2001).

Three zones defines the liquid spray Fan et al. (2010) :

— Spraying zone near the nozzle : the droplets wet the solid particles
— Drying zone : liquid instantaneously evaporates from the surface of wetted particles
— Heat-transfer zone : particles are heated up to begin the reaction

3.5 Levulinic acid to succinic acid

Levulinic acid (LEV) is one of the top 10 chemicals from carbohydrates Bozell and Petersen (2010). Industrially, LEV production is based on a continuous process of hydrolysis of carbohydrates with mineral acid at 210 °C to 230 °C and contact time of 13 s to 25 s Fitzpatrick (1997). To maximize the LEV production, the HMF produced from the hydrolysis of the C6 molecules is separated and further cleaved in another reactor. The yield exceeds the 60 % with hexoses as starting material Bozell et al. (2000).

In addition to the low production costs, the great advantages, compared to the hydrogenolysis or the oxidation of cellulose, are the process mild conditions and the absence of hydrogen or oxygen during the synthesis Pileidis and Titirici (2016). The huge potential of LEV is reflected in the variety of chemicals and fuels that can be synthesized from this bio-building block (Figure 3.7).

3.5.1 Levulinic acid valorization

Levulinic acid is a bio-based material, with extended applications in a large variety of fields. Methyltetrahydrofuran (MTHF) covers the majority of the levulinic acid market value, assessing for 10000 million lb per year to 100000 million lb per year Bozell et al. (2000). This bio-chemical is miscible with gasoline and acts like a fuel extenders. Upare et al. (2011) describes the direct hydrocyclization of LEV with Cu/SiO_2 at 265 °C and 25 bar of H_2, achieving a yield of 64 %. Esterification of levulinic acid produces bio-chemicals for the flavoring and fragrance industry, and also gasoline-additives. Industrially, the reaction occurs in the presence of alcohols and mineral acids, but this methodology is not environmental friendly. Solid acid catalysts, such as Amberlyst 70 Hu et al. (2013) and ZrO_2-SBA-15 Siva Sankar et al. (2016) replace the homogeneous catalysts and ensure less corrosion, easier recycling and increase the overall process safety.

Selective introduction of an amino group in position 5 forms Δ-aminolevulinic acid (DALA), a biodegradable herbicide. Condensation of levulinic acid with two molecules of phenol produces to diphenolic acid (DPA). With a similar spatial conformation to bisphenol A, it can replace this polymer to synthesize polycarbonates, epoxy resins and polyarylates Moore and Tannahill (2001). Homogeneous acids, such as HCl and H_2SO_4 are the most applied catalysts for this process. Recently, switching to mesoporous HPA, a solid particle, selectively produces DPA from LEV, and reduces the harmfulness of the reaction Guo et al. (2008).

Valeric acid is the levulinic acid hydrogenation product. EtOH and MeOH esterficate to produce ethyl valerate and methyl valerate, which present better fuel performances than the

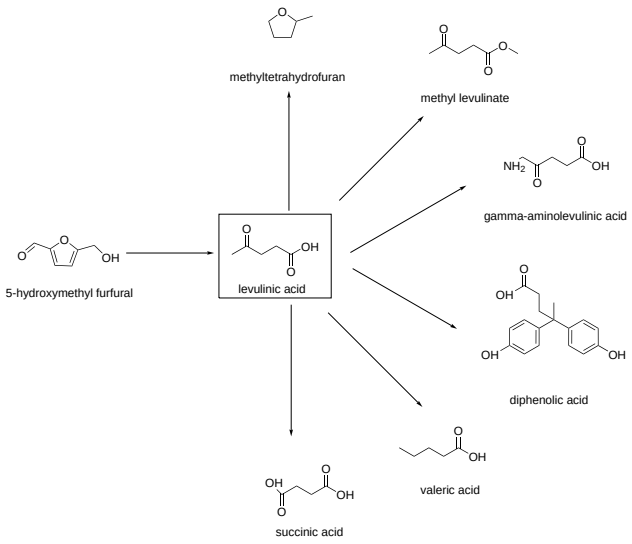

Figure 3.7 Hydrolysis of HMF leads to LEV, a potential bio-intermediate for a variety of bio-chemicals and bio-fuels.

current bio-fuels, such as ethanol, butanol and MTHF Lange et al. (2010).

Oxidation of levulinic acid produces succinic acid (SUCC), a precursor for polyesters.

Succinic acid

Succinic acid (SUCC) is a C4 diacid and one of the top 10 value added chemicals from biomass Bozell and Petersen (2010), with a market value of 400 billion USD per year Zeikus et al. (1999). Biologically, it is an intermediate in the Citric acid cycle and the anaerobic metabolism product. Industrially, *n*-butane is converted to maleic anhydride, which hydrogenates to succinic anhydride Li et al. (2011). With a conversion of around 15000 tons per year of C4 fraction, the price of succinic acid is around 6 \$ kg^{-1} to 9 \$ kg^{-1} Bechthold et al. (2008). Reverdia, a Royal DSM and Roquette joint venture, aims to produce bio-succinic acid. With a large-scale plant in Italy, it is the first commercial facility to produce 10000 tons per year with yeast.

Microorganisms, like fungi, yeast and bacteria, ferment cellulose and sugars to SUCC. The main drawback of the natural conversion are the higher concentration of organisms required, and the low selectivity of the reaction, which produces large amount of by-products. Mutated *Escherichia coli* aerobically converted glucose to succinic acid, achieving a maximum production of $58.3\,g\,L^{-1}$ after 59 h, but obtained as by-products pyruvic acid and acetic acid Lin et al. (2005).

The chemical valorization of succinic acid is classified in four main products categories : the

acyclic O-containing, the acyclic O,N-containing, the cyclic O-containing and the cyclic O,N-containing Bechthold et al. (2008). The first category includes the formation of 1,4-butanediol (BDO) and esters of succinic acid. Ru-Sn/AC reduced SUCC with a yield of 71 % in a trickle tubular bed, maintaining the activity for 96 h on stream Vardon et al. (2017). One example of cyclic O,N-containing group chemical is N-methyl-2-pyrrolidone (NMP), a petrochemical process solvent to recover 1,3-butandiene and acetylene.

Oxidation to succinic acid

Oxidation to succinic acid is an attractive route to upgrade levulinc acid. The first conversion included V_2O_5 as catalyst and temperatures in the range of 300 °C to 400 °C Dunlop and Shelbert (1952). Addition of HNO_3 decreased the temperature to 40 °C to 60 °C and the reaction time to 1 h to 4 h Van Der Klis et al. (2012). These methodologies achieve high yields, but strong acids combined with long contact time increase the system corrosion, and require high levels of safety. Shifting to more environmental technique will make the LEV conversion more accessible and less dangerous.

Acidic and metal-based catalysts successfully oxidized levulinic acid to succinic acid in both aqueous and organic solvents. Functionalized ruthenium nano particles posses both acidic and redox properties. A silica protection is coated with magnetite, and successively functionalized with aminopropyl groups. The particle is finally stabilized with ruthenium cations. The nano particles produced succinic acid in aqueous solution with a yield of 78 %, at 150 °C after 6 h. The oxidation agent was molecular oxygen, added until the reactor reached the pressure of 5 bar to 14 bar Podolean et al. (2013).

Kawasumi et al. (2017) developed a methodology based on I_2 and *t*-BuOK in *t*BuOH. The reaction evolves through the formation of *t*-BuOI, that chemoselectively demethylate the LEV to SUCC. The conversion demonstrated a selectivity of 87 % after 1 h at 25 °C. Molecular oxygen bubbled in the reaction media or pressurized into the reactor is the oxidizing agent.

The Baeyer-Villiger mechanism involves the nucleophilic addition of a hydroperoxide anion to the carbonyl carbon Rozhko et al. (2015). Hydrogen peroxide is a green oxidant, which decomposes to atomic oxygen and water. H_2O_2 oxidation catalysts involves Al_2O_3, H_2WO_4, titanium silicalite-1 and selenium. H_2O_2 and Amberlyst-15 converted furfural to succinic acid after 24 h with a yield of 74 %. H_2O_2 oxidize humic acids and lignite to malonic and succinic acid. After 4 h the succinic acid selectivity achieved a maximum of 62.2 %, and continued dropped to 7.4 % after 16 h reaction. The optimal conditions were 40 °C with 50 mL of 3 % weight of H_2O_2 Doskočil et al. (2014). Only few publications describes the oxidation of levulinic acid and levulinate to succinic acid and succinate. Wu et al. (2015) reported the

conversion of levulinic acid with H_2O_2, determining the influence of basic and acid catalysts on the reaction pathway ; the first one mainly produces 3-hydroxypropionic acid (3-HPA) — a precursor of acrylic acid—, while H_2SO_4 shows a maximum selectivity of 48 % to succinic acid. Increasing the catalyst acidity improved the SUCC production ; in fact, trifluoroacetic acid increased the selectivity up to 62 % at 90 °C after 2 h Dutta et al. (2015).

CHAPTER 4 ARTICLE 1 - GAS-PHASE FRUCTOSE CONVERSION TO FURFURAL IN MICRO-FLUIDIZED BED REACTOR

Davide Carnevali, Olivier Guévremont, Marco G. Rigamonti, Marta Stucchi, Fabrizio Cavani, and Gregory S. Patience

Article published in ACS Sustainable Chemistry & Engineering (I.F. 6.0)

4.1 Abstract

Specialty chemicals from sugars are destined to displace fermentation to alcohols due to their superior economic value and atom efficiency. Compared to bio-ethanol, retention of oxygen functional groups increase by 2 to 5 times the market value of specialty chemicals like furfural, 2,5-furan dicarboxylic acid, 2,5-dimethyl furan and γ-valerolactone. For the first time, we report a gas-phase process that converts C-6 monosaccharides to furfural in a micro-fluidized bed reactor. A spray nozzle inserted directly into the catalytic bed atomizes a fructose-water solution to micron-sized droplets ; water evaporates and WO_3/TiO_2 converts fructose to furfural. Furfural yield reached 22 % after 3 h time-on-stream with 15 % diformyl furan as co-product. Acetic acid yield was mostly below 10 % but was as high as 27 %. During the initial tests, coke and catalyst agglomerates blocked the sparger tip and run time varied between 1 h to 3 h. Insulating the nozzle leading into the bed reduced the injector wall temperature and improved reactor operability ; the 15 mm ID reactor ran continuously for 19 h after this modification.

Keywords

sugar, micro-reactor, fluidized bed, furfural, gas-phase, tungsten, atomization, diformyl furan

4.2 Introduction

Bio refineries require a diverse portfolio including speciality chemicals and monomers to achieve economic sustainability. The commercial value of bio building blocks is higher compared to biofuels Liu and Wu (2016) and has a market price ranging from 1 USD to 4 USD per kg ; a market study reported seventeen building blocks with an estimated total production capacity of 2.4 million tons in 2016, expected to reach 3.5 million tons in 2021, and

with a compound annual growth rate of 8 %.de Guzman (2017) In comparison, ethanol costs 0.5 USD per kg. NASDAQ (2017) Sugars, lignocellulosic feedstock, are mainly fermented to ethanol and this lignocellulosic-based alcohol accounts for approximately 97 % of the total ethanol produced in the United States.Shapouri and Salassi (2006) Considering that the average price of sugars in the US market is 0.3 USD per kg, profit on ethanol production is mediocre. US Department of Agiculture (2016) Lignocellulosic feedstock —cellulose and hemicellulose Vassilev et al. (2012) — is a valid starting material to produce high-value added molecules. Chemical processes Caratzoulas et al. (2014); Fanselow et al. (2007) ($T < 200\,°C$) lead mainly to C-6 and C-5 carbohydrates, while thermal processes ($T > 400\,°C$) produce C-1 to C-3 molecules ;Sun and Cheng (2002) Bozell and Petersen (2010) listed 14 bio platform chemicals from biorefinery carbohydrates that are potential candidates to replace petroleum feedstocks. Fructose is the second most abundant sugar on Earth ; it consists of 6 carbon atoms and six oxygen functional groups, thus it is more suitable than fossil fuels to produce oxidized green platform chemicals, such as 5-hydroxymethylfurfural Wang et al. (2016); Fachri et al. (2015); Leshkov et al. (2006); Antonetti et al. (2017), glucaric acid Derrien et al. (2017), 2,5-furandicarboxylic acid (FDCA) Zuo et al. (2016); Pasini et al. (2011), adipic acid Vardon et al. (2015) and 2,5-dimethyl furan Gawade et al. (2016). Furfural (FUR) is a precursor for furfuryl alcohol Sitthisa and Resasco (2011); Li et al. (2016b), furoic acid Verdeguer et al. (1994), methylfuran Zheng et al. (2006), tetrahydrofuran (THF) Ding et al. (2011) and γ-valerolactone Bui et al. (2013) and the market will double from 700 million USD in 2015 to 1.4 billion USD by 2022. Allied Market Research Report (2017) Its applications include selective extraction solvents Mariscal et al. (2016), agents for vulcanization Kuipers (1966), precursors for resins and plastics Pan et al. (2013), and flavouring agents. Yaghmur et al. (2002) The main reaction pathway contemplates the conversion of C-5 carbohydrates from hemicellulose to furfural by aqueous acid catalysts. Dutta et al. (2012) However, industrial yields are low and range between 44 % to 55 % ; furthermore, process issues include corrosion due to acids, high costs for heating during the product recovery, and difficult catalyst recover ; Peleteiro et al. (2016) moreover, secondary reactions produce formaldehyde, formic acid, acetaldehyde and humins. Karinen et al. (2011) Heterogeneous biphasic/triphasic reactors, ionic liquids or fluidized bed fast pyrolysis convert pentosan or xylose to furfural : Amberlyst 70 as solid catalyst converted furfural from xylose in an autoclave reactor at 160 °C, with 20 different solvents ; Hu et al. (2014) dimethyl sulfoxide gave a selectivity of 80 % to furfural after 60 min. H-mordenite reached 82 % selectivity from xylose to furfural, operating in γ-valero lactone (GVL) at 175 °C. Gürbüz et al. (2013) Niobium catalyst oxidized xylose to 5-hydroxymethyl furfural (HMF) and furfural with 90 % yield. Molina et al. (2015) Compared with the same mild conditions, ionic liquids exhibit higher selectivity ; for example, Tao et al.

(2011) converted 95 % of xylose with a selectivity of 91 % after 23 min working at 150 °C. These latter processes start from C-5 sugars derived from hemicellulose ; however, even C-6 sugars from cellulose are furfural precursors. The main advantages are its attractive price and abundance. In a continuous flow reactor, glucose reacts with water at 400 °C and 80 MPa to produce furfural ; maximum yield was 12 % at a residence time of 0.8 s. Aida et al. (2007) More recently, Sn-β zeolite converted glucose to furfural in GVL at 180 °C, yield approached 70 % after 33 min in a batch reactor. Zhang et al. (2017) Fast pyrolysis of biomass is another route to synthesize furfural. Chen et al. (2017b) Vanadyl pyrophosphate dehydrates xylose to furfural in the liquid phase, Sádaba et al. (2011) while in a fluidized bed reactor operating in the gas phase mainly produces maleic anhydride and acrylic acid. Ghaznavi et al. (2014) Fluidized bed reactors are more appropriate than fixed bed reactors Oh et al. (2013) due to higher heat and mass transfer rates and shorter contact times (<1 s). Dalil et al. (2015) reported the dehydration of glycerol to acrolein, while Keggin type catalyst oxidized 2-methyl-1,3-propanediol to methacrylic acid, spraying the reactants directly in the catalytic bed.Darabi Mahboub et al. (2016); Mahboub et al. (2018) As a first catalyst, we chose WO_3/TiO_2 because of its efficacy to dehydrate glycerol to acrolein operating under similar conditions.

Here, for the first time we report that fructose reacts to furfural and diformyl furan in the gas phase in a continuous micro fluidized bed reactor, with tungsten oxide over TiO_2 as catalyst. A nozzle atomizes the C-6 sugar solution in the catalytic bed ; thus, the physical conversion from liquid to gaseous feed is faster than the chemical caramelization of sugar, which blocks the nozzle and agglomerates the catalyst. Temperature ranged from 150 °C to 200 °C, WO_3 loading ranged from 0 % to 20 % and O_2/fructose ratio varied from 20 :1 to 40 :1. This revolutionary system indicates a new pathway for the conversion of fructose to furfural.

4.3 Experimental section

4.3.1 Materials

All the reagents are analytical grade without further purification. We acquired fructose (>99 %) from Alfa Aesar and acetone (>99 %), furfural (>99 %), acetic acid (99.7 %), 4-cyclopentene-1,3-dione (95 %), 5 - hydroxymethyl furfural (>99.7 %), 5-methyl furfural (99 %) and 2,5-furandicarboxaldehyde (97 %) from Sigma Aldrich. Air Liquide Canada supplied the gases : argon (> 99.7 %), 10.0 % O_2 balance Ar, and a mixture of CO (1.04 %), CO_2 (1.01 %), CH_4 (1.03 %) balance Ar. We purchased phosphotungstic acid ($H_3PW_{12}O_{40}$, 81 % of WO_3)

from Nippon Inorganic Colour & Chemical Co., LTD. Huntsman Corporation supplied the titanium dioxide (Hombikat 110100) and we sieved the powder to achieve particles from 90 µm to 150 µm in diameter.

4.3.2 Catalyst preparation

We prepared four catalysts with a mass fraction of 3 %, 5 %, 10 % and 20 % WO_3 by incipient wetness impregnation. We placed 50 g samples of dried support in a round-neck flask and drop wise added a 22 mL tungsten solution. A rotovapor operating at 300 mbar and 250 rpm mixed the catalyst thoroughly. After 3 h, the temperature ramped to 80 °C to remove the solvent. A furnace calcined the catalyst with a ramp of 2.5 °C min^{-1} up to 550 °C and thereafter held it for 3 h.

4.3.3 Catalytic tests and analytical methods

All experiments were conducted in a 15 mm ID quartz micro fluidized bed housed in a three-zone vertical furnace 450 mm tall. A quartz frit with a pore diameter from 150 µm to 200 µm distributed the gas feed homogeneously. Two mass flow controllers metered gas to the bottom of the reactor : Ar and O_2/Ar for fluidization. A HPLC pump metered the sugar solution to a 1.6 mm stainless steel tube (sparger). A third mass flow controller introduced Ar to this stream to atomize the solution entering the fluidized bed. The gas-to-liquid ratio influenced the homogeneity and the quality of the droplet size and spray quality Ghaznavi et al. (2014) : in these tests, 50 mL min^{-1} of argon atomized 0.05 mL min^{-1} of a mass fraction of 2 % sugar in water solution (Figure 4.2). The pressure in the sparger was stable at 35 kPa. The hot catalyst vaporizes the solution and reacts with the resulting aerosol. Catalyst and coke agglomerated and blocked the sparger in the early experiments ; the longest run time lasted up to 3 h. To achieve continuous operation, we insulated the nozzle leading to the bed, which reduced the injector wall temperature and so the reactor ran uninterrupted for 19 h.

A detector connected to the top and the bottom of the reactor monitored the total pressure and the ΔP. A heated coil maintained the exit line temperature above 110 °C to avoid product and solvent condensation in the exhaust line. An ice-quench trapped the products. Four thermocouples recorded temperature in the system : 5 mm below the distributor, 15 mm above the sparger tip (25 mm above the distributor in the catalytic bed), 20 mm above the catalytic bed (in the freeboard), and 160 mm above the distributor, at the exit line. The tests temperature related to the catalytic bed thermocouple. The presence of the other thermocouples measured the temperature profile in the reactor from the bed to the quench. A GC-MS with a thermal conductivity detector analysed the liquid sample composition withdrawn from the

quench periodically. An on-line mass spectrometer (MS), operating in the SCAN mode with a multiple ion detection (MID), monitored the non-condensable gas concentration. We derived response factors for each compound before an experiment with calibration gases from Air Liquide. After each experiment, air regenerated the catalyst at 400 °C. The MS monitored CO, CO_2, and O_2 in real time.Ghaznavi et al. (2014)

An online mass spectrometer (Pfeiffer Vacuum Thermostar^{TM} GSD 301 T) monitored the non-condensable gases—H_2, CH_4, CO, CO_2, O_2 and Ar at a frequency of 3 Hz—during the reaction and the regeneration of the catalyst. A GC-MS (Agilent 7890A with DB-Wax 30 m x 0.250 mm column, connected to a 5975C VL MSD with Triple-Axis Detector) analysed the liquid samples collected from the quench. The auto-sampler injected 0.5 µL of the products. The oven holds the temperature at 40 °C for 6 min, then reaches 200 °C with a ramp of 3.5 °C min^{-1} and after 250 °C with a ramp of 8 °C min^{-1}, holding it for 10 min.

The product selectivities (Eq. 4.1) is :

$$S_{prod} = \frac{n_{\text{prod}}^{\text{out}}}{n_{\text{fru}}^{\text{in}} - n_{\text{fru}}^{\text{out}}} \cdot \frac{\vartheta_{\text{prod}}}{\vartheta_{\text{fru}}} \cdot 100 \tag{4.1}$$

where $n_{\text{fru}}^{\text{in}}$ and $n_{\text{fru}}^{\text{out}}$ are the moles of fructose entering and coming out from the system, $n_{\text{prod}}^{\text{out}}$ the moles of product coming out. ϑ_{fru} and ϑ_{prod} are the number of carbon atoms of fructose and products.

Particle size distribution and minimum fluidization velocity

The Geldart powder classification assigns particles according to diameter and solid and fluid density difference : Type A powders are aeratable and typical for catalytic fluidization. Type B powders are generally larger in diameters and denser and are used in combustion type applications. Industrial catalysts are 70 µm in diameter and have 40 % between 20 µm to 40 µm. The TiO_2 powder behaves like a Type A powder. The larger particles minimize wall effects although contact between reagents and catalyst may suffer. The bulk density was 770 kg m^{-3} and the minimum fluidization velocity (U_{mf}) was 8 mm s^{-1} (Figure 4.3) : U_{mf} of commercial catalysts are closer to 2 mm s^{-1}. The reactor operated at 22.3 mm s^{-1} at 200 °C. The contact time of the feed with the catalytic bed was 0.3 s to 0.4 s. At these conditions, gas was well distributed and bubbles did not appear to channel through the bed. The flow regime deviates more from ideal plug flow with increasing gas velocity in the bubbling flow regime in which larger bubbles form.(Lorences et al., 2006)

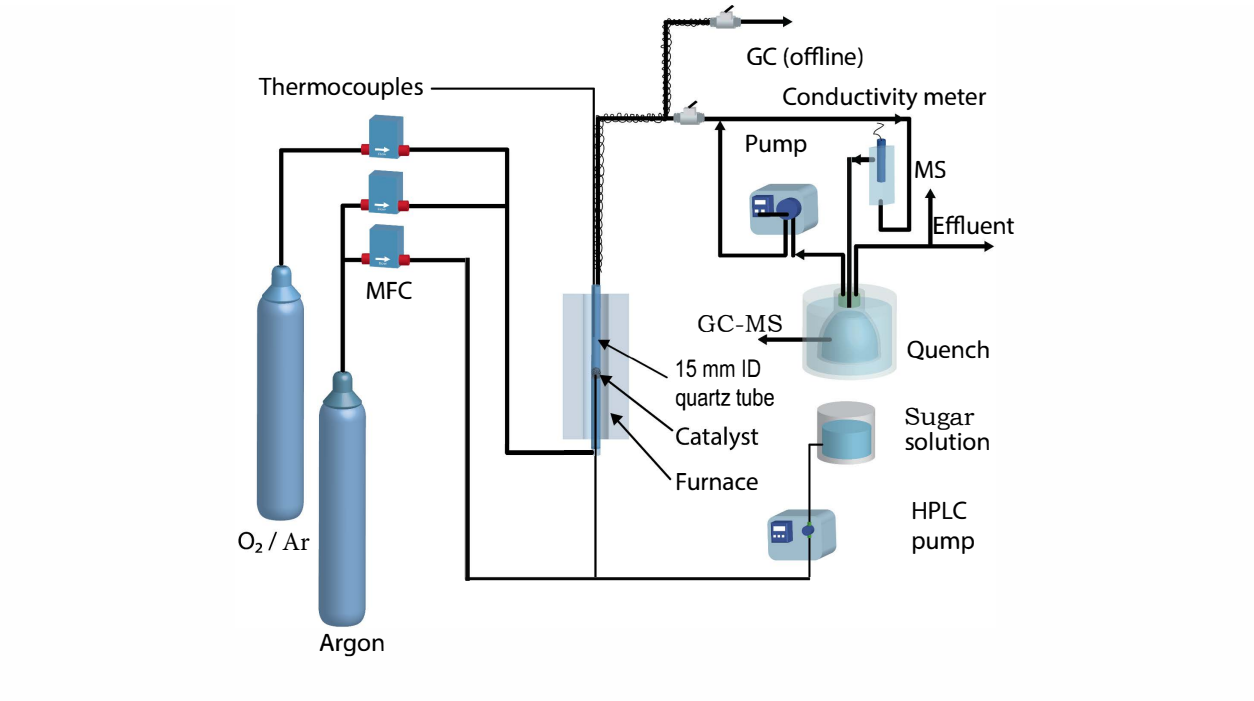

Figure 4.1 Micro-fluidized bed reactor : a furnace maintains the temperature constant in the 15 mm ID reactor. MS, GC and a conductivity meter monitor the products in the quench trap.

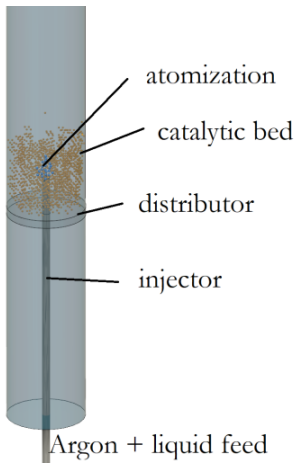

Figure 4.2 A jet nozzle atomizes 0.05 mL min^{-1} of sugar feed with 50 mL min^{-1} of argon in 5 g catalytic bed. A distributor prevents the catalyst from falling down and disperses the gases uniformly.

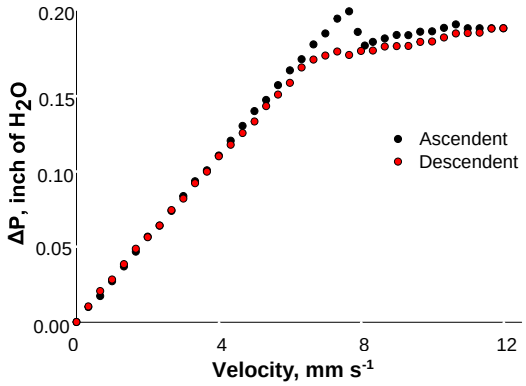

Figure 4.3 $8\,\mathrm{mm\,s^{-1}}$ is the minimum fluidization velocity at room temperature of the WO_3/TiO_2 catalyst in the micro fluidized bed reactor with a internal diameter of 15 mm and argon as fluidization gas.

4.3.4 Analytical instrumentation

A laser diffractometer (Horiba, LA-950) measured the particle size distribution (PSD) based on the Mie Theory, and we report the d_{10}, d_{50}, d_{90} and the volume moment mean diameter $D_{4,3}$:

$$D_{4,3} = \frac{\sum d_i^4 \cdot N_i}{\sum d_i^3 \cdot N_i} \tag{4.2}$$

where N_i is the number of particles with the corresponding diameter d_i. The particle refractive index was 2.75 + 0.00i (R and Chi parameter below 0.05).

A N_2 physisorption instrument (Quantachrome Autosorb-1) recorded at 77 K the adsorption and desorption isotherms, after degassing the sample under vacuum at 300 °C for 6 h.Orr and Dallavalle (1959) The Brunauer-Emmett-Teller (BET) theory regress the specific surface area at P/P_0 0.05-0.30 (C constant 100–200). The Barrett-Joyner-Hallender (BJH) theory estimates the mesopore size distribution over the desorption branch (P/P_0 0.15-0.995). The total pore volume is evaluated at the maximum filling pressure (P/P_0 0.995), considering all pores with a diameter smaller than 300 nm.

A Philips X'pert diffractometer scanned the catalyst samples with a Cu-Kα radiation source (1.542 Å at 50 kV and 40 mA) over 2 θ (20° to 70°) to identify the crystalline structure of the support and the metal phase.

A field emission scanning electron microscope (FE-SEM) (Jeol JSM-7600TFE) characterized the morphology of the fresh and used catalysts. An EDX detector determined the elemental distribution on the surface.

A CHN analyzer (LECO CS744) measured carbon build up on the catalyst surface after each experiment. It operated above 1000 °C in an oxidizing atmosphere. The internal balance, connected with the sample crucible, measured weight loss. The O_2 of the furnace environment, in addiction to the high temperature, converts the coke to CO and CO_2.

4.4 Results and discussion

Micro fluidized bed reactors have distinct advantages compared to fixed bed reactors to measure kinetics and develop processes relying on vaporizing liquids. Kaarsholm et al. (2007); Darabi Mahboub et al. (2016) Heat transfer rates are an order of magnitude higher, which ensures the reactor operates isothermally, minimize hot spots, but more importantly heat the aerosol from the sparger rapidly. Furthermore, solids mixing minimizes radial concentration gradients.

4.4.1 Catalyst characterization

Most of the particles (80 %) lie from 90 µm to 170 µm, thus the metal loading has mild effect on the size distribution (Figure 4.4). The shape of the curves are asymmetrical ; particle agglomeration in the PSD media can lead to higher scattering angles, with a consequently elongated tail.

4.4.2 Nitrogen physisorption

The support (TiO_2) dictated the specific surface area, pore size distribution and pore volume of all analysed samples. TiO_2 support and used catalyst possessed a type IV isotherm with a

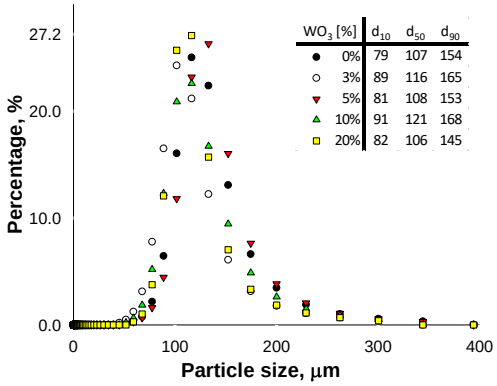

Figure 4.4 Particle size distribution is independent of metal loading, $d_{50} = 110\,\mu m$.

type 2 hysteresis loop (Fig.4.5), indicating a mesoporous structure with a narrow distribution of pore necks, inducing pore-blocking.Sing et al. (1985)

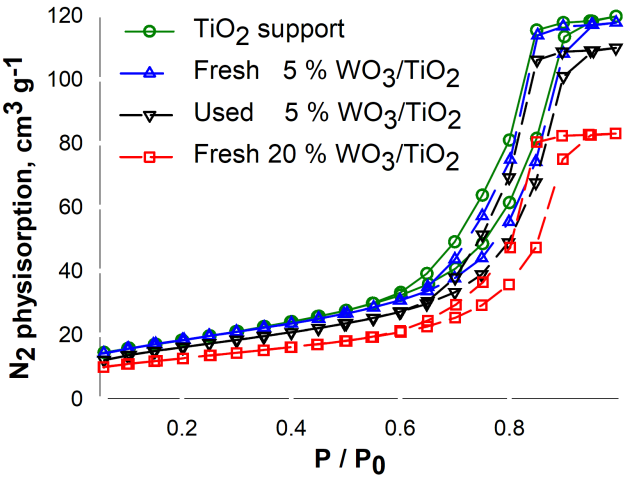

Figure 4.5 Adsorption-desorption isotherms : higher loading of catalyst on the support and coke deposition after reaction occluded the pores and decreased the amount of N_2 physisorbed, but the isotherm and hysteresis shape remained unaltered.

Indeed, Barrett-Joyner-Halenda (BJH) reported a well-defined surface and volume variation between 4 nm to 20 nm diameter (d_{98}). The BJH dV pore volume distribution shifted to bigger pore diameters with the WO_3 loading, as more catalyst filled selectively pores smaller than 10 nm (Fig. 4.6).

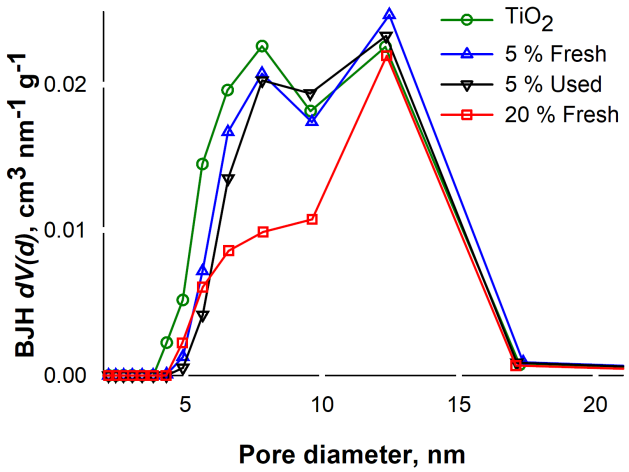

Figure 4.6 The pore fraction below 10 nm is filled as the WO_3 loading and coke formation increases.

Table 4.1 BET surface area by nitrogen physisorption, ϕ pore volume, Δ BJH $dV(d)$ mesopore median, Coke carbon content (0.05 % precision, 95 % variance). The relative standard deviation of the instrument is 1.5 % ($n = 3$).

	BET $m^2\,g^{-1}$	ϕ $cm^3\,g^{-1}$	Δ nm	*Coke* %
TiO_2	65	0.185	8.8	n/a
3 %	63	0.183	9.6	n/a
5 %	65	0.182	9.5	n/a
10 %	58	0.160	9.6	n/a
20 %	44	0.128	10.3	n/a
Used 3 %	57	0.154	9.0	1.60
Used 5 %	57	0.170	9.6	0.72
Used 10 %	57	0.158	9.7	0.43
Used 20 %	44	0.127	10.0	0.18

The pore volume (PV, $cm^3\,g^{-1}$) linearly decreased with the loading, as more catalyst (mass fraction, ω_{cat}, g/g WO_3 :total) occupied the internal pores of the bare support and when coke (ω_C, g/g coke :total) layered on the surface as the reaction progresses. Assuming a linear correlation (Eq. 4.3, $R^2 = 0.97$), the data regressed when $\rho_{\text{cat}} = 3300\,\text{kg}\,\text{m}^{-3}$ and $\rho_{\text{C}} = 700\,\text{kg}\,\text{m}^{-3}$, which referred to the WO_3 and coke apparent densities (Figure 4.7). This indicated a non-homogeneous surface coverage as the catalyst and the coke block the pores below 10 nm, decreasing the true density of the materials (true density $\rho_{WO_3} = 7100\,\text{kg}\,\text{m}^{-3}$, $\rho_{\text{coke}} = 1800\,\text{kg}\,\text{m}^{-3}$ to $2100\,\text{kg}\,\text{m}^{-3}$).

$$PV_{(\omega_{\text{cat}},\omega_C)} = PV_{TiO_2} - \frac{\omega_{\text{cat}}}{\rho_{\text{cat}}} - \frac{\omega_C}{\rho_{\text{C}}} \tag{4.3}$$

Similarly, the specific surface area (S_A, $m^2\,g^{-1}$) proportionally decreased with respect to the correlated pore volume ($PV_{(\omega_{\text{cat}},\omega_C)}$, $cm^3\,g^{-1}$). Assuming a linear correlation (Eq. 4.4), the data regressed with a $R^2 = 0.93$ (Figure 4.7) when basing the equation on the specific surface area and pore volume of the bare support, $\frac{S_{A,TiO_2}}{PV_{TiO_2}} = 350\,\text{m}^2\,\text{cm}^{-3}$ (Table 4.1).Rigamonti et al. (2018)

$$S_{A,(\omega_{\text{cat}},\omega_C)} = \frac{S_{A,TiO_2}}{PV_{TiO_2}} \cdot \left(PV_{TiO_2} - \frac{\omega_{\text{cat}}}{\rho_{\text{cat}}} - \frac{\omega_C}{\rho_{\text{C}}} \right) \tag{4.4}$$

XRD

The X-ray diffraction patterns of the fresh support and the four loadings of tungsten oxide (Figure 4.8) show spacing planes (101), (004), (200), (211) and (204). These patterns are

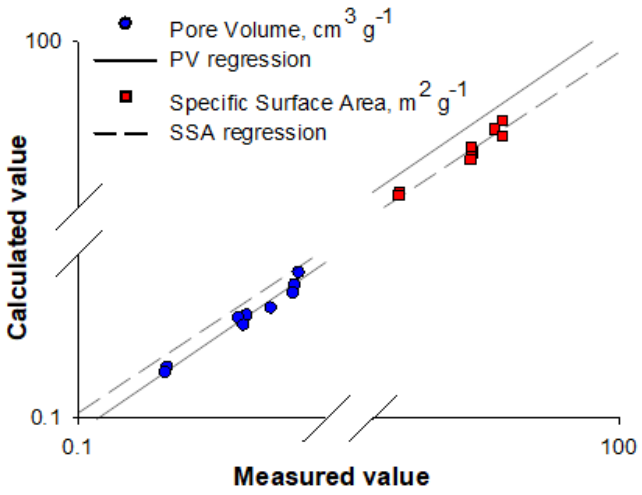

Figure 4.7 Pore volume and specific surface area model fitting.

characteristic of the anatase phase of titania that form after calcination at high temperature (550 °C).Hanaor and Sorrell (2011) The high temperature calcination step decomposes the phosphotungstic acid leaving only the metal oxide on the surface. Two characteristic peaks at 23.5° and 33.3°, highlighted by *, appear with increasing mass fraction of the WO_3 phase. The X-diffraction pattern identifies as orthorhombic (JCPDS 20-1324) the crystalline structure of tungsten oxide intermediate between monoclinic and orthorhombic above 400 °C. Ramana et al. (2006) These WO_3 peaks are too weak at 3 % and 5 %.

4.4.3 FE-SEM and EDX

The SEM images demonstrate that the particles are essentially spherical ($\phi = 1$); however, some particles have agglomerated (Figure 4.9). The shape conservation and the attrition resistance are two fundamental parameters to maintain the stability and the efficiency of the catalyst in a fluidized bed reactor. EDX analysis confirms the tungsten is well dispersed on the support surface (Figure 4.10a).

Coke built up on high acid spots of the catalyst. In fact, tungsten oxide shows both strong Lewis and Brønsted acid sites, which strongly affects the degradation of the feed on the surface. Dalil et al. (2016)

4.4.4 Conversion of fructose to furfural

Two blank tests at 150 °C and 20 :1 O_2/fructose molar ratio verified that the support is inert (Table 4.2). Conversion was complete as the TCD signal of the GC at the fructose retention

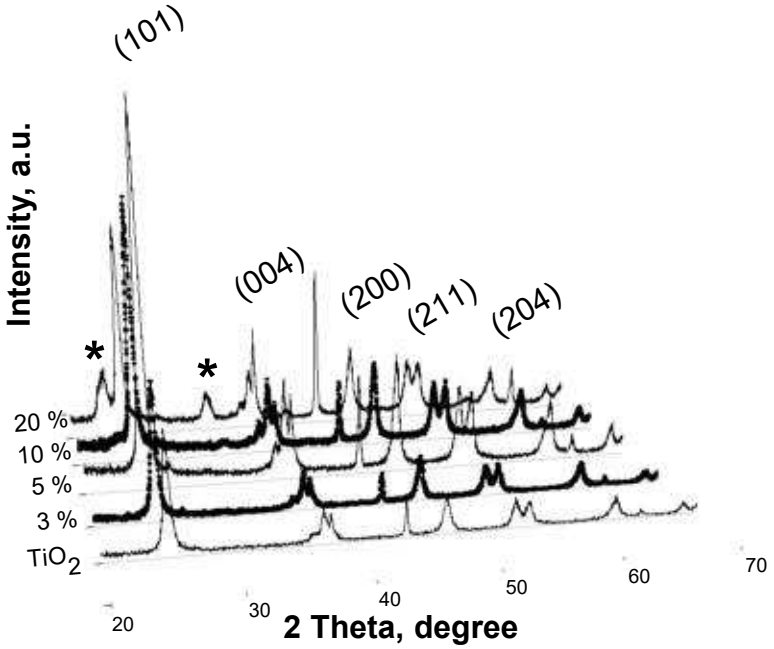

Figure 4.8 XRD patterns of fresh support and the 3 %, 5 %, 10 % and 20 % tungsten oxide loading. The peaks in brackets show the anatase form of TiO_2, while the * indicates the WO_3 crystalline phase.

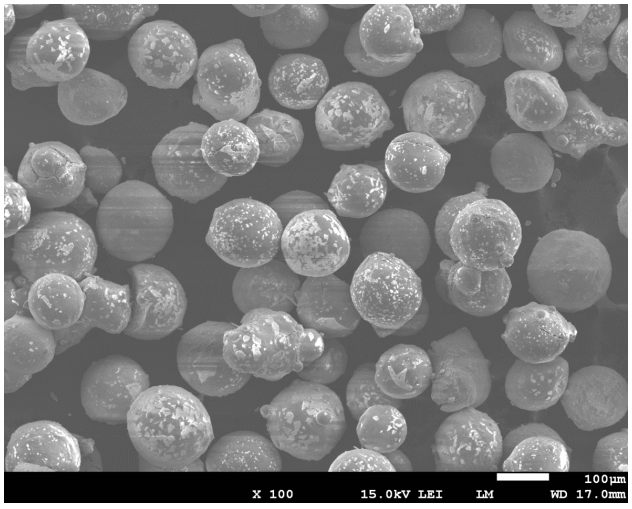

Figure 4.9 SEM of particles of 20 % tungsten oxide over titania.

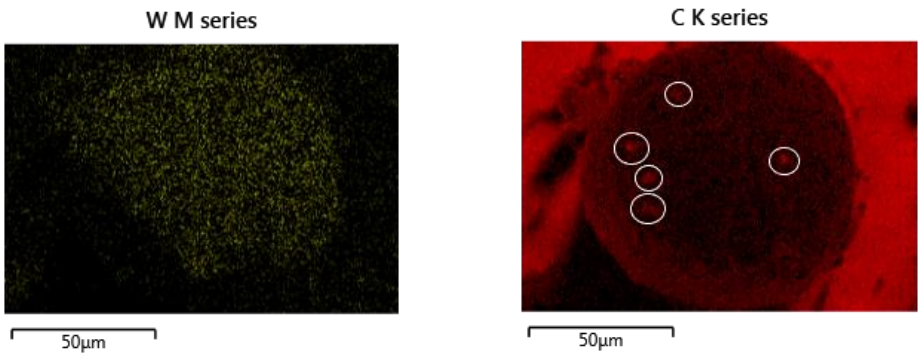

(a) Tungsten (b) Carbon

Figure 4.10 Tungsten is homogeneously dispersed on the surface. Carbon built up on all the surface of the catalyst, and aggregates to micro particles.

time was in the range of the noise. TiO_2 in oxidizing environments and high temperatures combusts fructose : CO selectivity was 59 %, while for CO_2 it was 14 % (balance coke) at 150 °C and a 20 :1 oxygen :fructose ratio. Coke that formed on the surface agglomerated the particles. Increasing the loading of tungsten oxide reduced the coke formation (Table 4.1).

The experimental plan considered 4 levels of metal oxide loading, 2 levels of O_2/fructose ratio at 2 temperatures. The main compounds detected were furfural, acetic acid, diformylfuran (DFF), CO, CO_2, and traces of formic acid, oxalic acid, 1,3-cyclopentendione and 5-methylfurfural. We calibrated the instrument for furan but its concentration was below the detection limit.

Furfural selectivity reached a maximum of 22 % at 200 °C, 5 % WO_3, and a ratio of 20 :1 oxygen to fructose. At this condition, the catalyst also produced 15 % diformylfuran (DFF), which translates to an overall C_5^+ selectivity of 37 % (Table 4.2). Presumably, the high temperature accelerated the desorption of the selective product. However, high WO_3 combined with high temperature reduce selectivity to furfural and DFF (experiment # 9, for example). Higher contact time and low desorption of the furfural and fructose on the catalytic surface lead to degradation of the molecules to acetic acid, COx or coke. Alternatively, at low temperature, the driving force to evaporate water/solvent was lower, which agglomerated the catalyst but also increased the contact time of the fructose with the active phase. The droplet wetted the surface at the sparger tip and the catalyst particle dried and reacted as it rejoins the bulk of the catalyst in the bed. Bruhns and Werther (2005) Selectivity to furfural dropped to 5 % with the higher catalyst loading (10 % and a 40 :1 O_2/fructose ratio). It further decreased at the 20 % loading. We detected DFF only at low catalyst loading (<10 %). The mass balance closed to within 80 % and it reached 90 % for many experiments

and includes the coke build-up during the reaction (measured by CHN analysis at the end of the 3 h experiment).

As a general trend, based on a non-linear regression analysis, acetic acid selectivity increases with temperature and oxygen/fructose ratio, and decreases with WO_3 loading. The highest selectivity was 27 % and at this condition, we also detected 3 % furfural (but not DFF). The catalyst produced acetic acid in many experiments, but the yields were predominantly below 10 % (Table 4.2).

At low temperature and low oxygen, the GC-MS analysis of the liquid quench showed traces of formic acid. Increasing temperature and oxygen content increased CO and CO_2 concentrations.

Excess oxygen minimized catalyst deactivation due to coke. Catalyst agglomerated and fructose formed carbonaceous structures on the sparger tip under anaerobic conditions and at an oxygen to fructose molar ratio of 7 and at 200 °C. At these conditions, conversion was complete and the on-line MS only detected CO and CO_2. Increasing oxygen content and temperature didn't affect the selectivity to furfural, but increased the carbon deposition (Table 4.1).

The CHN analyzer showed a carbon mass fraction of 0.04 % ±0.01 % after 3 h on stream. An additional 3 h on stream increased the coking rate by an order of magnitude (0.39 %). The standard deviation of the selectivity was ±4 % based on repeat runs of most experiments. The experimental error was due to condensation/degradation of products on the exit line, analytical uncertainty, coke, and degradation on the hot reactor walls.

4.4.5 Mechanism and steady state

Fructose conversion to furfural may follow various pathways, while the conversion of fructose to 2,5-diformyl furan has an unique mechanism. Paine et al. (2008) analyzed the glucose and fructose mechanism to furans by pyrolysis at 1000 °C with isotopic labelling. They proposed a mechanism involving four steps (Figure 4.11). The first step is the cyclic Grob fragmentation where a molecule of formic acid and water are lost. The C-5 compound forms a furan type ring and dehydrates further in the second step. The third step involves a keto-enolic equilibrium between the alcohol and aldehyde. The aldehyde dehydrates in the final step to furfural. The second mechanism is the triple dehydration to HMF, which can decarbonylate or oxidecarbonylate to lose a molecule of COx or formaldehyde. The latter rapidly converts to formic acid and consequently to COx. This transformation also requires a further oxidation of HMF to diformyl furan (Figure 4.12). Both these mechanisms explains the presence

Table 4.2 Selectivities to the main products and to CO_x after 180 min. Fructose conversion was always 100 %. Pure TiO_2 reacted all the fructose to CO, CO_2, and coke. Highest selectivity was at 5 % WO_3, 200 °C and 20 O_2/fructose ratio.

Exp #	T, °C	WO_3, %	O_2/fruct	S_{FF}, %	S_{AA}, %	S_{DFF}	S_{total}, %	S_{CO_x}, %
Blank	150	0	20	0	0	0	0	73
Blank	200	0	40	0	0	0	0	78
1	150	3	20	3	12	1	16	59
2	200	3	20	1	0	0	1	65
3	150	5	20	0	7	0	7	58
4	150	5	40	0	5	0	5	62
5	200	5	20	22	1	15	38	41
6	200	5	40	3	27	1	31	49
7	150	10	20	1	4	0	5	52
8	150	10	40	1	7	0	8	63
9	200	10	20	1	0	0	1	71
10	200	10	40	5	3	0	8	76
11	200	20	20	1	0	0	1	80
12	200	20	40	3	2	0	5	81
13	200	20	0	0	0	0	0	4
14	200	20	7	0	0	0	0	19

of furfural but only the second mechanism accounts for the presence of DFF, which is a C-6 compound. The first step of the first mechanism cleaves a carbon from fructose and all subsequent compounds are C-5. We can not confirm the second mechanism unequivocally since HMF was absent in the GC-MS chromatogram. Formic acid was detected only in particular cases, due to the higher activity at high levels of oxygen and temperature. In fact, formic acid easily converts to COx. Yu and Savage (1998)

Selectivity to furfural increased with time and reached a maximum after 3 h ; it then produces oxygenates at a steady rate while coke continues to build up. Dalil et al. (2016) demonstrated that the selectivity of acrolein from glycerol increased with an increasing mass fraction of coke on the surface for over 14 h operation. They showed that the coke covered acid sites (FTIR spectra recorded after pyridine adsorption) that were active for conversion. This behavior may explain the increase of the furfural and the decrease of the acetic acid selectivities (Figure 4.13).

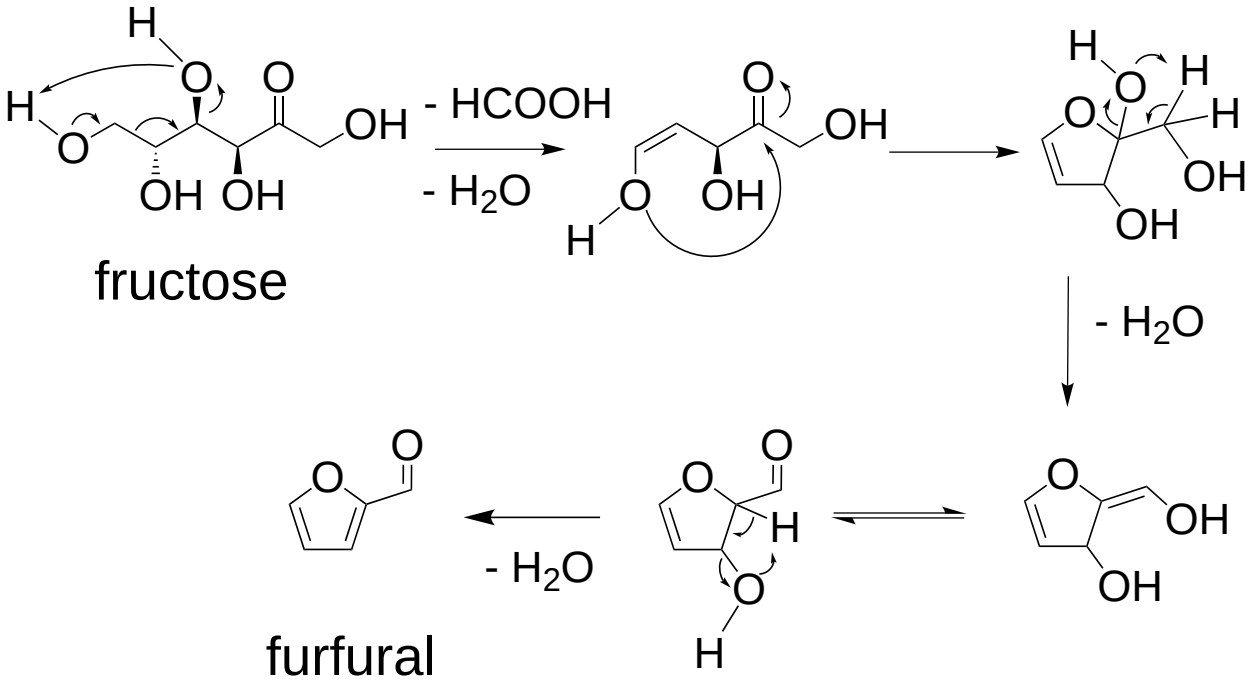

Figure 4.11 Fructose is triple dehydrated to produce furfural. The first step is the dehydration and the loss of a molecule of formic acid. The reaction proceed by the secondary dehydration and the keto-enolic equilibrium to form the aldehydic functional group. The loss of the third molecule of water leads to furfural.

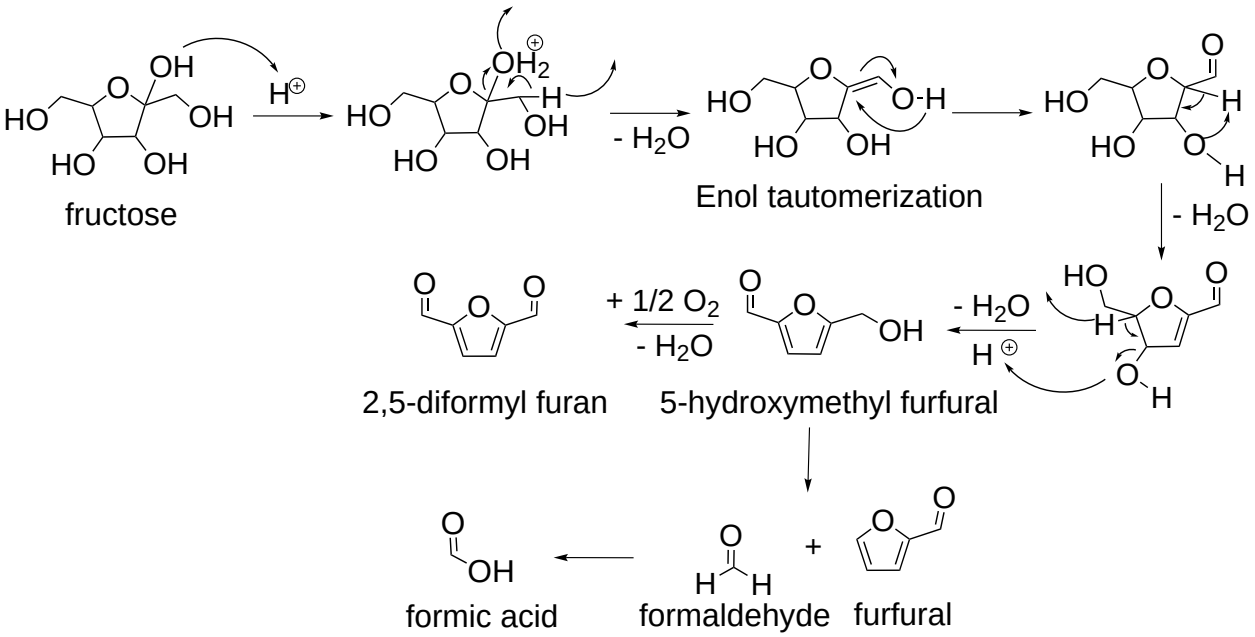

Figure 4.12 Triple dehydration from fructose to HMF. de Melo et al. (2014) A consequent oxidation leads to 2,5- diformylfuran, while the loss of formaldehyde or CO produces furfural. Li et al. (2016a)

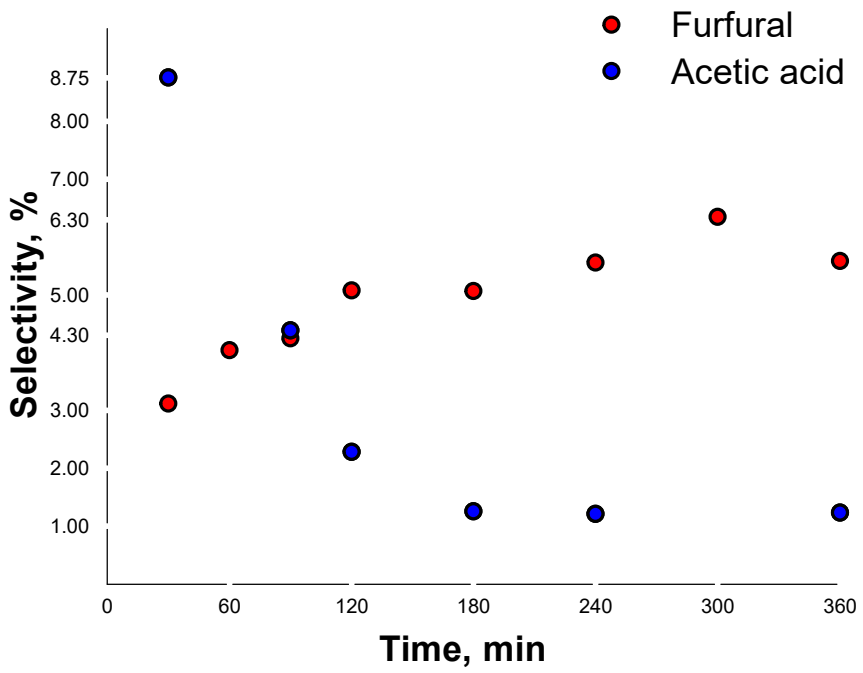

Figure 4.13 After 3 h, the system reaches the steady state. Decreasing the acidity leads to an increase of the selectivity to furfural and decrease to acetic acid.

4.5 Conclusion

We developed a micro-fluidized bed system that operates in the gas phase to convert fructose to value-added chemicals. We demonstrated that the kinetics forming dispersed aerosols is faster than caramelization kinetics and were able to operate 19 h continuously. Agglomeration and blocking at the sparger tip continues to affect operability and limit the range of conditions to test the reaction kinetics. The maximum selectivity to furfural was 22 % with 15 % of diformylfuran but in most experiments we produced acetic acid (generally < 10 %). Coke deposition has a deleterious affect on yield but may increase activity in the initial period. Future work will consider alternative catalyst compositions and promoters to increase yield.

CHAPTER 5 Pt-WO_3 OXIDEHYDRATION OF FRUCTOSE IN μ-FLUIDIZED BED REACTOR

5.1 Fructose to furans

The elevated oxygen/carbon ratio of carbohydrates versus petroleum constitutes an advantage to produce specialty chemicals and monomers. Sugar fermentation to bio-ethanol dominates the market at a maximum theoretical carbon atom yield of 67 % Macrelli et al. (2012). However, specialty chemicals command prices several-fold higher than that of bioethanol at fuel value. Fructose dehydrates to 5-hydroxymethyl furfural (HMF), a green intermediate, with a greater selectivity than glucose due to the similar spatial conformation and the faster enolisation reaction (Figure 5.1) Rosatella et al. (2011). Hydrogen reacts with HMF to dimethyl furan and dimethyl tetrahydrofuran (Figure 5.1)—a biofuel Ly et al. (2017)— while the hydrogenolytic ring opening produces adipic acid—a monomer for nylon-6,6 Tuteja et al. (2014). Oxygen reacts with HMF to 2,5-diformyl furan Lucarelli et al. (2016); Grasset et al. (2013); Le et al. (2013) and further to 2,5-furandicarboxlylic acid (FDCA) Wan et al. (2014); Zhang et al. (2015) (Figure 5.1). FDCA is the furanic substitute of terephthalic acid, which is a promising substitute for polyethylene terephthalate. Avantium developed the YXY technology that converts HMF to an ether with methanol/ethanol followed by an oxidation step to FDCA Avantium (2018). Acidic catalysts, ionic liquids, and supercritical water dehydrate fructose and glucose to HMF Choudhary et al. (2013); Antonetti et al. (2017); Li et al. (2013); Zhao et al. (2007); Cao et al. (2018); Bicker et al. (2005). Organic solvents are necessary to extract the product otherwise HMF hydrolyzes to levulinic acid and formic acid, or polymerizes to insoluble compounds—humins Patil and Lund (2011) (Figure 5.1).

Sn-Beta zeolite in tetrahydrofuran and water convert carbohydrates at 70 % selectivity. Other organic solvents include alkylphenol Pagán-Torres et al. (2012), dimethylsulfoxide (DMSO) and methylisobutylketone Chheda et al. (2007) and ethyl acetate Hu et al. (2009). These processes require contact times that range from minutes to hours because of the poor mass and heat transfer characteristic multiphasic reactors.

Metal-based catalysts Wan et al. (2014); Zhang et al. (2015); Liu et al. (2015); Yi et al. (2016) or enzymatic processes Koopman et al. (2010); Yuan et al. (2018) oxidize HMF to FDCA. Combination of the two steps in single reaction reduces the yield and requires special reactor or catalyst design. Leshkov et al. (2006) developed a multiphasic reactor with methylisobutyl ketone and 2-butanol as organic phase ; the aqueous solution dehydrates fructose to HMF, while the organic phase extracts it and further oxidize to FDCA. Pt/C oxidehydrates

fructose to FDCA in γ-valero lactone and H_2O Motagamwala et al. (2018). Combination of ionic liquids and not-noble metals avoid the organic phase and allows the one pot reaction Yan et al. (2018). Fluidized bed reactors operate at higher temperature with superior mass transfer and, consequently, reaction rates orders of magnitude higher. FBRs pyrolyze biomass into energy and chemicals Kan et al. (2016). Fast pyrolysis of cellulose in FBRs approach 62 % yields of levoglucosan, 3.5 % of HMF and 1 % of furfural Shen and Gu (2010). Immobilized anaerobic sludge produces biohydrogen and bioethanol citewu2007. A magnetically stirred fluidized bed reactor ferments glucose to ethanol within 95 % of the theoretical yield Liu et al. (2009).

We demonstrated the versatility of atomizing liquids into catalytic fluidized beds : VPO partially oxidizes xylose to C2-C4 carboxylic acids Ghaznavi et al. (2014) ; WO_3/TiO_2 dehydrates glycerol to acrolein Dalil et al. (2015, 2016) and decarbonylates fructose to furfural Carnevali et al. (2018) ; and, Keggin-type catalyst oxidehydrates 2-methyl,1-3-propanediol to methacrylic acid Darabi Mahboub et al. (2016). Here we investigated fructose dehydration to HMF in a μ-fluidized bed reactor. A nozzle atomized the aqueous liquid feed directly into the catalytic bed. We screened temperature, O_2 concentration, catalyst loading, Pt content on the catalyst, liquid flowrate, feed fructose mass concentration with a Plackett-Burman experimental design. The experimental plan was based on three levels of temperature and O_2 :fructose molar ratio and two levels for catalyst loading.

5.2 Experimental section

A furnace heated a 15 mm ID by 400 mm high quartz tube. Three thermocouples measured the temperature along the length at 20 mm below the bed, 5 mm — inside the bed, 90 mm above the distributor, and a fourth monitored the temperature in the exit line. The reactor operated at 1.4 bar while the ΔP between the inlet and outlet—0.001 bar during the reaction. A quartz frit, with a porosity of 150 µm to 200 µm, ensured the gas was distributed uniformly across the reactor diameter (Figure 5.2). A stream of O_2 in Ar fluidized the catalytic bed and burned the coke formed during the reaction. A nozzle atomized the aqueous fructose solution into the Pt-WO_3/TiO_2 catalytic bed. An HPLC pump injected the liquid feed at the desired flow, while 50 mL min^{-1} of argon improve the effervescent spray (Figure 5.3c) and a gauge recorded argon pressure in this line. A well dispersed spray with droplets less than 30 µm minimize catalyst agglomeration and blocking the nozzle. A ceramic tube enveloped the injector to reduce the heat transfer and ensure that the solvent evaporated in the bed rather than the injector ; when the temperature exceeded 100 °C, solvent evaporated and the sugar crystallized and blocked it. A stream of 50 mL min^{-1} of argon flushed the annular space

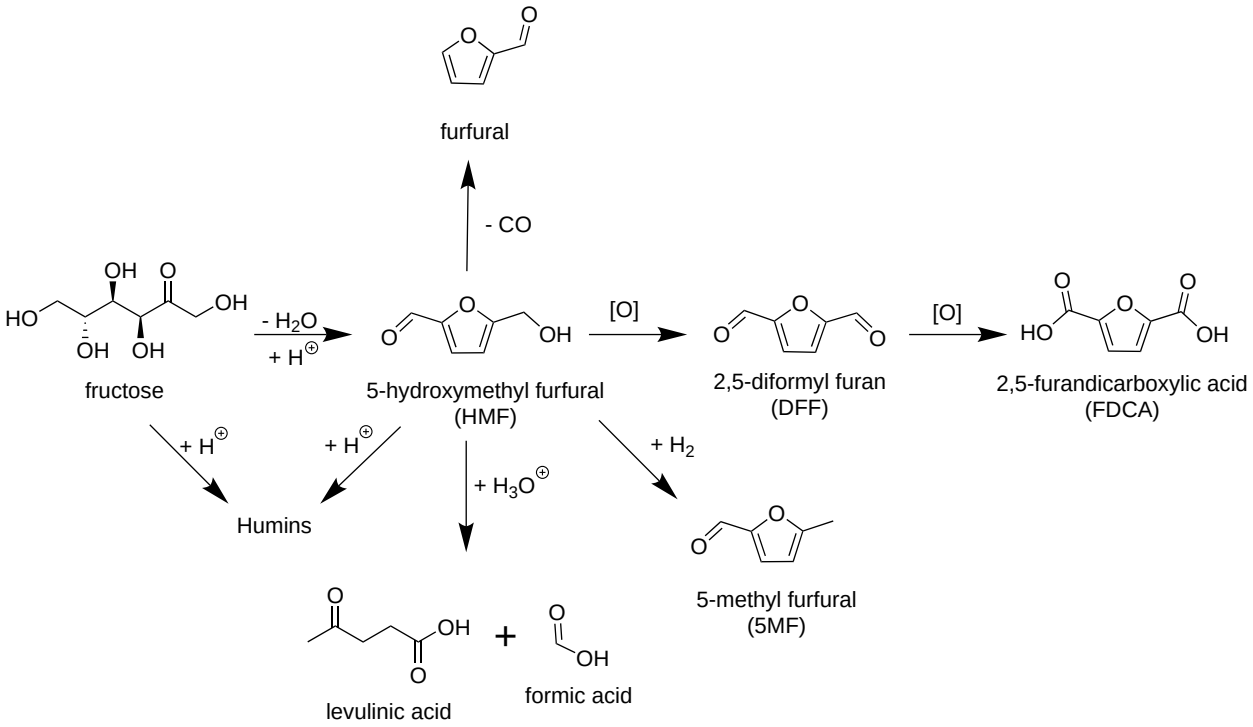

Figure 5.1 Fructose dehydrates to HMF. Organic solvents suppress the polymerization to humins and the rehydration to levulinic acid and formic acid. Decarbonylation leads to furfural, while the hydrogenation produces 5MF. HMF oxidation gives DFF and further FDCA, the furanic substitute of terephthalic acid.

between the injector and ceramic tube. The exit line (uninsulated) fed into a quench in an ice bath The quench fluid contained 25 g dimethyl sulfoxide to improve furanic solubility and 25 g H_2O. An on-line mass spectrometer (MS) with a multiple ion detector analyzed non-condensable gases — CO, CO_2, O_2, Ar, CH_4, while an HPLC quantified the liquid samples collected each 15 min during the first hour and then each 30 min until the end of the experiment (Figure 5.2). Glycerol was the internal standard for the HPLC analysis. At the end of each experiment we cleaned the exit line with 5 mL of water and analyzed this sample.

The selectivity to each product, S_i, is based on a molar balance around each component i, n_i^{out} :

$$S_i = \frac{\Sigma_j n_{i,j}^{\text{out}} / \vartheta_{i,j}}{n_{\text{fr}}^{\text{in}} - n_{\text{fr}}^{\text{out}}} \cdot 100 \tag{5.1}$$

where $n_{\text{fr}}^{\text{in}}$ and $n_{\text{fr}}^{\text{out}}$ are the moles of fructose entering and exiting the system and ϑ_i is the stoichiometric coefficient for the carbon component of each reaction j.

The following equation calculates the median drop size diameter, d_{50}, exiting the nozzle of an internal mixing air-assist atomizer Nasr et al. (2013) :

$$d_{50} = 20\ u_{\text{L}}^{0.5}\ m_L^{0.1}\ d_L^{0.1}\ \sigma^{0.2}\ \rho_g^{-0.3}\ \Delta U^{-1.0}\ \left[1 + \frac{m_{\text{L}}}{m_{\text{g}}}\right]^{0.5} \tag{5.2}$$

where u_{L} is the superficial velocity, m_{L} and m_{g} the mass flow of the liquid and the gas, d_{L} the orifice dimension, σ is the surface tension and the ΔU the relative velocity between the liquid and the gas.

5.2.1 Materials

All the reagents are analytical grade without further purification. We acquired D-fructose(99 %) from Alfa Aesar. We purchased 5-hydroxymethyl furfural (99 %), furfural (99 %), 5-hydroxymethyl-2-furancarboxylic acid, 5-formyl-2-furoic acid, 2,5-furandicarboxylic acid (97 %), 2,5-furan dicarboxaldehyde (97 %), 5-methyl-2-furaldehyde ($\geq$ 98 %), and tetraammineplatinum(II) nitrate ($\geq$ 99.9 %) and ammonium (para)tungstate hydrate (>99.99 %) from Sigma Aldrich. Air Liquide Canada supplied the gases : argon (> 99.7 %), 10.0 % O_2 balance Ar, and a mixture of CO (1.04 %), CO_2 (1.01 %), CH_4 (1.03 %) balance Ar. Huntsman Corporation supplied the titanium dioxide (Hombikat 110100).

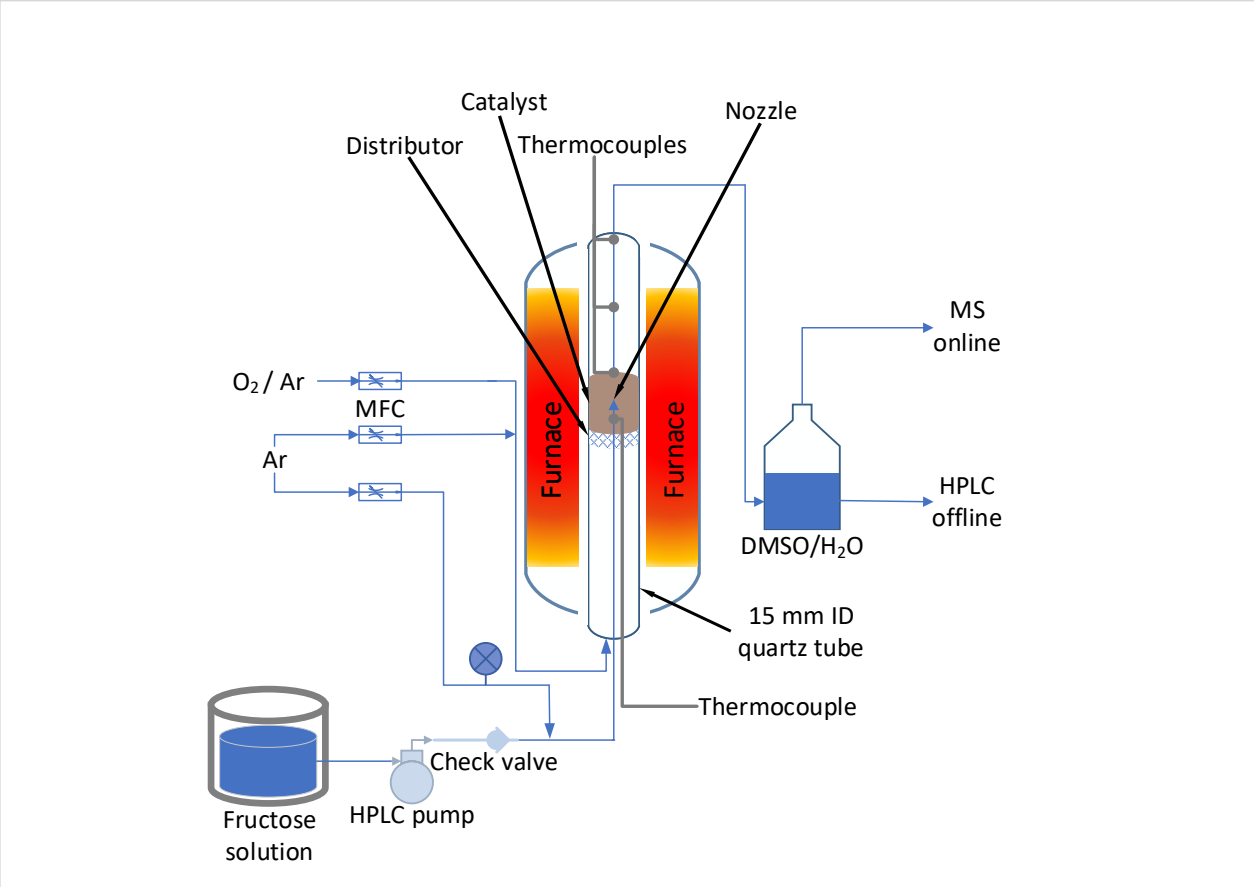

Figure 5.2 A nozzle atomizes the fructose solution directly into the catalytic bed. A DMSO/H_2O quench traps the products and an HPLC analyzes the trend. An online MS monitored non-condensable gases.

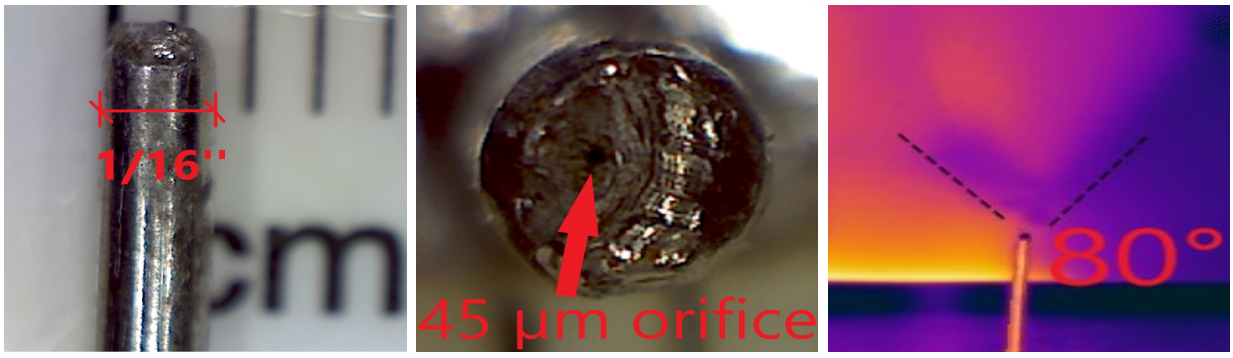

(a) (b) (c)

Figure 5.3 1/16" (1.59 mm) stainless steel pipe filed at the top to obtain an orifice of 45 µm. The IR camera shows that the atomization and the evaporation at the orifice decreased the temperature at the tip, forming a full cone with an angle of 80°.

5.2.2 Catalyst preparation

We sieved the support powder to 90 µm to 150 µm in diameter. The crystalline phase of the titania was pure anatase. A successive wetness impregnation method deposited firstly WO_3 and then Pt on the TiO_2 support. Initially we determined the total pore volume by dropwise addition of water. We dissolved the ammonium paratungstate in the calculated volume. For a more intimate contact between the active phase and the catalyst, we mixed the liquid and the solid in a rotary evaporator for 3 h at 100 rpm. After we increased the temperature to 70 °C and decreased the pressure to 300 mbar for 2 h to dry the catalyst. A furnace calcined the solid : first the temperature was maintained constant at 120 °C for 4 h to completely remove traces of water. With a ramp of 2.5 °C min^{-1} to 600 °C for 4 h in air. We repeated the same procedure for the Pt sample.

5.2.3 Analytical instrumentation

An X-ray diffractometer (Philips X'PERT) generated the XRD spectra with a monochromatic Cu-kα beam, $\lambda = 0.154\,06$ nm, at 50 kV and 40 mA. We scanned the gonio axis from 20° to 85°, at a rate of 0.01° s^{-1}. The crystalline phases were identified using the ICDD database and the Rietveld refinement (X'PERT highscore) gave a semi-quantitative characterization for the phases' weight composition. The Scherrer approximation defined the average cubic crystallite size : $D = 0.94\lambda/\beta \mathrm{Cos}\theta$, where λ is the mentioned instrument wavelength, β is the full-width at half-maximum peak height (FWHM, rad), and θ is the Bragg angle for the most intense peak (half of the 2θ position).

The FE-SEM-JEOL JSM-7600F scanning electron microscope (SEM) acquired the catalyst images between 5 kV to 30 kV, using secondary and backscattered electrons detectors (secondary electron image —SEI, low secondary electron image —LEI and backscatter image —LABe). The energy dispersive X-ray detector (EDX) mapped the surface of the catalyst and qualitatively quantified the composition and the different phase regions.

A laser diffractometer (Horiba, LA-950) evaluated the particle size distribution (PSD) based on the Mie Theory :

$$D_{4,3} = \frac{\sum d_i^4 \cdot N_i}{\sum d_i^3 \cdot N_i} \tag{5.3}$$

with N_i as number of particles with diameter d_i. The particle refractive index was 2.75 + 0.00i (R and Chi parameter below 0.05).

A N_2 physisorption instrument (Quantachrome Autosorb-1) recorded at 77 K the adsorption and desorption isotherms. A degasser, operating under vacuum at 300 °C for 6 h, removed

the gas adsorbed on the surface Orr and Dallavalle (1959). The Brunauer-Emmett-Teller (BET) theory regress the specific surface area at P/P_0 0.05 to 0.3. The instrument estimated the mesopore size distribution over the desorption branch (P/P_0 0.15-0.995), based on the Barrett-Joyner-Hallender (BJH) theory. The total pore volume is evaluated at the maximum filling pressure (P/P_0 0.995), considering all pores with a diameter smaller than 300 nm.

A CHN analyzer (LECO CS744) measured carbon build up on the catalyst surface after each experiment. An internal balance measured the sample weight loss, when heated above 1000 °C in air. A further CO trap converted the remaining carbon monoxide to CO_2.

A Varian ProStar 325 HPLC, equipped with UV detector at 260 nm analyzed the filtered liquid samples. A MetaCarb 87H column, kept at 60 °C, separated the compounds. The pump flowed a 0.05 N aqueous H_2SO_4 solution at 0.35 mL min^{-1}. Each analysis lasted 70 min to ensure the products separation.

5.3 Catalyst characterization

Fluidization and particle size distribution

Geldart classified particles into 4 categories based on the catalyst diameter and the differential of the particle density and the gas density Geldart (1973). Geldart group A particles are best for catalytic fluidized beds with diameters (d_{50}) on the order of 70 µm. Based on the Horiba LA-950, the average spherical particle diameter of calcined catalyst increased from 85 µm to 95 µm (Figure 5.4). Coke covered the surface (SEM-EDX) and increased the average particle diameter by 10 µm. The bulk density was 770 kg m^{-3}, so that we classify it as a group A powder.

The minimum fluidization velocity, u_{mf}, with 3 g of catalyst in the reactor was 8 mm s^{-1}. Catalyst attrition resistance is a major concern for fluidized beds particularly with high velocity jets where particles collide and fragments or cleaves surface asperities. To prevent this phenomena we opted for the catalyst synthesis by incipient wetness impregnation, which minimizes surface defects and thus asperities. We tested the attrition rate in an air jet mill according to the ASTM 5757 Tube et al. (2013). The high velocity simulates the mechanical stress coming from the nozzle and the distributor. A filtered vessel collected the elutriated fines after 24 h. The catalyst attrits at 5.4 mg h^{-1}, which is well within commercial practice Patience and Bockrath (2010).

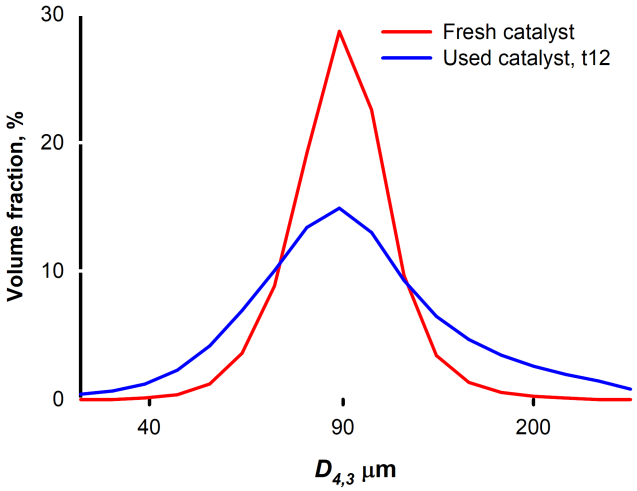

Figure 5.4 Catalyst particle size distribution in logarithmic scale. Coke deposits broadened the peak and increased the average.

Table 5.1 Variation of the catalyst physical characteristics after the reaction

Property	Calcined	Used
d_{50}, µm	85	95
SA, $m\,g^{-2}$	63	63
Pore volume, $mL\,g^{-1}$	0.183	0.183
u_{mf}, $mm\,s^{-1}$	8	
ρ_{bulk}, $kg\,m^{-3}$	770	
Attrition resistance, $mg\,h^{-1}$	5.4	5.4

XRD

We analyzed the calcined catalyst before reaction with a mass fraction of 5 % WO_3 on TiO_2 and 0.5 % Pt or 1.5 % Pt . We characterized catalyst at the end of experiment t12 that had 1.5 % Pt, which had the most coke. XRD analysis detected two crystalline phases : anatase for the titania (ref : 96-900-9087) and platinum (ref : 96-101-1114) while EDX confirmed the presence of W. The W concentration was below the XRD detection limit Carnevali et al. (2018). The titania support maintained a tetragonal structure during calcination and reaction. The platinum presented a cubic structure, with a submicron crystallinity, which increased with Pt loading and decreased by the coke deposition during the reaction. SEM confirmed the results, providing images of crystals with several hundred nanometers size and a round-prismatic shape. Each crystal contained several crystallites, growing in different directions (Figure 5.9). At50 kV, the X-ray penetrated the catalyst down to 35 µm (Pott's equation) Saadatkhah et al. (2017) : this surface analysis overestimated the Pt fraction with

respect the TiO_2 support. As coke builds up, the intensity of the Pt signals decrease, and become broader (Table 5.2). During calcination, WO_3 precursor penetrated the titania lattice thereby reducing the tungsten signal. Calcination at 600 °C was low enough to minimize phase segregation and so the WO_3 remained amorphous. A weak, unidentified peak emerged at 31.6° after reaction. Reaction conditions may have crystallized part of the amorphous WO_3 in the mesoporous titania structure however, SEM-EDX could not confirm WO_3 crystals on the surface of the catalyst but N_2 physisorption detected a decrease in pore size after reaction. The small crystallite size (30 nm) and the strong chemical interaction with the surrounding environment (coke and titania) shift the signal.

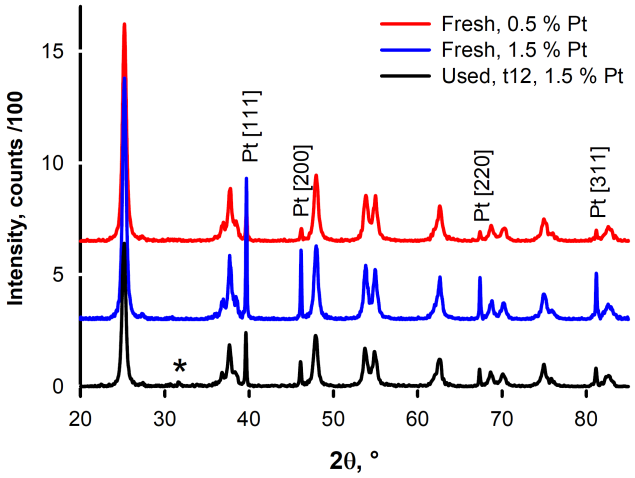

Figure 5.5 Stacked spectra recorded with the same conditions and smoothed with an 11 points cubic function, Cu-$k\alpha$ sidebands were removed : coke deposits on the used sample reduced the signal to noise ratio. Four sharp Pt signals (39.6°, 46.0°, 67.4°, 81.2°) and their respective planes $[hkl]$ have been identified. The remaining peaks belong to the titania support (anatase) Khan et al. (2018).

Table 5.2 D crystallite size (standard deviation among Pt signals) ; BET surface area by nitrogen physisorption, results are within 3 % precision (95 % variance) ; ϕ pore volume ; $\Delta_{\mathrm{d}V(d)}$ BJH $\mathrm{d}V(d)$ mesopore median ; Coke carbon content (0.05 % precision, 95 % variance).

	D nm	BET $m^2\,g^{-1}$	ϕ $mL\,g^{-1}$	$\Delta_{\mathrm{d}V(d)}$ nm	Coke %
Calcined 0.5 %Pt-WO_3/TiO_2	52(7)	63	0.183	9.6	na
Calcined 1.5 %Pt-WO_3/TiO_2	88(2)	63	0.183	9.6	na
Used, t12, 1.5 %Pt-WO_3/TiO_2	60(10)	63	0.183	9.6	48

BET

The TiO_2 support and tungsten salt precursor contribute most to the specific surface area (SSA), pore size distribution and pore volume (PV) of the catalyst after calcination (Figure 5.6) Carnevali et al. (2018). Calcined catalyst has a type IV isotherm and an $H2$ hysteresis loop : mesoporous structure with a narrow distribution of pore necks Sing et al. (1985). A mass fraction of 1.5 % Pt decreased the SSA with respect to calcined WO_3/TiO_2 catalyst. EDX images show Pt on the surface but not in the interior so the drop in SSA and PV is due to pore-blocking. Pt obstructed pores smaller than 10 nm, which increased the characteristic pore median ($\mathrm{d}S(d)$) by 1 nm. The "t12" catalyst has a type I-IV isotherm and an open $H4$ hysteresis : a microporous network developed as coke partially filled the internal mesoporous structure. Despite coke deposits, furanic selectivity improved with time. The SSA increased with respect to calcined catalyst, suggesting a selective coke deposit. This phenomenon decreased the reagent and product degradation, despite the pore size dropping from 11.0 nm to 0.7 nm) and the lower pore volume (Table 5.2).

The BJH surface distribution shrunk in the mesopore region. The quenched solid state functional theory (QSDFT) for SSA deviated less that than 5 % of the BET SSA. Based on the $V-t$ method, micropores in the calcined catalyst were negligble estimated a negligible micropore for the calcined samples, but for the used sample, micropores contributed almost 80 % of the SSA and 40 % of the pore volume (QSDFT method, $V-t$ method had 5 % deviation from those values). The higher pore-volume is strictly connected with the coke on the surface.

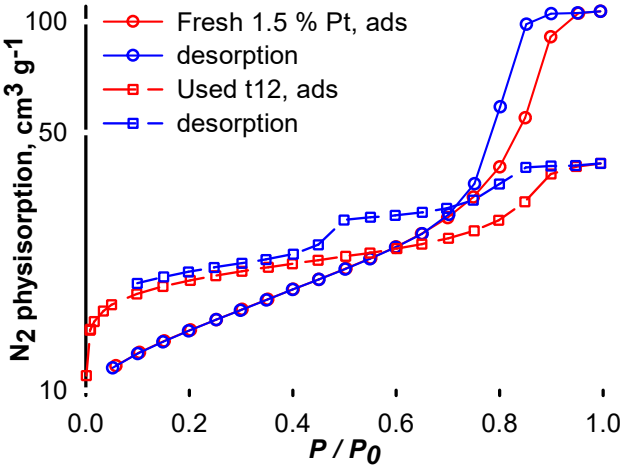

Figure 5.6 Nitrogen physisorption isotherms. The used catalyst loses the microporous fraction and the total pore volume decreases as a consequence. Carbon obstructing the mouth of the micropores accounts for the large reduction at $P/P_o > 0.7$.

Field Emission Scanning Electron Microscopy (FE-SEM)/EDX

The tungsten oxide was homogeneously dispersed on the titania support. Pt crystals were dispersed nonuniformly on the surface as SEM images show regions with bright spots with Pt particles (Figure 5.7). Furthermore, some particles have much more Pt than others. The Pt submicron crystals were 250 µm on average (Figure 5.8). After reaction, Pt submicron particles agglomerated into clusters of several hundred crystals but the powder remained free flowing. Only at the sparger tip, solids would agglomerate at the circumference Ghaznavi et al. (2014).

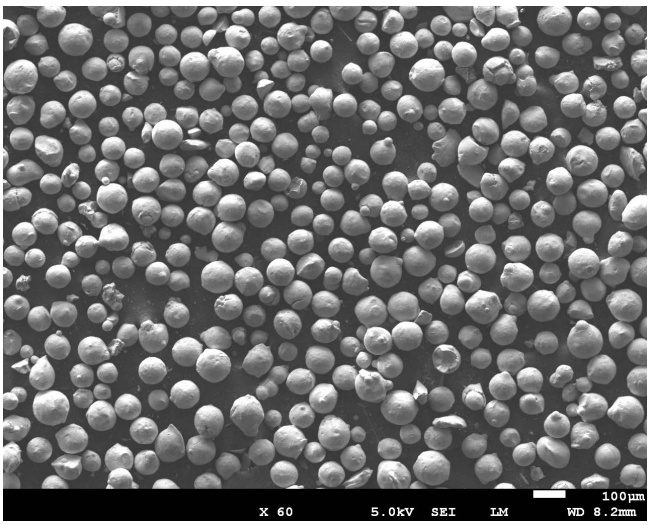

Figure 5.7 Calcined 1.5 % Pt over WO_3/TiO_2 particles. The LABe detector enhanced the signal from heavy elements and the Pt crystals appeared as bright white spots Patience (2017).

An EDX at 20 kV probed the catalyst surface to a depth of 10 µm and confirmed that W covered the surface uniformly. On the contrary, Pt forms submicron crystals rather than forming a monolayer on the surface or in the interior. Titanium-oxygen molar ratios were coherent with the TiO_2 composition. Pt was only in the metallic form since the EDX oxygen image showed dark spots corresponding to the Pt crystals (Figure 5.10).

We crushed used catalyst and the SEM images of the chunks showed no coke in the interior. As much as (20 µm) of coke covered some of the particles but most of it was homogeneously distributed on the surface (Figure 5.10). Clearly, since the carbon coverage was uniform WO_3 rather than Pt initiated the growth of the coke layer. An EDX spectrum on the coke deposit identified a molar composition of 90 % carbon and 10 % oxygen.

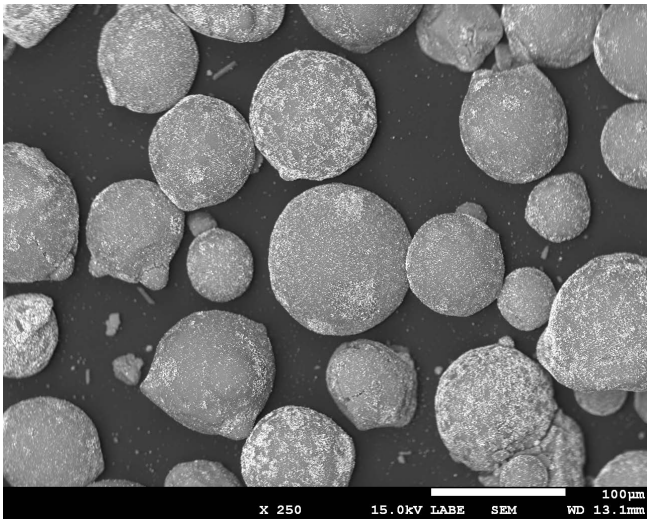

Figure 5.8 Calcined 1.5 % Pt over WO_3/TiO_2 particles. The metallic platinum crystals appeared as multi-facets prisms. Considering their sizes (submicron), the crystallite size of 88 nm (XRD) and the crystal structure of metallic Pt (cubic), several crystallites compose the crystal.

5.4 Internal-mixing two-fluid nozzle

Atomizing the fructose and HMF solutions into the fluidized bed reactor caused most of the interruptions. The large surface to volume ratio of the sparger was a contributing factor as the water would evaporate in the tube and the fructose would then crystalize. We injected Ar at 50 mL min^{-1} to reduce the residence time of the solution in the tube and improve the effervescent spray of the liquid. The gas and fluid first mix at the t-junction below the sparger tip. We reduce the internal diameter of the top part of a stainless steel pipe of 1.5875 mm OD and 0.127 mm ID (Figure 5.3a) to create an orifice of 45 µm±5 µm (Figure 5.3b), which is 65 % reduction of the internal diameter. The setup produced a full cone spray with an angle of 80°±5°, measured by infrared camera after heating the nozzle to 400 °C.

Equation 5.2 demonstrated a 0.5 median drop size of 5 µm. We calculated the results based on room temperature and approximating the viscosity of the 2 % sugar solution as pure water. An internal mixing increased the contact between the gas and the liquid, resulting in finer droplet size Nasr et al. (2013).

5.5 Screening test and full factorial design

A Plackett-Burman screening design investigated the influence of six parameters on the fructose oxidehydration. We evaluated temperature (150 °C and 300 °C), O_2 :fructose molar ratio

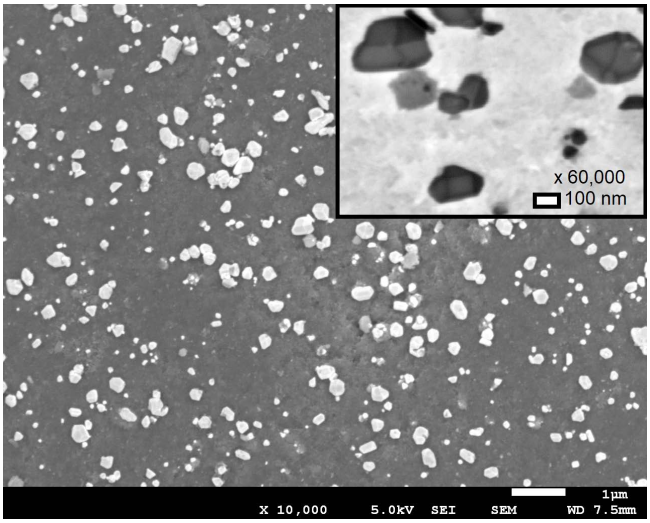

Figure 5.9 Used "t12" catalyst's surface. Shiny "metallic-lookalike" coke chunks were dispersed around the spherical catalyst particles after mechanical breakage. Some particles broke as well.

(2 :1 and 20 :1), mass catalyst loaded (2.5 g and 5 g), Pt loading (0.5 % and 1.5 %), feed flowrate (50 µL min^{-1} and 100 µL min^{-1}) and feed fructose mass concentration (2.5 % and 5 %). The design limited to 12 the number of experiments.

All the tests demonstrated total conversion of fructose. The molecule reacted with the catalyst to form the products, or degraded to coke or COx. Due to the hard conditions some molecule pyrolized on the walls or in the exit line, resulting in carbon loss.

The two levels of mass of catalyst loading varied the contact time, while two flowrates levels modified the weight hour space velocity and the gaseous partial pressure of water.

We computed the results with the statistical software STATISTICA®. Low catalyst loading is the most predominant parameter, decreasing the contact time and increasing the furanic products selectivity. The maximum total products selectivity never exceeded 6 %, due to the extreme conditions of the screening tests. CO_2 and CO rose with temperature, reaching 59 % and 4 % at 300 °C, respectively. Furthermore, higher oxygen concentration produced higher amount of CO_2. HMF, the dehydration product, increased with higher liquid flowrate and lower catalyst loading. Increasing the partial pressure of water rose the catalytic surface saturation, lowering the degradation kinetic. High contact time demonstrated higher HMF conversion. Furfural, the decarbonylation product of HMF (Figure 5.1), was dependent only on catalyst loading, which is favored by the longer contact time. Maximizing the contact time, determined the fructose and the intermediate degradation to coke and COx.

Oxygen reacted with HMF to HMFCA and DFF (Figure 5.1). Oxidation kinetics of the hy-

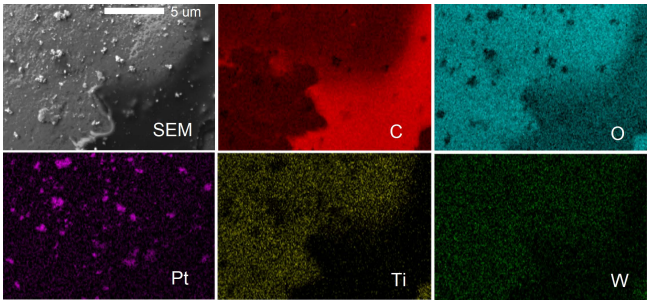

Figure 5.10 SEM and EDX mapping of the used "t12" catalyst's surface. Carbon (C, red) partially covered the surface and suppressed the underlying elements' signals. Oxygen (O, blue) was predominant were titanium was also present (Ti, yellow), less were carbon was present and absent were platinum was present (Pt, violet). Tungsten (W, green) was homogeneously distributed along with titanium.

droxyl moiety of HMF is faster than the conversion of the aldehydic functional group. DFF reached a maximum selectivity of 1 %, while HMFCA never exceeded the 0.05 %. Lower catalyst loading and higher temperature increase the selectivity. This behavior can be explained by the high energy of activation of the HMF oxidation, which increased with higher temperature. Furthermore, as all the furanic compounds, lower amount of catalyst reduced the contact time and the degradation process. A further oxidation of HMFCA and DFF formed FDCA. We determined that any of the parameters affects the selectivity. The amount of catalyst tested was high, leading to elevate contact time and increasing the degradation.

We developed a full factorial design, investigating temperature (300 °C, 350 °C and 400 °C), O_2 content (0.5, 1 and 10 molar ratio with fructose), and catalyst loading (1.5 g and 3 g). We kept constant Pt loading (1.5 %), increasing the liquid flowrate (300 µL min^{-1}) and keeping the fructose mass percentage in the feed at 2 % (Table 5.3).

The contact time τ between the sugar injected and the catalyst varied between 0.3 s to 0.4 s, while the weight hour space velocity ranged between 0.1 h^{-1} to 0.25 h^{-1}. Also for this set of experiments, the conversion was complete. We calculated the carbon balance for each experiment. The results ranged between 57 % to 97 %. The carbon loss is due to the degradation of the molecules on the reactor wall or inside the exit line.

Table 5.3 represents the selectivity to the main products, considering all the three hours reaction.

Higher temperature and lower catalyst loading increased the selectivity for all the products (Table 5.3). The CO_2 selectivity varied from almost 0 to 47 %. At higher catalyst loading — so higher contact time — and higher oxygen concentration, fructose decomposed more frequently

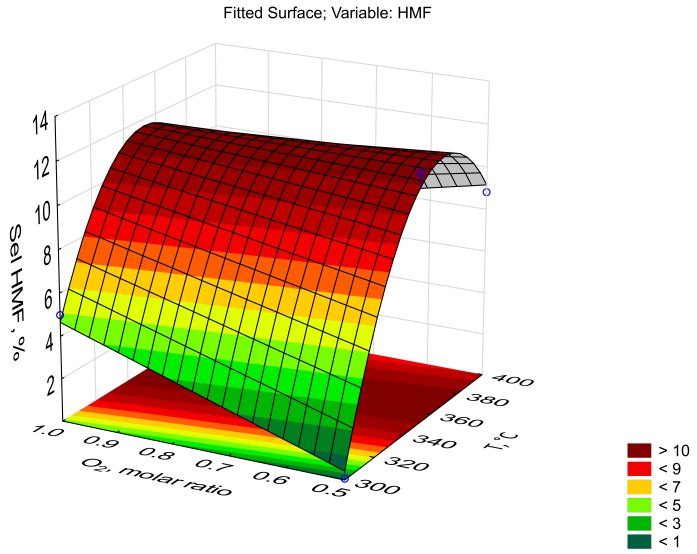

Figure 5.11 Surface chart of HMF selectivity with 1.5 g catalyst loading.

Table 5.3 Full factorial of catalyst loading, temperature and O_2 molar ratio. The selectivities are calculated from time 0 min to 180 min. HMF : 5-hydroxymethyl furfural ; FUR : furfural ; 5MF : 5-methyl furfural ; DFF : diformyl furan.

Exp #	**Cat** g	**T** °C	**O_2** Molar ratio	S_{CO_2} %	S_{CO} %	S_{CH_4} %	S_{Coke} %	S_{HMF} %	S_{FUR} %	S_{5MF} %	S_{DFF} %
1	3	300	0.5	6	6	9	8	0	5	3	1
2	3	400	1	12	10	5	10	4	5	1	1
3	1.5	300	10	20	4	17	6	6	4	0	1
4	1.5	400	1	2	3	1	12	9	3	0	0
5	3	350	10	4	3	4	55	3	2	1	1
6	3	300	1	3	12	2	43	3	1	0	0
7	1.5	350	10	0	2	0	21	1	1	0	0
8	3	350	0.5	8	5	4	54	0	5	4	3
9	1.5	300	0.5	2	0	1	13	0	1	0	0
10	1.5	300	1	4	2	3	36	5	6	1	1
11	3	350	1	12	6	5	57	1	5	4	3
12	1.5	350	1	7	5	5	49	11	6	1	2
13	1.5	350	0.5	4	3	4	31	12	6	1	1
14	1.5	400	1	7	3	5	48	7	3	1	3
15	3	400	10	47	1	17	43	0	0	0	0
16	3	300	10	41	1	15	66	1	2	0	1
17	3	400	0.5	4	2	2	24	1	9	6	2
18	1.5	400	10	11	8	3	20	0	7	4	2

to CO_2, which increased linearly with O_2 concentration. Oxidized products demonstrated stable selectivity at higher temperature. Lower O_2 concentration produced lower oxidized compounds. CH_4 has the maximum selectivity when the oxygen molar ratio was 0.5, achieving 17 %. Coke formation relates to the decomposition of the feed or the products on the catalyst. In all the experiments coke deposited on the catalytic surface, producing large agglomerates. A quadratic function of temperature, presenting a maximum at 350 °C, affected the coke formation. Furthermore, increasing the catalyst ratio increased the contact time, leading to a higher degradation of the products and higher coke formation. Oxygen seems not affecting the coke formation. The reason relates to the temperature, which is not high enough for activate the carbon to react with the O_2 to produce COx. As demonstrated by the screening test, HMF selectivity increased with lower contact time, reaching a maximum of 12 % at 350 °C and with 0.5 O_2 molar ratio. Considering low amount of O_2 — 0.5 :1 and 1 :1 molar ratio, and temperature at 350 °C, the selectivity to HMF remained almost constant, demonstrating the low impact of O_2 on the reaction at that temperature (Figure 5.11). To validate the results, we repeated test 12 and test 13 (Table 5.3). We calculated the standard deviation, which attested at 4 %

5.5.1 HMF to DFF

We investigated the oxidation of HMF to DFF with four temperatures (250 °C, 300 °C, 350 °C and 400 °C), and two catalysts loading (1.5 g and 5 g), maintaining the O_2 :HMF molar ratio of 2 (Table 5.4). Pt-WO_3/TiO_2 demonstrated a partial oxidation of HMF to DFF, and the inefficient oxidation power to further produce HMFCA and FDCA. HMF conversion was total with temperature above 350 °C, while decreased to 92 % at 300 °C and to 86 % when the temperature dropped to 250 °C. The main oxidation product was DFF, reaching a maximum of 42 % with the lowest temperature and catalyst loading. Higher contact time increased the degradation, resulting in lower DFF selectivity. In fact, with 5 g catalyst the maximum DFF never exceeded 4 %. On the contrary, at 1.5 %, the DFF selectivity increased with temperature.

5MF, the main by-product of the reaction, is mainly controlled by temperature and mass of catalyst. In fact, at higher contact time, the selectivity dropped to maximum 2 %, while decreasing the temperature from 400 °C to 250 °C, the selectivity increased from 12 % to a maximum of 18 %. Furfural, the other main by-product, remained almost stable around 6 % for all the reactions with lowest amount of catalyst, but presented lower values —around 1 % — for 5 g.

Coke built up on the catalyst, but seems independent of temperature and catalyst loading.

Table 5.4 Higher contact time increase the degradation kinetic. Decreasing the temperature decreases the conversion but enhances the DFF selectivity. CB : Carbon balance

Cat g	**T** °C	**O_2 :HMF** molar ratio	**Time** h	**Conversion** %	S_{CO_2} %	S_{CO} %	S_{coke} %	S_{CH_4} %	S_{FUR} %	S_{5MF} %	S_{DFF} %	**CB** %
1.5	250	2	3	86	10	12	12	2	6	18	42	116
1.5	300	2	3	92	3	28	22	3	1	11	30	98
1.5	350	2	3	100	15	15	13	5	9	11	26	94
1.5	400	2	3	100	23	6	4	4	4	12	16	69
5	400	2	3	100	36	15	12	2	1	2	4	72
5	350	2	3	100	27	15	16	10	0	1	0	69

Differently, for CO and CO_2 the selectivity varied with the two parameters. In fact, at low temperature and low catalyst loading, CO was higher than CO_2, but increasing the two variables, the ratio became 1 :1 and consequently in large favor to CO_2. The reason was the higher contact time, that increased the degradation of the molecules and the temperature than enhanced the formation of more oxidized products.

5.6 Conclusions

Fructose oxidehydration in gas-phase to DFF has a major impact on the fructose valorization, defining a new conversion pathway. The fluidized bed reactor avoid organic solvents, decreases the reaction time to fraction of seconds and facilitates the products separation. Fructose dehydrates to HMF, with the highest selectivity of 12 %, with the lowest catalyst loading (1.5 g) and low O_2 concentration (1.5 :1 molar ratio with fructose) at 350 °C. After 3 h the system did not reach the steady-state. HMF as starting material demonstrated a partial oxidation selectivity to DFF of 42 %, at 250 °C and 1.5 g catalyst. Coke built up on the catalytic surface, agglomerating the catalyst but also covering the strongest acid sites, enhancing the selectivity to the furanic compounds. Further addition of a second transition metal will promote the further oxidation of DFF to FDCA.

CHAPTER 6 ARTICLE 2 - LEVULINIC ACID UPGRADE TO SUCCINIC ACID WITH HYDROGEN PEROXIDE

Davide Carnevali, Marco G. Rigamonti, Tommaso Tabanelli, Gregory S. Patience, Fabrizio Cavani

Article published on Applied Catalysis A : General (I.F. 4.4)

6.1 Abstract

Levulinic acid is produced from the acidic aqueous degradation of 5-hydroxymethylfurfural, with potential applications in bio-value added chemicals synthesis. Here, we report for the first time, the solvent-free Baeyer-Villiger oxidation of levulinic acid to succinic acid, with hydrogen peroxide and tungstic acid. We investigated the effects of time, amount of reagent-to-catalyst molar ratio and H_2O_2-to-levulinic acid molar ratio. The maximum conversion was 57 %, while the maximum selectivity was 75 % after 6 h. We propose a reaction mechanism based on results obtained from the reactivity of the intermediates. The catalyst interacts with the substrate, forming a cyclic species that enhances the formation of succinic acid versus 3-hydroxypropanoic acid.

Keywords

levulinic acid, succinic acid, hydrogen peroxide, Baeyer-Villiger, oxidation, tungstic acid, H_2WO_4

6.2 Introduction

Biomass is a primary source of energy and a potential feedstock for bio- chemicals. Compared to fossil fuels, it has an elevated oxygen - carbon ratio, which makes it more suitable for the synthesis of highly functionalized value-added molecules, like to 5-hydroxymethylfurfural (HMF) by fructose dehydration Antonetti et al. (2017); Bin et al. (2017) ; a further oxidation of the intermediate forms 2,5-furandicarboxylic acid (FDCA) Pasini et al. (2011); Leshkov et al. (2006). The dehydration of fructose occurs with high temperature or by presence of an acidic Brønsted catalyst. The main synthesis hurdle is that HMF degrades in aqueous acidic condition, and forms insoluble polymers (humins), or cleaves to make levulinic acid

(LEV) and formic acid. Most works in this area apply multi-phasic reactors Kroger et al. (2000), membrane reactors Xie et al. (2012) or ionic liquids Kumar et al. (2017) to reduce humins. LEV is an important bio-building block for valeric acid Upare et al. (2011), methyltetrahydrofuran Manikandan and Cheralathan (2017), alkyl levulinate Guo et al. (2007), diphenolic acid Tan et al. (2016), δ-amino levulinic acid, γ-valerolactone Sun et al. (2016); Manzer (2004), α-methylene-γ- valerolactone Lewkowski (2005) and succinic acid. Derivatives applications regard mainly the production of rubber, plasticizers, pharmaceuticals and textiles Szabolcs et al. (2013). Biomass is the preferred starting material to produce LEV Antonetti et al. (2016); Pileidis and Titirici (2016); Werpy and Petersen (2004). LEV and succinic acid are in the top 10 value added chemicals from biomass Bozell and Petersen (2010); Zeikus et al. (1999). The succinic acid market value reached 400 billionUSD per year Li et al. (2011). Industrially, the favored route to succinic anhydride is the hydrogenation of maleic anhydride, derived from fossil fuel *n*-butane Mandelli et al. (2001). On the contrary, the main bio-pathway is the sugars fermentation. LEV reacts with basic, acidic and metal oxide catalysts to form succinic acid ; most studies add solvent to increase product yield (Table 6.1). One promising reaction is the Baeyer-Villiger oxidation with hydrogen peroxide as an oxidizing agent. Adding catalyst increases the reaction rate and improves the selectivity to the desired products. Examples of catalysts include alumina Van Der Klis et al. (2012), tungstic acid Podolean et al. (2013), tin Xia et al. (2016), titanium silicalite-1 (TS-1) Wang et al. (2015), selenium Caretto and Perosa (2013) and bio-enzymes Choudhary et al. (2013). The mechanism comprises the nucleophilic addition of a hydroperoxide anion to the carbonyl carbon Kawasumi et al. (2017). Environmental conditions modulate the intermediate rearrangement ; acidic catalysts react with the substrate to form the methyl ester, while in basic conditions it produces the acetate through an intramolecular addition. Starting from humic acids, hydrogen peroxide achieved 93 % malonic acid or 62 % succinic acid Wu et al. (2015).

Dutta et al. (2015) described the basic oxidation of LEV with H_2O_2 to 3-hydroxypropionic acid (HPA), a precursor of acrylic acid. On the contrary, hydrogen peroxide, combined with

Table 6.1 Review of the conversion with reaction parameters and yields. LEV : levulinic acid ; M- LEV : methyl levulinate ; SUCC : succinic acid ; M-SUCC : methyl succinate ; DM-SUCC : dimethyl succinate ; MA : maleic anhydride.

Reagent	T, °C	Catalyst	Solvent	Time, h	Products	Yield, %	Ref.
LEV	300 – 400	V_2O_5			SUCC		Dunlop and Shelbert (1952)
LEV	40 – 60	V_2O_5 + HNO_3		1 - 4	SUCC		Van Der Klis et al. (2012)
LEV	150	Ru-based magnetic nano particles +O_2	H_2O	6	SUCC	78	Podolean et al. (2013)
LEV	90	Mn-based catalyst	AcOAc	10	SUCC, MA	9, 26	Xia et al. (2016)
M-LEV	80	Amberlyst-15 + H_2O_2	Methanol	6	M-SUCC	41	Wang et al. (2015)
LEV	200	K_2CO_3	Dimethyl carbonate	6	DM-SUCC	21	Caretto and Perosa (2013)
Furfural	80	Amberlyst-15 + H_2O_2	H_2O	24	SUCC	74	Choudhary et al. (2013)
LEV	25	I_2	*t*-BuOH	1	SUCC	87	Kawasumi et al. (2017)

sulfuric acid, achieved a maximum of 48 % succinic acid selectivity. Replacing H_2SO_4 with trifluoroacetic acid, increased selectivity to 62 %, at 90 °C after 2 h Weiss et al. (1966). Here for the first time, we describe the acidic solvent-free Baeyer-Villiger oxidation of LEV to succinic acid with H_2O_2 and H_2WO_4. We investigated the effects of time (1 h, 3 h and 6 h), reagent :catalyst ratio (100, 50 and 10) and H_2O_2 :LEV ratio (1.5, 3 and 5) on the LEV conversion and on the main products selectivity. Furthermore, we investigated the reaction pathway, testing the intermediates reactivity.

6.3 Experimental

6.3.1 Materials

We used all reagents without further purification. The purity of LEV was greater than => 97 %, succinic acid > 99 %, formic acid purity varied between 95 % to 97 %, propionic acid >99.5 % , α-angelica lactone purity was 98 %, malonic acid was 99 %, and stabilized hydrogen peroxide 27 % w/w in H_2O), sulfuric acid (ACS reagent, 95 % to 98 %) and potassium permanganate (97 %) from Sigma Aldrich. Glacial acetic acid (ACS Reag. Ph Eur) was acquired from Carlo Erba, while oxalic acid (98 % anhydrous) from Acros Organics. We purchased the 3-hydroxypropionic acid sodium salt from Toronto Research Chemicals. The tungstic acid (99 %) catalyst was purchased from Sigma Aldrich.

6.3.2 Catalytic experiment

We designed a full factorial set of experiments with 3 factors and 3 levels each (27 tests) with the statistical software *Minitab*®. The reactions time were at 1 h, 3 h, 6 h, with a LEV :H_2WO_4 ratio of 100 :1, 50 :1, 10 :1 and H_2O_2 :LEV ratio of 1.5 :1, 3 :1, 5 :1. An oil bath kept the temperature constant at 90 °C. We derived the sample standard deviation, s (Table 6.2), by repeating experiments at three different conditions.

We investigated the reaction pathway, evaluating the reactivity of the intermediates at 1 h

Table 6.2 Repetition of three tests at various conditions. * H_2O_2 :LEV molar ratio, ** LEV : H_2WO_4 molar ratio. Conversion (X) and Selectivities (S) are in %. Succ : succinic acid ; acet : acetic acid ; mal : malonic acid ; oxal : oxalic acid, form : formic acid, AL : α-angelica lactone ; HPA : 3-hydroxypropionic acid ; gly+glyox : glycolic acid and glyoxylic acid ; prop : propionic acid.

	Conv	S_{succ}	S_{acet}	S_{mal}	S_{form}	S_{AL}	S_{HPA}	$S_{gly+glyox}$	S_{prop}
Sample standard deviation *s*	2	2	0.5	0.3	0.2	1	0.4	0	0.3

and 6 h, with a LEV :H_2WO_4 molar ratio of 100 and H_2O_2 :LEV molar ratio of 5. In a standard reaction procedure, we added 5 mmol (0.58 g) of LEV into an Erlenmeyer flask, with the specified amount of catalyst (H_2WO_4, i.e. 0.124 g for a LEV :H_2WO_4 molar ratio of 10) and H_2O_2 solution (aqueous solution 27 % w/w, i.e. 0.93 g for a H_2O_2 :LEV molar ratio of 1.5). The mixture was homogenized for few minutes, while an oil bath heated it to the desired temperature (90 °C). The flask was equipped with a reflux condenser to avoid an excessive evaporation of the solution. By means of gas-chromatography we qualitatively analyzed the non-condensable gases inside the flask, which turned out to contain CO_2. At the end of the test, the mixture was cooled rapidly from 90 °C down to room temperature, diluted with distilled water and filtered using a disposable syringe equipped with 0.20 µm PTFE filter to preserve the HPLC column. Tungstic acid is insoluble in cold water (only slightly soluble in hot water), however in the presence of H_2O_2 the catalyst is soluble in the state of pertungstic acid (H_2WO_5). This means that working at high H_2O_2 conversion would favor the precipitation of the catalyst facilitating its recovery by filtration Weiss et al. (1966). For catalyst recycle tests, we put the mixture in the rotavapor, in order to completely evaporate water and traces of residual H_2O_2. In order to remove the adsorbed organic compounds, the catalyst was washed with acetone, and dried in the oven at 80 °C overnight. This procedure allowed to recover the 70 % of the initial H_2WO_4 amount, in the form of a yellow solid.

6.3.3 Analytical procedure

A Varian CP-3380 gas chromatography equipped with a packed Carbosieve SII column (2 m length, stationary phase of active carbons of 80 mesh to 100 mesh) was used to analyze the non-condensable gases. A TCD monitored the concentration of CO, CO_2, O_2 and N_2, with He as the carrier gas. The oven was maintained at 40 °C for 7 min, then the temperature was ramped up until 220 °C with a rate of 30 °C min^{-1}, and finally left isothermal for 10 min. An HPLC Agilent Technologies 1260 Infinity, equipped with an Aminex HPX-87H Ion Exclusion column (300 mm x 7.8 mm), maintained at 30 °C, measured the concentration of the crude products. The autosampler injected 10 µL of the solution, while the eluent was a 5 mM H_2SO_4 solution, flowing at 0.4 mL min^{-1}. The instrument monitored the response of the samples at 8 wavelengths (from 210 nm to 284 nm). The LEV conversion (Eq. 6.1) and the products selectivity based on carbon (Eq. 6.2) were calculated as follows :

$$X_{\mathrm{LEV}} = \frac{n^{i}_{\mathrm{LEV}} - n^{fi}_{\mathrm{LEV}}}{n^{i}_{\mathrm{LEV}}} \cdot 100 \tag{6.1}$$

$$S_{\mathrm{PROD}} = \frac{n^f_{\mathrm{PROD}}}{n^i_{\mathrm{LEV}} - n^f_{\mathrm{LEV}}} \cdot \frac{\theta_{\mathrm{PROD}}}{\theta_{\mathrm{LEV}}} \cdot 100 \tag{6.2}$$

where n^i_{LEV} and n^f_{LEV} are the initial moles and the final LEV moles in the system, n^f_{PROD} the final moles of product analyzed by HPLC. θ_{LEV} and θ_{PROD} are the number of carbon atoms of LEV and products. We evaluated the amount of unconverted hydrogen peroxide with a 0.3 N potassium permanganate solution and a diluted 1 :4 aqueous sulfuric acid solution. The titration proceeded with the addition of distilled water and 10 mL of acidic solution to the sample. We titrated the sample using a calibrated burette until the solution turned permanent pink USP Technologies (2018). The mass percentage of H_2O_2 by (Eq. 6.3) :

$$H_2O_2, \%\ \mathrm{g\,g^{-1}} = \frac{\mathrm{mL}_{\mathrm{KMnO_4}} \cdot N_{\mathrm{KMnO_4}} \cdot 0.0170 \cdot 1000}{\mathrm{g}_{\mathrm{sample}}} \tag{6.3}$$

where N is the normality of the $KMnO_4$ solution, $\mathrm{mL}_{\mathrm{KMnO_4}}$ is the volume of permanganate used for the titration and 0.0170 is the mass per milliequivalent of H_2O_2.

6.4 Results and discussion

6.4.1 LEV reactivity and selective oxidation

Reactivity screening tests at three H_2O_2 concentration (H_2O_2 :LEV molar ratio of 1 :1, 1.5 :1 and 3 :1), three temperatures (50 °C,70 °C and 90 °C) and constant H_2WO_4 :LEV molar ratio of 100 demonstrated a very low LEV conversion, reaching a minimum of 5 % at the lowest temperature and peroxide content (Test 31, Table 6.3). Increasing the temperature led to an increased conversion of LEV. Therefore, all the further experiments were carried out at 90 °C. Time, catalyst mass and H_2O_2 content affect succinic acid selectivity and LEV conversion (Figure 6.1, Table 6.3). The maximum variation of conversion was recorded at H_2O_2 :LEV ratio of 3 and LEV :H_2WO_4 ratio of 50 ; the value increased from 28 % after 1 h to 46 % after 6 h reaction time (Table 6.3, entries 13 and 15). Addition of H_2O_2 and H_2WO_4 amplified the oxidative power and the acidity of the reaction media, enhancing the reactivity of the substrate. The highest LEV conversion was shown at 6 h, reaching 57 % at the highest hydrogen peroxide concentration and catalyst loading (Table 6.3, entry 27). Furthermore, at these conditions, we recorded the highest conversion after 1 h of reaction (Figure 6.1).

Succinic acid selectivity increased from 10 % (Table 6.3, entry 1) to 49 % (entry 9) with increasing H_2O_2 and time. Increasing the H_2WO_4, its behavior changed ; at 50 :1 LEV :H_2WO_4 molar ratio, the selectivity increased with peroxide concentration, reaching a maximum after

3 h, but then decreased (entries 10-18).

This trend was accentuated at higher catalyst loading, where the highest selectivity was registered after 1 h, and then decreased with time (entries 19-27). Figure 6.2 summarizes the effect of the two main reaction parameters on selectivity to succinic acid at 3 h.

We measured acetic acid, malonic acid, oxalic acid, formic acid, α-angelica lactone, 3-hydroxypropionic acid, propionic acid, glycolic acid and glyoxylic acid concentration by means of HPLC (Table 6.3). Some intermediates reacted further to CO_2 and volatile compounds Feng et al. (2018), which were undetected. Acetic acid was the main by-product and it formed in all tests. Many compounds decomposed to this acid, which accounts for its high selectivity, and increased with H_2WO_4 and H_2O_2 concentration and longer time. Selectivity to acetic acid approached 10 % after 1 h, and rose to 20 % after 6 h. The highest selectivity was 23 % (Table 6.3, entry 23). We detected low concentrations of oxalic acid in all the reactions, but it never exceeded 5 %, and mainly remained below 1 %. Oxalic acid easily oxidizes in the presence of acidic oxidizing environment, releasing CO_2 Ignaczak et al. (2017). For LEV :H_2WO_4 catalytic ratio higher than 50, selectivity hardly were higher than 1 %, while at ratio of 10, values increased from 2 % to 5 %.

Glycolic and glyoxylic acids showed low selectivity, which remained almost always lower than 1 %. Formic acid presented a similar trend : selectivity varied between 0 % to 5 %, with a general increase with time and H_2WO_4 loading. Results at low H_2O_2 concentration showed that the absence of reactive oxygen stopped the Baeyer-Villiger oxidation, favouring the dehydration of LEV to α-angelica lactone. In acidic conditions and low H_2O_2 concentrations (LEV :H_2O_2 molar ratio 1 :1), selectivity to α-angelica lactone was 50 percent from LEV. At higher H_2O_2 concentration, α-angelica lactone degraded to acetic acid and malonic acid (Table 6.4). α-Angelica lactone selectivity decreased with reaction time and was the greatest

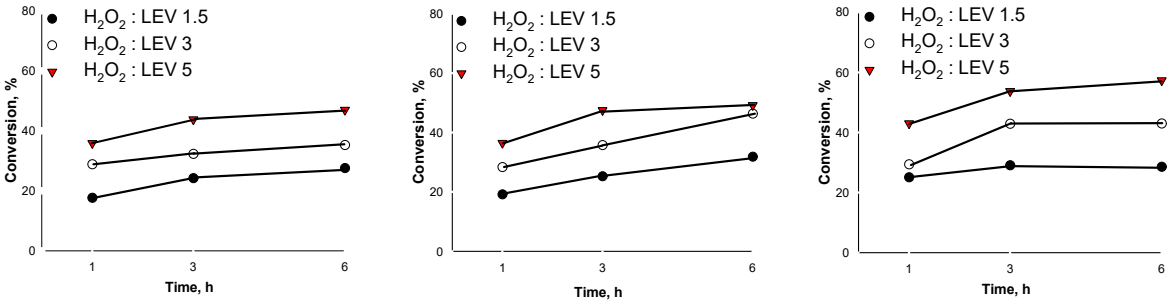

(a) (b) (c)

Figure 6.1 Effects of various amount of H_2O_2 and H_2WO_4 on the conversion at 1 h, 3 h and 6 h. LEV :H_2WO_4 molar ratio : 100 (left figure), 50 (middle), 10 (right)

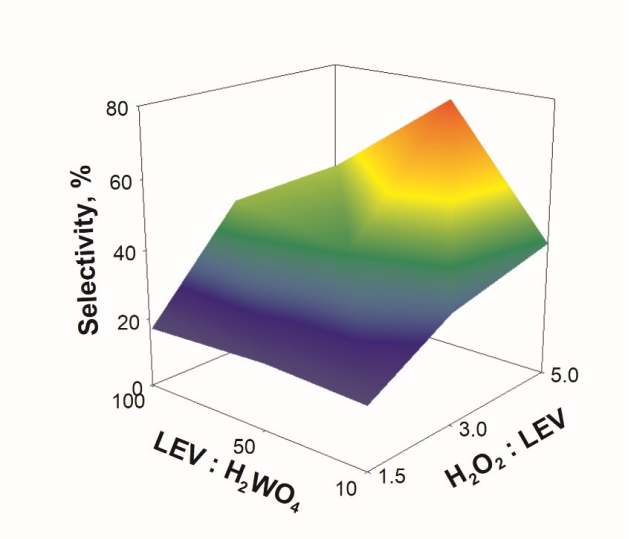

Figure 6.2 Succinic acid selectivity reached a maximum with the highest concentration of H_2O_2 and LEV :H_2WO_4 ratio of 50, after 3 h.

with low tungstic acid loading (Table 6.3, entries 1, 4 and 7) : at 1 h, 3 h, and 6 h, selectivity dropped from 38 % down to 21 %, and 14 %, respectively. In experiments at a 1.5 :1 H_2O_2 :LEV ratio and 100 :1 LEV :H_2WO_4 ratio, after 1 h the lactone selectivity was 38 %, but dropped to 2 % after 6 h (entries 1-3). This behavior could be attributed to the degradation of the lactone, which is highly unstable in the presence of oxidizing agents and acids. Selectivity to the lactone was very high in experiments carried out with a H_2O_2 :LEV ratio of 0.5 (entries 28-30). The selectivity to 3-hydroxypropionic acid was always lower than 4 % with the lowest H_2O_2 concentration. However, the selectivity increased with H_2O_2 concentration and reached 25 % at a H_2O_2 :LEV ratio of 5 :1 (entries 8 and 9 in Table 6.3). Generally, the selectivity reached a maximum after 3 h, and then slowly decreased. Furthermore, higher H_2WO_4 loading boosted the reactivity of 3-hydroxypropionic acid, resulting in selectivity values lower than 1 %. Succinic acid may decarboxylate to propionic acid. At the highest amount of H_2WO_4 (low LEV :H_2WO_4 ratio) almost no propionic acid was detected, due to its degradation to acetic acid and CO_2. The highest values of propionic acid selectivity were shown with the lowest catalyst loading and highest hydrogen peroxide concentration, reaching a selectivity of 6 % (Table 6.3, entries 8 and 9).

In the three experiments at H_2O_2 :LEV ratio 0.5 :1 and LEV :H_2WO_4 ratio 100 :1 (Table 6.3, entries 28-30), H_2O_2 conversion approached 100 % after 1 h reaction time; in fact, LEV conversion showed a moderate growth, passing from 15 % at the first hour to 17 % after 6 h. Besides the usual by-products, we also detected the formation of acrylic acid (not shown

Table 6.3 Effects of time, H_2WO_4 and H_2O_2 content on conversion and selectivity. * H_2O_2 :LEV molar ratio, ** LEV :H_2WO_4 molar ratio. Succ : succinic acid ; acet : acetic acid ; mal : malonic acid ; oxal : oxalic acid, form : formic acid, AL : α-angelica lactone ; HPA : 3-hydroxypropionic acid ; gly+glyox : glycolic acid and glyoxylic acid ; prop : propionic acid. *** Test 31 at 50 °C, adding one drop of H_2O_2 every 10 s, and at the end leaving the reaction run for 20 min more.

Exp	H_2O_2*	H_2WO_4**	Time, h	Conv, %	S_{succ}, %	S_{acet}, %	S_{mal}, %	S_{oxal}, %	S_{form}, %	SAL, %	S_{HPA}, %	$S_{gly+glyox}$, %	S_{prop}, %
1	1.5	100	1	18	10	14	5	0.7	2	38	1	4	0.6
2	1.5	100	3	24	17	18	7	0.7	3	4	3	0.1	2
3	1.5	100	6	28	19	20	7	2	3	2	4	0.2	0.3
4	3	100	1	29	10	8	6	0.3	0.6	21	4	2	2
5	3	100	3	32	47	13	6	0.6	0.9	0.2	14	0.5	3
6	3	100	6	35	48	17	6	0.8	1	0.3	11	0.1	3
7	5	100	1	36	2	3	3	0.2	0.4	14	0.6	0.5	4
8	5	100	3	44	48	8	4	0.4	1	0.6	25	0.1	6
9	5	100	6	47	49	12	4	0.5	1	2	25	0	6
10	1.5	50	1	19	12	11	5	0.8	3	29	1	0.2	0.5
11	1.5	50	3	25	19	17	8	3	3	3	3	0.2	0.3
12	1.5	50	6	32	18	18	6	2	3	2	2	0.2	0.1
13	3	50	1	28	32	4	3	0.3	0.2	9	0	0.1	2
14	3	50	3	36	41	18	7	2	2	1	11	0.2	3
15	3	50	6	46	29	22	5	2	2	4	3	0.2	0.5
16	5	50	1	37	23	1	2	0.1	1	10	0	0	2
17	5	50	3	48	75	9	4	0.7	0.6	3	15	0.1	5
18	5	50	6	49	71	17	4	0.9	0.8	0	12	0.1	3
19	1.5	10	1	25	35	13	7	5	3	4	1	2	0.2
20	1.5	10	3	29	18	19	8	3	4	3	1	0.2	0
21	1.5	10	6	43	11	13	4	2	3	0	1	0.2	0
22	3	10	1	29	62	9	9	5	3	6	2	0	0.9
23	3	10	3	43	32	23	7	5	4	3	1	0.2	0.6
24	3	10	6	32	22	20	6	3	5	1	1	0.1	0
25	5	10	1	43	58	12	5	4	2	4	1	1	2
26	5	10	3	54	39	21	5	0.3	3	1	1	1	0.3
27	5	10	6	57	35	22	4	4	3	1	1	0	0
28	0.5	100	1	15	7	5	3	0.3	1	53	0.7	0.4	0.2
29	0.5	100	3	16	10	11	4	0.6	2	50	0.8	0.2	0
30	0.5	100	6	17	7	8	3	0.4	2	49	0.7	0.3	0.1
31***	3	100	0.35	5	6	2	1	0	0	24	0	0	0

in Table 6.3) ; its selectivity was 8 % after 1 h, slightly increasing to 13 % after 3 h and then decreasing down to 10 % after 6 h. In order to check the stability and recyclability of H_2WO_4, the catalyst was recovered after reaction (see Experimental), and recycled a few times. Differences of catalytic performance between each experiment were within the standard deviation ; therefore, the behavior of the recycled catalyst can be considered to be the same as that one of the fresh catalyst (Annexes B).

6.4.2 Selectivity versus time

Most of the by-products selectivity were invariant with time (Figure 6.3) : 3-HPA selectivity was 1 %, malonic acid 8 %, formic acid 4 %, oxalic acid about 2 %, whereas α-angelica lactone varied from 0 % to 5 %. Succinic acid selectivity decreased from 35 % to 11 % after 6 h. Acetic acid, the main by-product, reached a maximum of 19 % at 3 h after which it dropped to 13 %. LEV conversion was 25 % after 1 h and increased to 43 % at 6 h. We did not detect the formation of propionic acid. The total carbon selectivity decreased from 75 % after 1 h down to 40-45 % after 6 h reaction time. This drop is due to the product overoxidation occurring along with the increasing LEV conversion. We did not close the carbon mass balance due to the formation of volatile molecules (mainly CO_2) that left the reactor and the formation of insoluble polymers, which slightly changed the color of the solution during the reaction. For short reaction times the solution was colourless. We calculated the H_2O_2 remaining in the reaction mixture by titration. When the hydrogen peroxide was the limiting reagent (H_2O_2 :LEV ratio 0.5 :1), the oxidant conversion was almost complete (98 %). When the oxidant was in slight excess (ratio 1.5 :1), after 1 h reaction time H_2O_2 conversion was 86 % (overall selectivity to oxidized products, calculated with respect to converted H_2O_2, was 56 % ; therefore, 44 % of converted H_2O_2 decomposed), which increased up to 92 % after 3 h (selectivity 54 %). Working in large oxidant excess (ratio 5 :1) and the highest catalyst loading, the H_2O_2 conversion dropped to 64 %.

6.4.3 The reaction network

The oxidation pathway proceeds with the formation of various by-products and intermediates. The Baeyer-Villiger mechanism consists of the addition of an oxygen atom to convert a ketone to an ester. Oxygen from a peroxide compound attacks the molecule with two competitive mechanisms to form methyl succinate or 3-acetoxypropanoic acid Kawasumi et al. (2017). Moreover, in the presence of an acidic environment or high temperature, LEV dehydrates to α-angelica lactone Enslow and Bell (2015) (Figure 6.4). Wu et al. (2015) found that the regioselectivity of the Baeyer-Villiger oxidation with hydrogen peroxide is pH controlled :

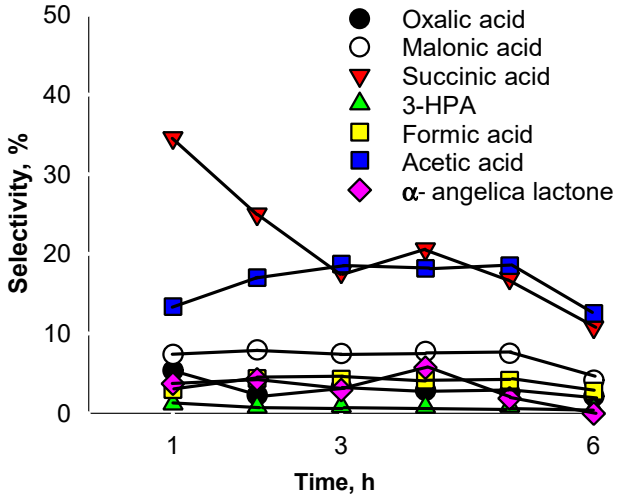

Figure 6.3 Variation of the selectivity of the products with time. LEV :H_2WO_4 = 10 ; H_2O_2 :LEV = 1.5 ; T 90 °C.

under alkaline conditions the insertion of oxygen is favored on the secondary carbon, leading to the 3-acetoxypropanoic acid intermediate and subsequently to 3-HPA and acetic acid, with 50 % yield. In strong acidic conditions — trifluoroacetic acid as solvent — the migration of the less substituted carbon is favored. This mechanism produces methyl succinate as the intermediate, with subsequent acidic cleavage of the ether to methanol and succinic acid, with 60 % yield. As a side reaction, 10 % 3-HPA is also recovered Dutta et al. (2015).

Methanol can further react with H_2O_2 to form oxidized derivatives : formaldehyde, formic acid and finally CO_2, but MeOH and CH_2O were absent in the HPLC chromatogram traces. These compounds oxidize to CO_2 in the presence of hydrogen peroxide. 3-HPA, formed by hydrolysis of 3-acetoxypropanoic acid, can dehydrate to acrylic acid in the absence of oxidizing agents Dishisha et al. (2015), or can follow the retro-aldolic reaction to acetic acid and formaldehyde. The latter, in an oxidizing environment reacts to formic acid Dutta et al. (2015). In an alternative pathway, oxidation of the hydroxyl group of 3-HPA gives malonic acid Shende and Levee (1999). In order to confirm that the reaction network was similar also with our catalyst and reaction conditions, we carried out experiments by testing the reactivity of both succinic acid and main by-products/intermediates, using the lowest level of H_2WO_4 and the highest of H_2O_2, at 1 h and 6 h reaction time (Table 6.4). The experiments with succinic acid as substrate demonstrated an increase in the conversion with time, from 1 % registered after 1 h reaction time to 7 % after 6 h. Those low values provided evidence for the high stability of the product in the reaction mixture. Decarboxylation of succinic acid led to propionic acid, which further can lose a molecule of CO_2 producing acetic acid. Propionic acid

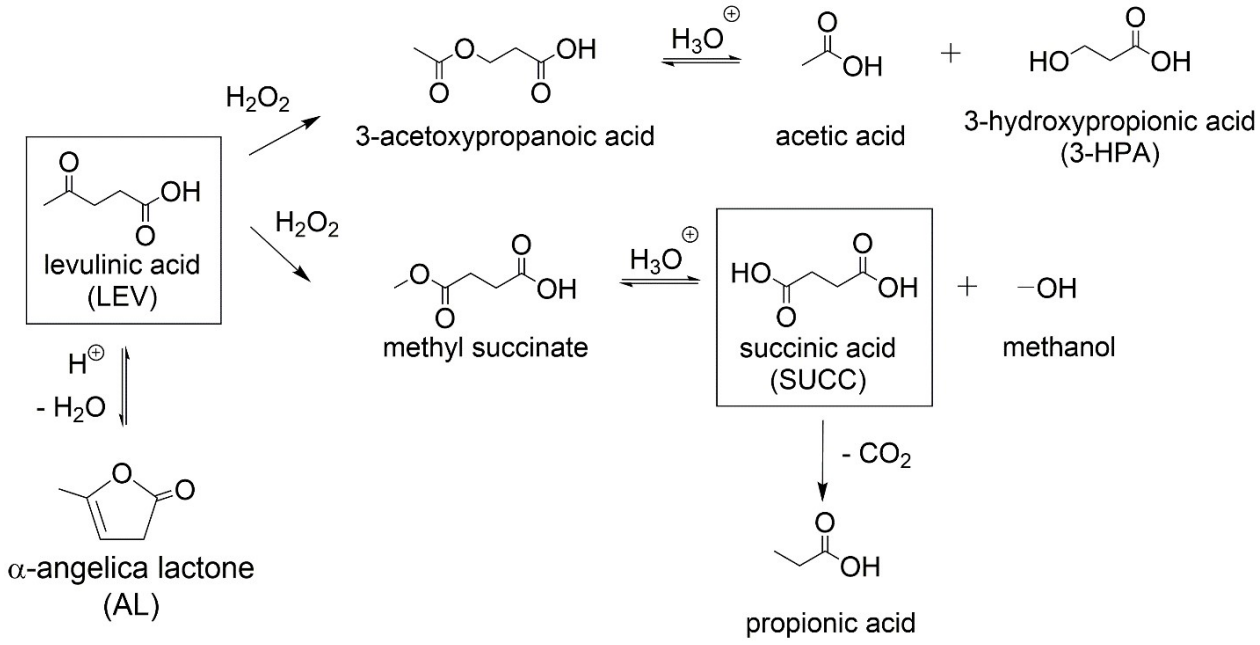

Figure 6.4 Hydrogen peroxide adds an oxygen to LEV with two competitive mechanisms. The first leads to 3-acetoxypropanoic acid and consequently to 3-HPA, while the second produces methyl succinate, which is in equilibrium with succinic acid.

selectivity reached 10 % after the first hour of reaction, and consequently dropped to 1 % at 6 h (Table 6.4). In tests carried out starting from propionic acid, the acid conversion slightly increased from 18 % to 25 % along with the increase of reaction time. The main products were glycolic and glyoxylic acid and acetic acid. The firsts remained almost constant after 6 h at 5 %, while the acetic acid increased from 0.6 % to 3 %. It is worth noting that in the experiments with succinic acid we did not detect the presence of glycolic/glyoxylic acid. Experiments carried out starting from 3-HPA confirmed the oxidizing pathways proposed in the literature ; at the end of the reaction, we detected acetic acid, malonic acid, oxalic acid and formic acid. Formic acid selectivity attested at 7 %, while acetic acid was around 22 % and malonic acid around 6 %.

The tests on malonic acid degradation showed that at high H_2O_2 concentration, the molecule presented high reactivity ; in this case the conversion attested around 70 %. Malonic acid oxidized to acetic acid, which continued the pathway to glycolic acid and oxalic acid ; the analysis showed an increase of around 15 % to glycolic acid and glyoxylic acid from 1 h to 6 h. The two experiments with glycolic acid as starting material demonstrated an high reactivity of the substrate when in contact with H_2O_2 (conversion around 75 %). However, we were unable to detect any key products, due to the complete degradation to volatile compounds.

Table 6.4 Oxidation of the intermediates and the by-products at T 90 °C, reactant :H_2WO_4 molar ratio 100 and H_2O_2 :reactant ratio 5. Succ : succinic acid ; acet : acetic acid ; mal : malonic acid ; oxal : oxalic acid, form : formic acid, AL : α-angelica lactone ; HPA : 3-hydroxypropionic acid ; gly+glyox : glycolic acid and glyoxylic acid ; prop : propionic acid

Reagent	t, h	Conv, %	S_{succ}, %	S_{acet}, %	S_{mal}, %	S_{oxal} %	S_{form}, %	S_{AL}, %	S_{HPA}, %	$S_{gly+glyox}$ %	S_{prop}, %
Succinic acid	1	1	-	0	0	1	0	0	0	0	10
Succinic acid	6	7	-	3	4	6	1	0	0	0	1
Malonic acid	1	72	-	1	-	17	2	-	0	6	0.4
Malonic acid	6	70	-	4	-	12	3	-	0	21	0
3 – HPA	1	22	-	22	6	3	7	-	-	0	0
3 – HPA	6	20	-	25	7	0.1	8	-	-	0.1	0.5
Glycolic acid	1	77	-	0	-	0	0	-	-	-	-
Glycolic acid	6	74	-	0.1	-	0	6	-	-	-	-
Propionic acid	1	18	-	0.6	0	0	0	-	0	6	-
Propionic acid	6	25	-	3	0	0	0	-	0	4	-
α-angelica lactone	1	47	0	52	27	10	4	-	0	1	9
α-angelica lactone	6	60	4	58	23	10	4	-	0	0.3	0

Three experiments of LEV oxidation at low loading of H_2O_2 (entries 28-30, Table 6.3) showed that under conditions of oxidant starvation LEV preferably converted to α-angelica lactone instead of being oxidized to succinic acid or 3-HPA. The lactone is in equilibrium with the starting material Chatzidimitriou and Bond (2015). In experiments carried out starting from the lactone (Table 6.4), the latter was converted mainly to acetic acid and malonic acid.

6.4.4 The regioselectivity in Baeyer-Villiger oxidation of LEV

Results shown in Table 6.3 demonstrate that the H_2WO_4 controls the regioselectivity of the two competitive pathways from LEV to either succinic acid or 3-HPA. In fact, by modulating the catalyst loading we obtained a selectivity ratio succinic acid :3-HPA of $> 98\,\%$, after 6 hour and at 10 % molar ratio of catalyst (Table 6.3, entry 27). Each increment of H_2O_2 also augmented the selectivity ratio of the two-competitive kinetics, enhancing the role of catalyst in a proportional fashion (Figure 6.5).

Based on these results, we propose that H_2WO_4 in an organic solvent free environment arranges with the carboxylic group of LEV to form an octagonal cyclic adduct by hydrogen bonding (Figure 6.6).

This conformation locks the molecule and impedes the Baeyer-Villiger migration of the secondary carbon by steric hindrance. Indeed, we also found that this interaction locks LEV and impedes the dehydration and the consequent cyclization to α-angelica lactone. In fact, selectivity to the lactone decreased with increasing the catalyst loading. The major example is the reduction from 38 % to 4 % lactone selectivity after 1 h reaction time, indicating the interaction of the H_2WO_4 with LEV (Table 6.3, entries 1 and 19).

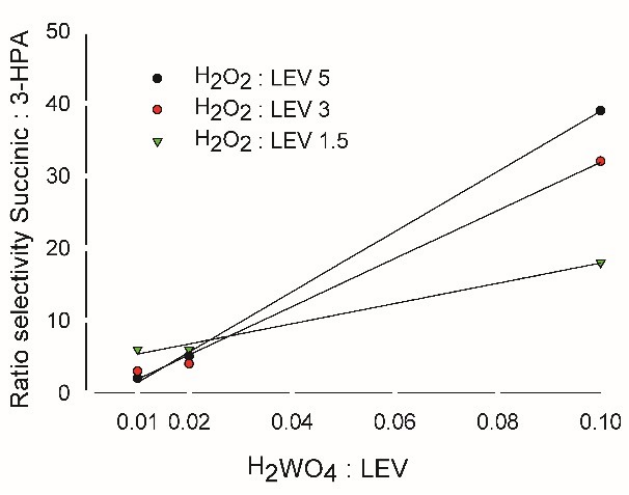

Figure 6.5 Direct correlation between the H_2WO_4 catalyst and the selectivity ratio succinic acid :3-HPA.

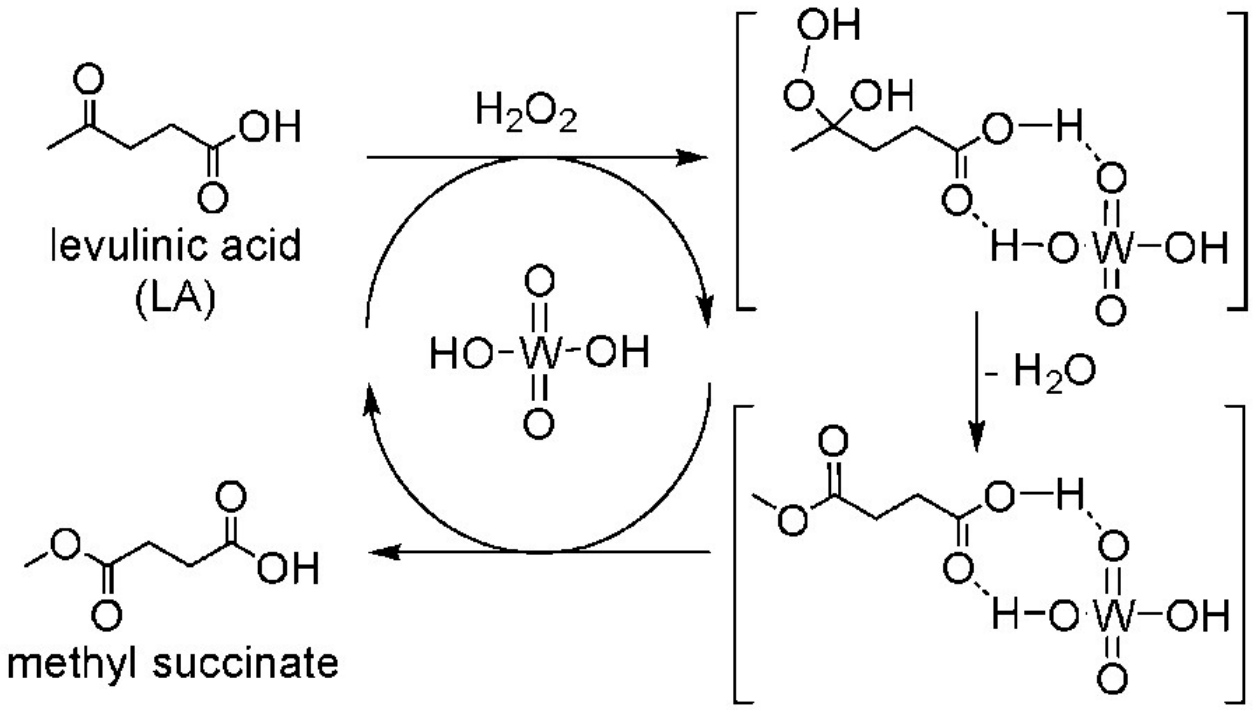

Figure 6.6 The H_2WO_4 catalyst interacts with LEV, forming an octagonal cyclic adduct, which due to sterical hindrance, reduced the migration of the most substituted carbon, and consequently enhances the formation of the methyl succinate.

6.5 Conclusions

Tungstic acid catalyzed the conversion of levulinic acid to succinic acid with hydrogen peroxide and no organic solvent. We investigated the effects of time, ratio between H_2O_2 and both H_2WO_4 and the substrate. The results confirmed an interaction mechanism of the tungstic acid with the substrate, which indicates the regioselectivity of the catalyst and the decrease of LEV dehydration to α-angelica lactone. Controlling the catalyst loading modulated the selectivity of the two-competitive kinetics, achieving more than 97 % ratio between selectivities of succinic acid and 3-HPA. We achieved a maximum conversion of 48 % and 75 % selectivity to succinic acid with LEV :H_2WO_4 molar ratio of 50 and H_2O_2 :LEV of 5. To investigate the decomposition pathway, we ran experiments with increasing time testing each intermediate's reactivity, with lowest amount of catalyst and a H_2O_2 :LEV molar ratio of 5. We demonstrated the decomposition pathway of succinic acid, which formed acetic acid as main by-product, followed by malonic acid and formic acid.

CHAPTER 7 GENERAL DISCUSSION

Sugars are outstanding sources for bio-chemicals and bio-fuels. Enzymatic fermentation to bio-ethanol is the main valorization process, but it is limited by the low theoretical yield and the lower market value compared to other bio-chemicals from carbohydrates. Fructose is an excellent starting material, with an elevate oxygen-carbon ratio. This characteristic makes it more suitable to synthesize bio-building blocks rather than fossil fuels. Dehydration to 5-hydroxymethyl furfural (HMF) is the most attracting reaction, due to the elevate application versatility. The main limitations are the aqueous acidic cleavage to levulinic acid and formic acid, and the degradation to insoluble polymers called humins. HMF converts to 2,5-dimethyl furan, a valid substitute of bio-ethanol as gasoline additive. HMF oxidation produces 2,5-furandicarboxylic acid (FDCA), the furanic substitute of terephthalic acid for bio-polymers. Polymerization with ethylen glycol form poly(ethylen furanoate) (PEF), a superior chemical and physical plastic for bottles and packaging. One of the main hurdle on the conversion of sugars to furanic compounds is their low solubility in water. To overcome this limitation, application of organic solvents increases the dissolution of the products. Furthermore, products extraction minimize the degradation process and increase the final purity, which is fundamental for the plastic industry to avoid change in the product's colour.

This PhD project aims to develop a new process to valorize fructose and at the same time establish a new route to convert the dehydration by-product — levulinic acid — to a highly value-added chemicals for environmental friendly applications.

The first part of the project identified and demonstrated the feasibility to convert fructose into a fluidized bed reactor. We identified WO_3/TiO_2 as potential catalyst for the dehydration of fructose to HMF. Furthermore, it ensured a spherical geometry of the particles and a high attrition resistance. The support, TiO_2 was inert for the dehydration reaction of fructose. The incipient wetness impregnation deposited the tungsten on the titania. We prepared 4 levels of WO_3/TiO_2. A sparger, directly inserted into the catalytic bed, atomized the aqueous solution. Argon and oxygen flowed from the bottom of the reactor, ensuring the fluidization of the catalyst. We improved the atomization, modulating the liquid-to-gas ratio, and adding a ceramic tube on the injector to reduce the heat transfer. This modification reduced the coke formation on the tip of the sparger, which causes the pressure to increase and the consequent blockage of the nozzle. A furnace, coupled with four thermocouples in various point of the reactor, maintained the temperature constant for all the experiences. A water/dimethyl sulfoxide (DMSO) quench dissolved the products. An online MS monitored

the non-condensable gases, while HPLC analysis determined the products concentration at various intervals.

Fructose decarbonylated to furfural, with a maximum yield of 22 % after 6 h, with 5 % WO_3 loading on TiO_2. Acetic acid was the predominant by-product, which generally accounted to less than 10 % molar. DFF was the co-product of the reaction, demonstrating a maximum of 15 % yield. COx concentration were elevate, reaching up to 81 %. Fructose partially degraded inside the catalytic bed, forming coke that agglomerated the particles. SEM investigated the surface of the material, showing a well disperse tungsten on the surface and the formation of small coke particles. After 6 h the reaction reaches the steady-state. The selectivity to furfural increases with time, while the acetic acid showed a rapid decrease for the first 3 h, to then further stabilize. Improving the heat exchanged between the sparger and the reactor demonstrates a continuous feed injection for 19 h. The main limitation of the system is the carbon efficiency.

After demonstrated the feasibility to convert fructose in a gas-phase fluidized bed reactor, we implemented and further optimized the setup and the reaction conditions, targeting the oxidehydration of fructose to FDCA. Adding Pt on the surface of a 5 % WO_3/TiO_2 catalyst, we screened six reaction variables : temperature, O_2 :fructose molar ratio, mass catalyst loaded, Pt loading, feed flowrate and feed fructose mass concentration. Lower contact time and higher temperature increased the formation of HMF and other furanic compounds. We develop a full factorial design, with three levels of temperature (300 °C,350 °C and 400 °C), and of O_2 concentration (0.5 :1, 1 :1 and 10 :1) and two levels for catalyst mass (1.5 g and 3 g). Pt loading (1.5 %), liquid flowrate (300 µL min^{-1}) and fructose mass percentage in the feed (2 % remained constant for all the tests. Higher temperature and lower contact time increased the selectivity of the furanic compounds. HMF selectivity reached the maximum of 12 % at 350 °C, 1.5 g catalyst and with 0.5 molar ratio of O_2. The main by-products were furfural, 5-methylfurfural and diformyl furan. The three variables investigated demonstrated no influence on the FUR selectivity. DFF surprising remained low for all the tests, never exceeding the 3 %. Further investigation on the HMF oxidation showed at low catalyst (1.5 g) and low temperature (250 °C) a maximum DFF selectivity of 42 %, with an HMF conversion of 86 %. Higher contact time drastically reduced all the furanic products.

The third part of the project, developed at University of Bologna, focused on the valorization of levulinic acid, the by-product of the fructose dehydration. We investigated the Baeyer-Villiger oxidation to succinic acid with H_2O_2 and H_2WO_4 in the liquid phase, without organic solvents. We designed a set of experiments, evaluating the influence of time (1 h, 3 h and 6 h), levulinic acid : H_2WO_4 molar ratio (100 :1, 50 :1 and 10 :1) and the

H_2O_2 :LEV molar ratio (1.5 :1, 3 :1 and 5 :1). In an Erlenmeyer flask, maintained at 90 °C, we added the starting material with the catalyst and the hydrogen peroxide. The flask was covered but not completely closed. HPLC measured the liquid products concentration, while GC qualitatively analyzed the non-condensable gases. The oxidation to succinic acid follows two possible pathways : formation of the 3-acetoxypropanoic acid or the methyl succinate. LEV conversion increased with time and amount of H_2O_2. Succinic acid selectivity reached a maximum of 75 % with a levulinic acid conversion of 48 %. The main by-product of the reaction was acetic acid, followed by malonic acid and formic acid. We further investigated the reaction pathway, reacting the intermediates at the same conditions and evaluating the products. The catalyst reacted with the substrate, forming an octagonal cyclic abduct. Catalyst loading modulate the selectivity of the two competitive kinetics, achieving a maximum of 97 % molar ratio between succinic acd and 3-HPA. We evaluated the recycling of catalyst ; after reaction we purified and recovered 70 percent of H_2WO_4, and further tests with the same material demonstrated similar results with respect to the fresh catalyst.

CHAPTER 8 CONCLUSION

8.1 Conclusion

Sugars posses a tremendous potential to a variety of chemicals and bio-fuels. They are mainly fermented to bio-ethanol, but bio-chemicals from carbohydrates present higher market value and carbon efficiency. The project demonstrate the catalytic valorization of sugars, focusing on developing a fluidized bed reactor to convert fructose in the gas-phase, and oxidizing levulinic acid to succinic acid with hydrogen peroxide.

The main limitations for the conversion of sugars in the liquid phase are the long contact time, and the application of organic solvents to reduce the degradation to humins.

The first step was to develop a solid-liquid-gas phase μ-fluidized bed reactor, where the liquid feed is continuously injected through a sparger, and atomized directly into the catalytic bed. The system did not require any organic solvent and the contact time was from 0.3 s to 0.4 s. We investigated the effects of O_2, temperature and tungsten loading on the decarbonylation of fructose to furfural by WO_3/TiO_2. The main by-products are acetic acid and diformyl furan. After 6 h reaction, the reaction reached the steady state. Protecting the sparger, increased the continuous injection up to 19 h.

The main limitation was the low carbon atom efficiency, due to the loss of a molecule of carbon per mole of furfural produced. We added Pt on the 5 % WO_3/TiO_2 catalyst. Mass catalyst and temperature mainly influence the dehydration of fructose to HMF.

The catalyst mainly dehydrated fructose to HMF, reaching a maximum of 12 % after 6 h. To further investigate the oxidation power of the catalyst, tests with HMF as starting material and lower amount of catalyst demonstrated a maximum selectivity of 42 % to DFF. The catalyst does not possess enough oxidizing power to further convert DFF to FDCA, which reflects the low amount of FDCA quantified during the analysis with fructose as substrate. This technology define a new pathway for the conversion of sugars to value-added chemicals and bio-fuels.

The last part of the project focused on the oxidation of levulinic acid to succinic acid. Levulinic acid is the degradation product of HMF. Industrially is synthesized from fossil fuels, but switching to renewable resource will reduce is appealing. We demonstrated the green Baeyer-Villiger transformation of LEV, with H_2O_2 and tunsgtic acid as catalyst. We investigated the effects of H_2O_2, H_2WO_4 and time on the conversion of LEV. Increasing reaction time, concentration of reagents and catalyst increased the conversion. The oxidation follows

to possible pathways : formation of succinic acid or 3-hydroxypropionic acid. Catalyst loading modulate the two competitive kinetics. We propose the formation of an adduct that explains the interaction between the substrate and the tungstic acid. We obtained the maximum selectivity to succinic acid of 75 % after 3 h with H_2O_2 :LEV ratio of 5 and LEV :H_2WO_4 of 50.

8.2 Limitation of the solution proposed

In the micro-fluidized bed reactor, injection of highly concentrated liquid sugar solution may drastically increase the coke formation and the particles agglomeration. Furthermore, higher temperature will favor the degradation process, resulting into cleavage of the molecule and low carbon efficiency.

8.3 Recommendations for the future research

Here we present for the first time the conversion of hexoses in micro-fluidized bed reactor, operating in the gas-phase. Furthermore, levulinic acid is oxidized to succinic acid through the Baeyer-Villiger mechanism, without any organic solvent at mild conditions.

Pt-WO_3/TiO_2 demonstrated a selective dehydration of fructose to HMF, and the oxidation of HMF to DFF. This technology is just at the beginning of its development, and many parameters and active phases should be investigated. Noble metals (such as Au, Pd or Rh) could improve the oxidation step, directly oxidehydrate fructose to FDCA. Furthermore, addition of a third active phase, which will play as promoter (like K, Na or Ce), can improve the final yield. Replacing expensive metals with low cost materials (like Mn, V or Fe) will decrease the catalyst price, making them more affordable for a future scale-up.

Liquid injection in fluidized bed reactor is a wide technology employed to insert reagents into the catalytic bed. Commercially there are no micro injector able to sustain high temperature and low fluid flowrate ; for this reason we produced each injector filing a 1/16 ” stainless steel tube. Scaling-up the system allows to equip the reactor with a commercial injector, which will create a more reliable and similar spray between each experiment.

Finally, tests with glucose as starting material could reduce the costs of the process even further.

For the levulinic acid oxidation to succinic acid, we tested only few catalysts (TS-1, Al_2O_3 and H_2WO_4), but then we developed the research only on the tungstic acid. The first step could be the screening of other type of catalyst that demonstrate good activity in the Baeyer-

Villiger oxidation. Furthermore, the methodology to add H_2O_2 is fundamental for the reaction — add dropwise the peroxide, or directly include it in the reaction mixture. At the end, tests with sugars as starting material, and addition of a second catalyst for the dehydration step of sugar to HMF, could make a one-pot synthesis and intensify the process.

LIST OF REFERENCES

T. M. Aida, Y. Sato, M. Watanabe, K. Tajima, T. Nonaka, H. Hattori, et K. Arai, "Dehydration of d-glucose in high temperature water at pressures up to 80 mpa", *J. Supercrit. Fluids*, no. 3, pp. 381–388, 2007. DOI : 10.1016/j.supflu.2006.07.027

S. Akgöl, Y. Kaçar, A. Denizli, et M. Y. Arca, "Hydrolysis of sucrose by invertase immobilized onto novel magnetic polyvinylalcohol microspheres", *Food Chemistry*, vol. 74, no. 3, pp. 281–288, 2001. DOI : 10.1016/S0308-8146(01)00150-9

G. R. Akien, L. Qi, et I. T. Horváth, "Molecular mapping of the acid catalysed dehydration of fructose", *Chemical Communications*, vol. 48, no. 47, p. 5850, 2012. DOI : 10.1039/c2cc31689g

S. Albonetti, T. Pasini, A. Lolli, M. Blosi, M. Piccinini, N. Dimitratos, J. A. Lopez-Sanchez, D. J. Morgan, A. F. Carley, G. J. Hutchings, et F. Cavani, "Selective oxidation of 5-hydroxymethyl-2-furfural over TiO_2-supported gold-copper catalysts prepared from preformed nanoparticles : Effect of Au/Cu ratio", *Catalysis Today*, vol. 195, no. 1, pp. 120–126, 2012. DOI : 10.1016/j.cattod.2012.05.039

S. Albonetti, A. Lolli, V. Morandi, A. Migliori, C. Lucarelli, et F. Cavani, "Conversion of 5-hydroxymethylfurfural to 2,5-furandicarboxylic acid over Au-based catalysts : Optimization of active phase and metal-support interaction", *Applied Catalysis B : Environmental*, vol. 163, pp. 520–530, 2015. DOI : 10.1016/j.apcatb.2014.08.026

Allied Market Research Report, "Furfural market by raw material (corn cob, rice husk, sugarcane bagasse, and others), application (furfuryl alcohol and solvent), and end user industry (petroleum refineries, agricultural formulations, paints & coatings, pharmaceuticals, and others) — global opportunity analysis and industry forecast, 2014-2022", 2017. En ligne : https://www.alliedmarketresearch.com/furfural-market

D. M. Alonso, S. H. Hakim, S. Zhou, W. Won, O. Hosseinaei, J. Tao, V. Garcia-Negron, A. H. Motagamwala, M. A. Mellmer, K. Huang, C. J. Houtman, N. Labbé, D. P. Harper, C. T. Maravelias, T. Runge, et J. A. Dumesic, "Increasing the revenue from lignocellulosic biomass : Maximizing feedstock utilization", *Science Advances*, vol. 3, no. 5, 2017. DOI : 10.1126/sciadv.1603301

D. An, A. Ye, W. Deng, Q. Zhang, et Y. Wang, "Selective conversion of cellobiose and

cellulose into gluconic acid in water in the presence of oxygen, catalyzed by polyoxometalate-supported gold nanoparticles", *Chemistry - A European Journal*, vol. 18, no. 10, pp. 2938–2947, 2012. DOI : 10.1002/chem.201103262

C. Antonetti, D. Licursi, S. Fulignati, G. Valentini, et A. Raspolli Galletti, "New Frontiers in the Catalytic Synthesis of Levulinic Acid : From Sugars to Raw and Waste Biomass as Starting Feedstock", *Catalysts*, vol. 6, no. 12, p. 196, 2016. DOI : 10.3390/catal6120196

C. Antonetti, M. Melloni, D. Licursi, S. Fulignati, E. Ribechini, S. Rivas, J. C. Parajó, F. Cavani, et A. M. Raspolli Galletti, "Microwave-assisted dehydration of fructose and inulin to HMF catalyzed by niobium and zirconium phosphate catalysts", *Applied Catalysis B : Environmental*, vol. 206, pp. 364–377, 2017. DOI : 10.1016/j.apcatb.2017.01.056

F. S. Asghari et H. Yoshida, "Acid-catalyzed production of 5-hydroxymethyl furfural from D-fructose in subcritical water", *Industrial and Engineering Chemistry Research*, vol. 45, no. 7, pp. 2163–2173, 2006. DOI : 10.1021/ie051088y

Avantium, "Avanitum - FDCA", 2018. En ligne : https://www.avantium.com/yxy/products-applications/

Avantium, "YXY technology for bio-based packaging", 2018. En ligne : https://www.synvina.com/technology/process

BASF. (2016) Synvina : Joint venture of BASF and Avantium established. En ligne : www.basf.com

I. Bechthold, K. Bretz, S. Kabasci, R. Kopitzky, et A. Springer, "Succinic acid : A new platform chemical for biobased polymers from renewable resources", *Chemical Engineering and Technology*, vol. 31, no. 5, pp. 647–654, 2008. DOI : 10.1002/ceat.200800063

S. H. Bhosale, M. B. Rao, et V. V. Deshpande, "Molecular and industrial aspects of glucose isomerase." *Microbiological reviews*, vol. 60, no. 2, pp. 280–300, 1996.

M. Bicker, J. Hirth, et H. Vogel, "Dehydration of fructose to 5-hydroxymethylfurfural in sub- and supercritical acetone", *Green Chemistry*, vol. 5, no. 2, pp. 280–284, 2003. DOI : 10.1039/b211468b

M. Bicker, D. Kaiser, L. Ott, et H. Vogel, "Dehydration of D-fructose to hydroxymethylfurfural in sub- and supercritical fluids", *Journal of Supercritical Fluids*, vol. 36, no. 2, pp. 118–126, 2005. DOI : 10.1016/j.supflu.2005.04.004

Z. Bin, C. Xueshan, Z. Cunshan, Y. Xiaojie, M. Haile, Z. Jing, et B. Xinjie, "Highly-Efficient and Low-Cost Synthesis of 5-Hydroxymethylfurfural from Monosaccharides Catalyzed by Surface Treated Biomass", *The Canadian Journal of Chemical Engineering*, no. September, 2017. DOI : 10.1002/cjce.23077

A. Boisen, T. B. Christensen, W. Fu, Y. Y. Gorbanev, T. S. Hansen, J. S. Jensen, S. K. Klitgaard, S. Pedersen, A. Riisager, T. St ? ?hlberg, et J. M. Woodley, "Process integration for the conversion of glucose to 2,5-furandicarboxylic acid", *Chemical Engineering Research and Design*, vol. 87, no. 9, pp. 1318–1327, 2009. DOI : 10.1016/j.cherd.2009.06.010

T. R. Boussie, E. L. Dias, Z. M. Fresco, V. J. Murphy, S. James, A. Raymond, et J. Hong, "Production of adipic acid and derivatives from carbohydrates-containing materials", 2010, Patent # WO 2010/144862 A2.

J. J. Bozell et G. R. Petersen, "Technology development for the production of biobased products from biorefinery carbohydrates—the US Department of Energy's "Top 10" revisited", *Green Chemistry*, vol. 12, no. 4, p. 539, 2010. DOI : 10.1039/b922014c

J. J. Bozell, L. Moens, D. C. Elliott, Y. Wang, G. G. Neuenscwander, S. W. Fitzpatrick, R. J. Bilski, et J. L. Jarnefeld, "Production of levulinic acid and use as a platform chemical for derived products", *Resources, Conservation and Recycling*, vol. 28, no. 3-4, pp. 227–239, 2000. DOI : 10.1016/S0921-3449(99)00047-6

S. Bruhns et J. Werther, "An investigation of the mechanism of liquid injection into fluidized beds", *AIChE Journal*, vol. 51, no. 3, pp. 766–775, 2005. DOI : 10.1002/aic.10336

L. Bu, Y. Tang, Y. Gao, H. Jian, et J. Jiang, "Comparative characterization of milled wood lignin from furfural residues and corncob", *Chemical Engineering Journal*, vol. 175, no. 1, pp. 176–184, 2011. DOI : 10.1016/j.cej.2011.09.091

L. Bui, H. Luo, W. R. Gunther, et Y. Rom á n Leshkov, "Domino reaction catalyzed by zeolites with brönsted and lewis acid sites for the production of γ-valerolactone from furfural", *Angew. Chem. Int. Ed.*, vol. 52, no. 31, pp. 8022–8025, 2013. DOI : 10.1002/anie.201302575

S. K. Burgess, O. Karvan, J. R. Johnson, R. M. Kriegel, et W. J. Koros, "Oxygen sorption and transport in amorphous poly(ethylene furanoate)", *Polymer*, vol. 55, no. 18, pp. 4748–4756, 2014.

S. K. Burgess, J. E. Leisen, B. E. Kraftschik, C. R. Mubarak, R. M. Kriegel, et W. J. Koros,

"Chain mobility, thermal, and mechanical properties of poly(ethylene furanoate) compared to poly(ethylene terephthalate)", *Macromolecules*, vol. 47, no. 4, pp. 1383–1391, 2014.

S. K. Burgess, D. S. Mikkilineni, D. B. Yu, D. J. Kim, C. R. Mubarak, R. M. Kriegel, et W. J. Koros, "Water sorption in poly(ethylene furanoate) compared to poly(ethylene terephthalate). part 1 : Equilibrium sorption", *Polymer*, vol. 55, no. 26, pp. 6861–6869, 2014.

S. K. Burgess, R. M. Kriegel, et W. J. Koros, "Carbon dioxide sorption and transport in amorphous poly(ethylene furanoate)", *Macromolecules*, vol. 48, no. 7, pp. 2184–2193, 2015.

Business insider, "Sugar price commodity", 2018. En ligne : `http://markets.businessinsider.com/commodities/sugar-price`

S. Camarero Espinosa, T. Kuhnt, E. J. Foster, et C. Weder, "Isolation of thermally stable cellulose nanocrystals by phosphoric acid hydrolysis", *Biomacromolecules*, vol. 14, no. 4, pp. 1223–1230, 2013. DOI : `10.1021/bm400219u`

L. Cao, I. K. Yu, S. S. Chen, D. C. Tsang, L. Wang, X. Xiong, S. Zhang, Y. S. Ok, E. E. Kwon, H. Song, et C. S. Poon, "Production of 5-hydroxymethylfurfural from starch-rich food waste catalyzed by sulfonated biochar", *Bioresource Technology*, vol. 252, no. October 2017, pp. 76–82, 2018. DOI : `10.1016/j.biortech.2017.12.098`

S. Caratzoulas, M. E. Davis, R. J. Gorte, R. Gounder, R. F. Lobo, V. Nikolakis, S. I. Sandler, M. A. Snyder, M. Tsapatsis, et D. G. Vlachos, "Challenges of and insights into acid-catalyzed transformations of sugars", *J. Phys. Chem. C*, vol. 118, no. 40, pp. 22 815–22 833, 2014. DOI : `10.1021/jp504358d`

A. Caretto et A. Perosa, "Upgrading of levulinic acid with dimethylcarbonate as solvent/reagent", *ACS Sustainable Chemistry and Engineering*, vol. 1, no. 8, pp. 989–994, 2013. DOI : `10.1021/sc400067s`

T. R. Carlson, J. Jae, Y. C. Lin, G. A. Tompsett, et G. W. Huber, "Catalytic fast pyrolysis of glucose with HZSM-5 : The combined homogeneous and heterogeneous reactions", *Journal of Catalysis*, vol. 270, no. 1, pp. 110–124, 2010. DOI : `10.1016/j.jcat.2009.12.013`

T. R. Carlson, Y.-T. Cheng, J. Jae, et G. W. Huber, "Production of green aromatics and olefins by catalytic fast pyrolysis of wood sawdust", *Energy Environ. Sci.*, vol. 4, no. 1, pp. 145–161, 2011. DOI : `10.1039/C0EE00341G`

D. Carnevali, O. Guévremont, M. G. Rigamonti, M. Stucchi, F. Cavani, et G. S. Patience, “Gas-Phase Fructose Conversion to Furfural in a Microfluidized Bed Reactor”, *ACS Sustainable Chemistry & Engineering*, vol. 6, no. 4, pp. 5580–5587, 2018. DOI : 10.1021/acssuschemeng.8b00510

M. Carrier, A. Loppinet-Serani, D. Denux, J. M. Lasnier, F. Ham-Pichavant, F. Cansell, et C. Aymonier, “Thermogravimetric analysis as a new method to determine the lignocellulosic composition of biomass”, *Biomass and Bioenergy*, vol. 35, no. 1, pp. 298–307, 2011. DOI : 10.1016/j.biombioe.2010.08.067

Chao Wang, Liming Zhang, T. Zhou, J. Chen, et F. Xu, “Synergy of Lewis and Brønsted acids on catalytic hydrothermal decomposition of carbohydrates and corncob acid hydrolysis residues to 5-hydroxymethylfurfural”, *Scientific Reports*, no. 7, 2017. DOI : 10.1038/srep40908

A. Chatzidimitriou et J. Q. Bond, “Oxidation of levulinic acid for the production of maleic anhydride : breathing new life into biochemicals”, *Green Chem.*, vol. 17, no. 8, pp. 4367–4376, 2015. DOI : 10.1039/C5GC01000D

H. Chen, Z. Zheng, Z. Chen, et X. T. Bi, “Reduction of hematite (Fe_2O_3) to metallic iron (Fe) by CO in a micro fluidized bed reaction analyzer : A multistep kinetics study”, *Powder Technology*, vol. 316, pp. 410–420, 2017. DOI : 10.1016/j.powtec.2017.02.067

J. D. Chen, B. F. Kuster, et K. Van Der Wiele, “Preparation of 5-hydroxymethylfurfural via fructose acetonides in ethylene glycol dimethyl ether”, *Biomass and Bioenergy*, vol. 1, no. 4, pp. 217–223, 1991. DOI : 10.1016/0961-9534(91)90006-X

X. Chen, H. Yang, Y. Chen, W. Chen, T. Lei, W. Zhang, et H. Chen, “Catalytic fast pyrolysis of biomass to produce furfural using heterogeneous catalysts”, *J. Anal. Appl. Pyrolysis*, no. January, pp. 0–1, 2017. DOI : 10.1016/j.jaap.2017.07.022

S. W. Cheung et B. C. Anderson, “Laboratory investigation of ethanol production from municipal primary wastewater solids”, *Bioresource Technology*, vol. 59, no. 1, pp. 81–96, 1997. DOI : 10.1016/S0960-8524(96)00109-5

J. N. Chheda, Y. Román-Leshkov, et J. A. Dumesic, “Production of 5-hydroxymethylfurfural and furfural by dehydration of biomass-derived mono- and poly-saccharides”, *Green Chem.*, vol. 9, no. 4, pp. 342–350, 2007. DOI : 10.1039/B611568C

V. Choudhary, S. H. Mushrif, C. Ho, A. Anderko, V. Nikolakis, N. S. Marinkovic, A. I.

Frenkel, S. I. Sandler, et D. G. Vlachos, “Insights into the interplay of Lewis and Brønsted acid catalysts in glucose and fructose conversion to 5-(hydroxymethyl) furfural and levulinic acid in aqueous media”, *Journal of the American Chemical Society*, vol. 135, no. 10, pp. 3997–4006, 2013. DOI : 10.1021/ja3122763

H. Cui et J. R. Grace, “Fluidization of biomass particles : A review of experimental multiphase flow aspects”, *Chemical Engineering Science*, vol. 62, no. 1-2, pp. 45–55, 2007. DOI : 10.1016/j.ces.2006.08.006

J. Cui, J. Tan, T. Deng, X. Cui, Y. Zhu, et Y. Li, “Conversion of carbohydrates to furfural via selective cleavage of the carbon–carbon bond : the cooperative effects of zeolite and solvent”, *Green Chem.*, vol. 18, no. 6, pp. 1619–1624, 2016. DOI : 10.1039/C5GC01948F

M. Dalil, D. Carnevali, J. L. Dubois, et G. S. Patience, “Transient acrolein selectivity and carbon deposition study of glycerol dehydration over WO_3/TiO_2 catalyst”, *Chemical Engineering Journal*, vol. 270, pp. 557–563, 2015. DOI : 10.1016/j.cej.2015.02.058

M. Dalil, D. Carnevali, M. Edake, A. Auroux, J. L. Dubois, et G. S. Patience, “Gas phase dehydration of glycerol to acrolein : Coke on WO_3/TiO_2 reduces by-products”, *Journal of Molecular Catalysis A : Chemical*, vol. 421, pp. 146–155, 2016. DOI : 10.1016/j.molcata.2016.05.022

M. J. Darabi Mahboub, M. Rostamizadeh, J.-L. Dubois, et G. S. Patience, “Partial oxidation of 2-methyl-1,3-propanediol to methacrylic acid : experimental and neural network modeling”, *RSC Advances*, vol. 6, pp. 114 123–114 134, 2016. DOI : 10.1039/c6ra16605a

D. de Guzman, “Bio-based building blocks and polymers. global capacities and trends 2016—2021”, 2017. En ligne : http://www.bio-based.eu/reports

F. C. de Melo, R. F. de Souza, P. L. A. Coutinho, et M. O. de Souza, “Synthesis of 5-hydroxymethylfurfural from dehydration of fructose and glucose using ionic liquids”, *J. Braz. Chem. Soc.*, vol. 25, no. 12, pp. 2378–2384, 2014. DOI : 10.1038/nature08274

R. L. de Souza, H. Yu, F. Rataboul, et N. Essayem, “5-Hydroxymethylfurfural (5-HMF) Production from Hexoses : Limits of Heterogeneous Catalysis in Hydrothermal Conditions and Potential of Concentrated Aqueous Organic Acids as Reactive Solvent System”, *Challenges*, vol. 3, no. 2, pp. 212–232, 2012. DOI : 10.3390/challe3020212

A. Demirbaş, “Bioethanol from cellulosic materials : A renewable motor fuel from biomass”, *Energy Sources*, vol. 27, no. 4, pp. 327–337, 2005. DOI : 10.1080/00908310390266643

E. Derrien, M. Mounguengui-Diallo, N. Perret, P. Marion, C. Pinel, et M. Besson, “Aerobic oxidation of glucose to glucaric acid under alkaline-free conditions : Au-based bimetallic catalysts and effect of residues in a hemicellulose hydrolysate”, *Ind. Eng. Chem. Res.*, pp. 13 175–13 189, 2017. DOI : 10.1021/acs.iecr.7b01571

M. E. Diaz De Villegas, P. Villa, M. Guerra, E. Rodriguez, D. Redondo, et A. Martinez, “Conversion of furfural into furfuryl alcohol by *saccharomyces cervisiae 354*”, *Acta Biotechnologica*, vol. 12, no. 4, pp. 351–354, 1992. DOI : 10.1002/abio.370120420

G. Ding, Y. Zhu, H. Zheng, H. Chen, et Y. Li, “Vapour phase hydrogenolysis of biomass-derived diethyl succinate to tetrahydrofuran over CuO−ZnO/solid acid bifunctional catalysts”, *J. Chem. Technol. Biotechnol.*, vol. 86, no. 2, pp. 231–237, 2011. DOI : 10.1002/jctb.2503

T. Dishisha, S. H. Pyo, et R. Hatti-Kaul, “Bio-based 3-hydroxypropionic- and acrylic acid production from biodiesel glycerol via integrated microbial and chemical catalysis”, *Microbial Cell Factories*, vol. 14, no. 1, pp. 1–11, 2015. DOI : 10.1186/s12934-015-0388-0

L. Doskočil, L. Grasset, D. Válková, et M. Pekař, “Hydrogen peroxide oxidation of humic acids and lignite”, *Fuel*, vol. 134, pp. 406–413, 2014. DOI : 10.1016/j.fuel.2014.06.011

G. Düll, “Action of oxalic acid on inulin”, *Chem. Ztg*, vol. 19, pp. 216–220, 1895.

A. Dunlop et S. Shelbert, “Preparation of succinic acid”, 1952. En ligne : http://www.google.com/patents/WO2012044168A1?cl=en

S. Dutta, S. De, B. Saha, et M. I. Alam, “Advances in conversion of hemicellulosic biomass to furfural and upgrading to biofuels”, *Catal. Sci. Technol.*, vol. 2, no. 10, p. 2025, 2012. DOI : 10.1039/c2cy20235b

S. Dutta, L. Wu, et M. Mascal, “Efficient, metal-free production of succinic acid by oxidation of biomass-derived levulinic acid with hydrogen peroxide”, *Green Chemistry*, vol. 17, no. 4, pp. 2335–2338, 2015. DOI : 10.1039/C5GC00098J

K. R. Enslow et A. T. Bell, “SnCl ₄ -catalyzed isomerization/dehydration of xylose and glucose to furanics in water”, *Catal. Sci. Technol.*, vol. 5, no. 5, pp. 2839–2847, 2015. DOI : 10.1039/C5CY00077G

B. A. Fachri, R. M. Abdilla, H. H. D. Bovenkamp, C. B. Rasrendra, et H. J. Heeres, “Experimental and kinetic modeling studies on the sulfuric acid catalyzed conversion of

d -fructose to 5-hydroxymethylfurfural and levulinic acid in water", *ACS Sustain. Chem. Eng.*, vol. 3, no. 12, pp. 3024–3034, 2015. DOI : 10.1021/acssuschemeng.5b00023

Y. Fan, E. Chenglin, M. Shi, C. Xu, J. Gao, et C. Lu, "Diffusion of feed spray in fluid catalytic cracker riser", *AIChE Journal*, vol. 56, no. 4, pp. 858–868, 2010. DOI : 10.1002/aic.12035

M. Fanselow, J. Holbrey, K. R. Seddon, et K. Seddon, "Preparing water-soluble cellulose hydrolysis products e.g. glucose involves mixing cellulose with ionic liquid comprising cations and anions, and treating resulting solvate/solution with acid in presence of water", 2007.

J. Feng, X. Zhang, J. Fu, et H. Chen, "Catalytic ozonation of oxalic acid over rod-like ceria coated on activated carbon", *Catalysis Communications*, vol. 110, no. March, pp. 28–32, 2018. DOI : 10.1016/j.catcom.2018.03.001

S. W. Fitzpatrick, "Production of levulinic acid from carbohydrate-containing materials", 1997, US Patent # 5,608,105. DOI : 10.1074/JBC.274.42.30033.(51)

C. Fu, X. Xiao, Y. Xi, Y. Ge, F. Chen, J. Bouton, R. A. Dixon, et Z. Y. Wang, "Down-regulation of Cinnamyl Alcohol Dehydrogenase (CAD) Leads to Improved Saccharification Efficiency in Switchgrass", *Bioenergy Research*, vol. 4, no. 3, pp. 153–164, 2011. DOI : 10.1007/s12155-010-9109-z

P. Gallezot, "Conversion of biomass to selected chemical products", *Chem. Soc. Rev.*, vol. 41, no. 4, pp. 1538–1558, 2012. DOI : 10.1039/C1CS15147A

J. Gao, C. Xu, S. Lin, G. Yang, et Y. Guo, "Simulations of Gas-Liquid-Solid 3-Phase Flow and Reaction in FCC Riser Reactors", *AIChE Journal*, vol. 47, no. 3, pp. 677–692, 2001. DOI : 10.1002/aic.690470315

T. Gao, Y. Yin, W. Fang, et Q. Cao, "Highly dispersed ruthenium nanoparticles on hydroxyapatite as selective and reusable catalyst for aerobic oxidation of 5-hydroxymethylfurfural to 2, 5-furandicarboxylic acid under base-free conditions", *Molecular Catalysis*, vol. 450, no. January, pp. 55–64, 2018. DOI : 10.1016/j.mcat.2018.03.006

W. Gao, M. R. Farahani, M. Rezaei, A. Qudair Baig, M. K. Jamil, M. Imran, et R. Rezaee-Manesh, "Kinetic modeling of biomass gasification in a micro fluidized bed", *Energy Sources, Part A : Recovery, Utilization and Environmental Effects*, vol. 39, no. 7, pp. 643–648, 2017. DOI : 10.1080/15567036.2016.1236302

A. B. Gawade, M. S. Tiwari, et G. D. Yadav, "Biobased green process : Selective hydrogenation of 5-hydroxymethylfurfural to 2,5-dimethyl furan under mild conditions using

Pd−$Cs_2 \cdot 5\,H_0 \cdot 5\,PW_{12}O_{40}$ /k-10 clay", *ACS Sustainable Chemistry & Engineering*, vol. 4, no. 8, pp. 4113–4123, 2016. DOI : 10.1021/acssuschemeng.6b00426

A. B. Gawade, A. V. Nakhate, et G. D. Yadav, "Selective synthesis of 2, 5-furandicarboxylic acid by oxidation of 5-hydroxymethylfurfural over MnFe2O4catalyst", *Catalysis Today*, vol. 309, no. August 2017, pp. 119–125, 2018. DOI : 10.1016/j.cattod.2017.08.061

D. Geldart, "Types of gas fluidization", *Powder Technology*, vol. 7, no. 5, pp. 285–292, 1973. DOI : 10.1016/0032-5910(73)80037-3

T. Ghaznavi, C. Neagoe, et G. S. Patience, "Partial oxidation of D-xylose to maleic anhydride and acrylic acid over vanadyl pyrophosphate", *Biomass and Bioenergy*, vol. 71, pp. 285–293, 2014. DOI : 10.1016/j.biombioe.2014.09.029

J. Gotro, "Polyethylene Furanoate (PEF) : 100% Biobased Polymer to Compete with PET ?" 2013. En ligne : https://polymerinnovationblog.com/

F. L. Grasset, B. Katryniok, S. Paul, V. Nardello-Rataj, M. Pera-Titus, J.-M. Clacens, F. De Campo, et F. Dumeignil, "Selective oxidation of 5-hydroxymethylfurfural to 2,5-diformylfuran over intercalated vanadium phosphate oxides", *RSC Advances*, vol. 3, no. 25, p. 9942, 2013. DOI : 10.1039/c3ra41890a

G. D. Guerrero Peña, Y. A. Hammid, A. Raj, S. Stephen, T. Anjana, et V. Balasubramanian, "On the characteristics and reactivity of soot particles from ethanol-gasoline and 2,5-dimethylfuran-gasoline blends", *Fuel*, vol. 222, no. February, pp. 42–55, 2018. DOI : 10.1016/j.fuel.2018.02.147

F. Guo, Y. Dong, Z. Lv, P. Fan, S. Yang, et L. Dong, "Pyrolysis kinetics of biomass (herb residue) under isothermal condition in a micro fluidized bed", *Energy Conversion and Management*, vol. 93, pp. 367–376, 2015. DOI : 10.1016/j.enconman.2015.01.042

Y. Guo, K. Lib, et J. H. Clark, "The synthesis of diphenolic acid using the periodic mesoporous $H_3PW_{12}O_{40}$-silica composite catalysed reaction of levulinic acid", *Green Chemistry*, pp. 839–841, 2007. DOI : 10.1039/b702739g

Y. Guo, K. Li, X. Yu, et J. H. Clark, "Mesoporous $H_3PW_{12}O_{40}$-silica composite : Efficient and reusable solid acid catalyst for the synthesis of diphenolic acid from levulinic acid", *Applied Catalysis B : Environmental*, vol. 81, no. 3-4, pp. 182–191, 2008. DOI : 10.1016/j.apcatb.2007.12.020

E. I. Gürbüz, J. M. R. Gallo, D. M. Alonso, S. G. Wettstein, W. Y. Lim, et J. A. Dumesic, "Conversion of hemicellulose into furfural using solid acid catalysts in gamma-valerolactone", *Angewandte Chemie - International Edition*, vol. 52, no. 4, pp. 1270–1274, 2013. DOI : 10.1002/anie.201207334

D. A. H. Hanaor et C. C. Sorrell, "Review of the anatase to rutile phase transformation", *J. Mater. Sci.*, vol. 46, no. 4, pp. 855–874, 2011. DOI : 10.1007/s10853-010-5113-0

J. D. Hind, F. H. Crayton, et W. Richmond, "Tobacco flavorants", 1963, US Patent 3,095,882.

Q. Hou, M. Zhen, L. Liu, Y. Chen, F. Huang, S. Zhang, W. Li, et M. Ju, "Tin phosphate as a heterogeneous catalyst for efficient dehydration of glucose into 5-hydroxymethylfurfural in ionic liquid", *Applied Catalysis B : Environmental*, vol. 224, no. July 2017, pp. 183–193, 2018. DOI : 10.1016/j.apcatb.2017.09.049

S. Hu, Z. Zhang, Y. Zhou, J. Song, H. Fan, et B. Han, "Direct conversion of inulin to 5-hydroxymethylfurfural in biorenewable ionic liquids", *Green Chemistry*, vol. 11, no. 6, p. 873, 2009. DOI : 10.1039/b822328a

X. Hu, Y. Song, L. Wu, M. Gholizadeh, et C. Z. Li, "One-pot synthesis of levulinic acid/ester from C5 carbohydrates in a methanol medium", *ACS Sustainable Chemistry and Engineering*, vol. 1, no. 12, pp. 1593–1599, 2013. DOI : 10.1021/sc400229w

X. Hu, R. J. Westerhof, D. Dong, L. Wu, et C. Z. Li, "Acid-catalyzed conversion of Xylose in 20 solvents : Insight into interactions of the solvents with Xylose, furfural, and the acid catalyst", *ACS Sustainable Chemistry and Engineering*, vol. 2, no. 11, pp. 2562–2575, 2014. DOI : 10.1021/sc5004659

Y.-B. Huang et Y. Fu, "Hydrolysis of cellulose to glucose by solid acid catalysts", *Green Chemistry*, vol. 15, no. 5, p. 1095, 2013. DOI : 10.1039/c3gc40136g

A. Ignaczak, E. Santos, W. Schmickler, et T. F. da Costa, "Oxidation of oxalic acid on boron-doped diamond electrode in acidic solutions", *Journal of Electroanalytical Chemistry*, vol. 819, no. November, pp. 410–416, 2017. DOI : 10.1016/j.jelechem.2017.11.036

International Sugar Organization, "Daily sugar prices", 2018. En ligne : https://www.isosugar.org/prices.php

J. Isaksson, A. Åsblad, et T. Berntsson, "Influence of dryer type on the performance of a

biomass gasification combined cycle co-located with an integrated pulp and paper mill", *Biomass and Bioenergy*, vol. 59, pp. 336–347, 2013. DOI : 10.1016/j.biombioe.2013.10.002

J. Jae, G. A. Tompsett, A. J. Foster, K. D. Hammond, S. M. Auerbach, R. F. Lobo, et G. W. Huber, "Investigation into the shape selectivity of zeolite catalysts for biomass conversion", *Journal of Catalysis*, vol. 279, no. 2, pp. 257–268, 2011. DOI : 10.1016/j.jcat.2011.01.019

M. I. Jahirul, M. G. Rasul, A. A. Chowdhury, et N. Ashwath, "Biofuels production through biomass pyrolysis- A technological review", *Energies*, vol. 5, no. 12, pp. 4952–5001, 2012. DOI : 10.3390/en5124952

M. E. Janka, C. E. J. Sumner, S. K. Kirk, A. S. Shaikh, et K. R. Parker, "Purifying crude furan 2,5-dicarboxylic acid by hydrogenation", 2013, u.S. Patent 8,748,479. DOI : US 2010/0311130 A1

L. Juslin, O. Antikainen, P. Merkku, et J. Yliruusi, "Droplet size measurement : I. Effect of three independent variables on droplet size distribution and spray angle from a pneumatic nozzle", *International Journal of Pharmaceutics*, vol. 123, no. 2, pp. 247–256, 1995. DOI : 10.1016/0378-5173(95)00081-S

M. Kaarsholm, F. Joensen, J. Nerlov, R. Cenni, J. Chaouki, et G. S. Patience, "Phosphorous modified zsm-5 : Deactivation and product distribution for mto", *Chem. Eng. Sci.*, vol. 62, no. 18-20, pp. 5527–5532, 2007. DOI : 10.1016/j.ces.2006.12.076

T. Kan, V. Strezov, et T. J. Evans, "Lignocellulosic biomass pyrolysis : A review of product properties and effects of pyrolysis parameters", *Renewable and Sustainable Energy Reviews*, vol. 57, pp. 126–1140, 2016. DOI : 10.1016/j.rser.2015.12.185

R. Karinen, K. Vilonen, et M. Niemel, "Biorefining : Heterogeneously catalyzed reactions of carbohydrates for the production of furfural and hydroxymethylfurfural", *ChemSusChem*, vol. 4, no. 8, pp. 1002–1016, 2011. DOI : 10.1002/cssc.201000375

R. Kawasumi, S. Narita, K. Miyamoto, K.-i. Tominaga, R. Takita, et M. Uchiyama, "One-step Conversion of Levulinic Acid to Succinic Acid Using I_2/t-BuOK System : The Iodoform Reaction Revisited", *Scientific Reports*, vol. 7, no. 1, p. 17967, 2017. DOI : 10.1038/s41598-017-17116-4

F. K. Kazi, A. D. Patel, J. C. Serrano-Ruiz, J. A. Dumesic, et R. P. Anex, "Techno-economic analysis of dimethylfuran (DMF) and hydroxymethylfurfural (HMF) production from pure

fructose in catalytic processes", *Chemical Engineering Journal*, vol. 169, no. 1-3, pp. 329–338, 2011. DOI : 10.1016/j.cej.2011.03.018

H. Khan, M. G. Rigamonti, G. S. Patience, et D. C. Boffito, "Spray dried TiO_2/WO_3 heterostructure for photocatalytic applications with residual activity in the dark", *Applied Catalysis B : Environmental*, vol. 226, pp. 311–323, 2018. DOI : https://doi.org/10.1016/j.apcatb.2017.12.049

S. Kilambi et K. L. Kadam, "Production of fermentable sugars and lignin from biomass using supercritical fluids", 2015. DOI : 10.1016/j.(73)

M. Kishimoto, Y. Nitta, Y. Kamoshita, T. Suzuki, et K. I. Suga, "Ethanol production in an immobilized cell reactor coupled with the recycling of effluent from the bottom of a distillation column", *Journal of Fermentation and Bioengineering*, vol. 84, no. 5, pp. 449–454, 1997. DOI : 10.1016/S0922-338X(97)82006-5

T. Kläusli, "AVA Biochem : commercialising renewable platform chemical 5-HMF", *Green Processing and Synthesis*, vol. 3, no. 3, pp. 235–236, 2014. DOI : 10.1515/gps-2014-0029

F. Koopman, N. Wierckx, J. H. D. Winde, et H. J. Ruijssenaars, "Bioresource Technology Efficient whole-cell biotransformation of 5-(hydroxymethyl) furfural into FDCA , 2 , 5-furandicarboxylic acid", *Bioresource Technology*, vol. 101, no. 16, pp. 6291–6296, 2010. DOI : 10.1016/j.biortech.2010.03.050

M. Kroger, U. Prüße, et K.-D. Vorlop, "A new approach for the production of 2 , 5-furandicarboxylic acid by in situ oxidation of 5-hydroxymethylfurfural starting from fructose", *Topics in Catalysis*, vol. 13, pp. 237–242, 2000. DOI : 10.1023/A:1009017929727

R. Kuipers, "Vulcanization of saturated polymers with furfural or furfural condensates", 1966, US Patent 3,262,986. En ligne : https://www.google.com/patents/US3262986

P. Kumar, D. M. Barrett, M. J. Delwiche, et P. Stroeve, "Methods for Pretreatment of Lignocellulosic Biomass for Efficient Hydrolysis and Biofuel Production", *Industrial and Engineering Chemistry (Analytical Edition)*, vol. 48, no. 8, pp. 3713–3729, 2009. DOI : 10.1021/ie801542g

V. V. Kumar, G. Naresh, S. Deepa, P. G. Bhavani, M. Nagaraju, M. Sudhakar, K. V. R. Chary, J. Tardio, S. K. Bhargava, et A. Venugopal, "Influence of W on the reduction behaviour and Brønsted acidity of Ni / TiO_2 catalyst in the hydrogenation of levulinic acid to

valeric acid : Pyridine adsorbed DRIFTS study", *"Applied Catalysis A, General"*, vol. 531, pp. 169–176, 2017. DOI : 10.1016/j.apcata.2016.10.032

D. Kunii et O. Levenspiel, "{CHAPTER} 1 - introduction", dans *Fluidization Engineering (Second Edition)*, D. Kunii et O. Levenspiel, éds. Boston : Butterworth-Heinemann, 1991, pp. 1 – 13. DOI : https://doi.org/10.1016/B978-0-08-050664-7.50007-X

——, "{CHAPTER} 2 - industrial applications of fluidized beds", dans *Fluidization Engineering (Second Edition)*, D. Kunii et O. Levenspiel, éds. Boston : Butterworth-Heinemann, 1991, pp. 15 – 59. DOI : https://doi.org/10.1016/B978-0-08-050664-7.50008-1. En ligne : https://www.sciencedirect.com/science/article/pii/B9780080506647500081

E. Kurkela, M. Nieminen, et P. Simell, "Development and commercialization of biomass and waste gasification technologies from reliable and robust co-firing plants towards synthesis gas production and advanced power cycles", dans *Proc. of Second World Biomass Conference*, 2004, pp. 10–14.

B. F. Kuster, "5-Hydroxymethylfurfural (HMF). A Review Focussing on its Manufacture", *Starch - Stärke*, vol. 42, no. 8, pp. 314–321, 1990. DOI : 10.1002/star.19900420808

J. Kuusisto, J. P. Mikkola, P. P. Casal, H. Karhu, J. Väyrynen, et T. Salmi, "Kinetics of the catalytic hydrogenation of d-fructose over a CuO-ZnO catalyst", *Chemical Engineering Journal*, vol. 115, no. 1-2, pp. 93–102, 2005. DOI : 10.1016/j.cej.2005.09.020

J. P. Lange, R. Price, P. M. Ayoub, J. Louis, L. Petrus, L. Clarke, et H. Gosselink, "Valeric biofuels : A platform of cellulosic transportation fuels", *Angewandte Chemie - International Edition*, vol. 49, no. 26, pp. 4479–4483, 2010. DOI : 10.1002/anie.201000655

N. T. Le, P. Lakshmanan, K. Cho, Y. Han, et H. Kim, "Selective oxidation of 5-hydroxymethyl-2-furfural into 2,5-diformylfuran over $VO_2^+$and Cu_2^+ ions immobilized on sulfonated carbon catalysts", *Applied Catalysis A : General*, vol. 464-465, pp. 305–312, 2013. DOI : 10.1016/j.apcata.2013.06.002

P. Lenihan, A. Orozco, E. O'Neill, M. N. M. Ahmad, D. W. Rooney, et G. M. Walker, "Dilute acid hydrolysis of lignocellulosic biomass", *Chemical Engineering Journal*, vol. 156, no. 2, pp. 395–403, 2010. DOI : 10.1016/j.cej.2009.10.061

Y. Leshkov, J. N. Chheda, et J. A. Dumesic, "Phase modifiers promote efficient production of hydroxymethylfurfural from fructose", *Science*, vol. 312, no. 5782, pp. 1933–1937, 2006.

DOI : 10.1126/science.1126337

J. Lewkowski, "Synthesis, chemistry and applications of 5-hydroxymethyl-furfural and its derivatives", *Arkivoc*, vol. 2001, no. 1, pp. 17–54, 2005. DOI : 10.3998/ark.5550190.0002.102

F. Li, B. Cao, R. Ma, J. Liang, H. Song, et H. Song, "Performance of Cu/TiO_2-SiO_2 catalysts in hydrogenation of furfural to furfuryl alcohol", *Can. J. Chem. Eng.*, vol. 94, no. October, pp. 1368–1374, 2016. DOI : 10.1002/cjce.22503

H. Li, S. Yang, A. Riisager, A. Pandey, R. S. Sangwan, S. Saravanamurugan, et R. Luque, "Zeolite and zeotype-catalysed transformations of biofuranic compounds", *Green Chem.*, vol. 18, no. 21, pp. 5701–5735, 2016.

J. Li, W. P. Tian, X. Wang, et L. Shi, "Nickel and nickel-platinum as active and selective catalyst for the maleic anhydride hydrogenation to succinic anhydride", *Chemical Engineering Journal*, vol. 175, no. 1, pp. 417–422, 2011. DOI : 10.1016/j.cej.2011.09.023

X. Li, M. Liu, et Y. Li, "Hydrodynamic behavior of liquid–solid micro-fluidized beds determined from bed expansion", *Particuology*, vol. 38, pp. 103–112, 2018. DOI : 10.1016/j.partic.2017.08.002

Y. Li, H. Liu, C. Song, X. Gu, H. Li, W. Zhu, S. Yin, et C. Han, "The dehydration of fructose to 5-hydroxymethylfurfural efficiently catalyzed by acidic ion-exchange resin in ionic liquid", *Bioresource Technology*, vol. 133, pp. 347–353, 2013. DOI : 10.1016/j.biortech.2013.01.038

H. Lin, G. N. Bennett, et K. Y. San, "Metabolic engineering of aerobic succinate production systems in Escherichia coli to improve process productivity and achieve the maximum theoretical succinate yield", *Metabolic Engineering*, vol. 7, no. 2, pp. 116–127, 2005. DOI : 10.1016/j.ymben.2004.10.003

B. Liu, Y. Ren, et Z. Zhang, "Aerobic oxidation of 5-hydroxymethylfurfural into 2,5-furandicarboxylic acid in water under mild conditions", *Green Chem.*, vol. 17, no. 3, pp. 1610–1617, 2015. DOI : 10.1039/C4GC02019G

C. M. Liu et S. Y. Wu, "From biomass waste to biofuels and biomaterial building blocks", *Renew. Energ.*, vol. 96, pp. 1056–1062, 2016. DOI : 10.1016/j.renene.2015.12.059

C. Z. Liu, F. Wang, et F. Ou-Yang, "Ethanol fermentation in a magnetically fluidized bed reactor with immobilized Saccharomyces cerevisiae in magnetic particles", *Bioresource Technology*, vol. 100, no. 2, pp. 878–882, 2009. DOI : 10.1016/j.biortech.2008.07.016

X. Liu, G. Xu, et S. Gao, “Micro fluidized beds : Wall effect and operability”, *Chemical Engineering Journal*, vol. 137, no. 2, pp. 302–307, 2008. DOI : 10.1016/j.cej.2007.04.035

Livestrong, “Sorbitol Vs. Mannitol”, 2018. En ligne : https://www.livestrong.com/article/502638-sorbitol-and-bloating-from-gas/

M. J. Lorences, J. P. Laviolette, G. S. Patience, M. Alonso, et F. V. Díez, “Fluid bed gas rtd : Effect of fines and internals”, *Powder Technol.*, vol. 168, no. 1, pp. 1—9, 2006. DOI : 10.1016/j.powtec.2006.06.010

C. Lucarelli, S. Galli, A. Maspero, A. Cimino, C. Bandinelli, A. Lolli, J. Velasquez Ochoa, A. Vaccari, F. Cavani, et S. Albonetti, “Adsorbent-Adsorbate Interactions in the Oxidation of HMF Catalyzed by Ni-Based MOFs : A DRIFT and FT-IR Insight”, *Journal of Physical Chemistry C*, vol. 120, no. 28, pp. 15 310–15 321, 2016. DOI : 10.1021/acs.jpcc.6b05428

N. Ly, K. Al-Shamery, C. E. Chan-Thaw, L. Prati, P. Carniti, et A. Gervasini, “Impact of Support Oxide Acidity in Pt-Catalyzed HMF Hydrogenation in Alcoholic Medium”, *Catalysis Letters*, vol. 147, no. 2, pp. 345–359, 2017. DOI : 10.1007/s10562-016-1945-9

S. Macrelli, J. Mogensen, et G. Zacchi, “Techno economic evaluation of 2nd generation bioethanol production from sugar cane bagasse and leaves integrated with the sugar based ethanol process”, *Biotechnology for Biofuels*, vol. 5, p. 22, 2012. DOI : 10.1186/1754-6834-5-22.

M. J. D. Mahboub, J. Wright, D. C. Boffito, J.-L. Dubois, et G. S. Patience, “Cs, V, Cu keggin–type catalysts partially oxidize 2–methyl–1, 3–propanediolto methacrylic acid”, *Appl. Catal., A*, 2018.

D. Mandelli, M. C. Van Vliet, R. A. Sheldon, et U. Schuchardt, “Alumina-catalyzed alkene epoxidation with hydrogen peroxide”, *Applied Catalysis A : General*, vol. 219, no. 1-2, pp. 209–213, 2001. DOI : 10.1016/S0926-860X(01)00693-7

K. Manikandan et K. K. Cheralathan, “Heteropoly acid supported on silicalite–1 possesing intracrystalline nanovoids prepared using biomass – an efficient and recyclable catalyst for esterification of levulinic acid”, *Applied Catalysis A : General*, vol. 547, no. August, pp. 237–247, 2017. DOI : 10.1016/j.apcata.2017.09.007

L. E. Manzer, “Catalytic synthesis of α-methylene-γ-valerolactone : A biomass-derived acrylic monomer”, *Applied Catalysis A : General*, vol. 272, no. 1-2, pp. 249–256, 2004. DOI : 10.1016/j.apcata.2004.05.048

R. Mariscal, P. Maireles-Torres, M. Ojeda, I. Sádaba, et M. López Granados, “Furfural : a renewable and versatile platform molecule for the synthesis of chemicals and fuels”, *Energy Environ. Sci.*, vol. 9, no. 4, pp. 1144–1189, 2016. DOI : 10.1039/C5EE02666K

Market Research Reports Search Engine, “Biomass Power Generation Market by Feedstock (Woody Biomass, Agriculture & Forest Residues, Biogas & Energy Crops, Urban Residues, and Landfill Gas Feedstock) and by Technology (Anaerobic Digestion, Combustion, Gasification, Co-firing & CHP, and Landfill ”, p. 269, 2015. En ligne : https://www.smartcitiesdive.com/press-release/20180115-biomass-power-generation-market-worth-us5052-billion-by-2022/

Markets & Markets, “Specialty chemicals market by type (pesticides, construction chemicals, specialty oilfield chemicals, food additives, specialty polymer and others), by function (antioxidants, biocides, surfactants, and others) - global trends & forecasts to 2020””, 2018. En ligne : https://www.marketsandmarkets.com/PressReleases/specialty-chemicals-market.asp

——, “Succinic acid market by type and by region - global forecast to 2021”, 2018. En ligne : https://www.marketsandmarkets.com/PressReleases/succinic-acid.asp

C. Megías-Sayago, J. L. Santos, F. Ammari, M. Chenouf, S. Ivanova, M. A. Centeno, et J. A. Odriozola, “Influence of gold particle size in Au/C catalysts for base-free oxidation of glucose”, *Catalysis Today*, vol. 306, pp. 183–190, 2018. DOI : 10.1016/j.cattod.2017.01.007

S. Michailos, D. Parker, et C. Webb, “A techno-economic comparison of Fischer–Tropsch and fast pyrolysis as ways of utilizing sugar cane bagasse in transportation fuels production.” *Chemical Engineering Research and Design*, vol. 118, pp. 206–214, 2017. DOI : 10.1016/j.cherd.2017.01.001

M. J. C. Molina, M. L. Granados, A. Gervasini, et P. Carniti, “Exploitment of niobium oxide effective acidity for xylose dehydration to furfural”, *Catal. Today*, vol. 254, pp. 90–98, 2015. DOI : 10.1016/j.cattod.2015.01.018

J. A. Moore et T. Tannahill, “Homo- and co-polycarbonates and blends derived from diphenolic acid”, *High Performance Polymers*, vol. 13, no. 2, pp. S305–S316, 2001. DOI : 10.1088/0954-0083/13/2/326

N. Mosier, C. Wyman, B. Dale, R. Elander, Y. Y. Lee, M. Holtzapple, et M. Ladisch, “Features of promising technologies for pretreatment of lignocellulosic biomass”, *Bioresource Technology*, vol. 96, no. 6, pp. 673–686, 2005. DOI : 10.1016/j.biortech.2004.06.025

A. H. Motagamwala, W. Won, C. Sener, D. M. Alonso, C. T. Maravelias, et J. A. Dumesic, "Toward biomass-derived renewable plastics : Production of 2,5-furandicarboxylic acid from fructose", *Science Advances*, vol. 4, no. 1, p. eaap9722, 2018. DOI : 10.1126/sciadv.aap9722

R. M. Musau et R. M. Munavu, "The preparation of 5-hydroxymethyl-2-furaldehyde (HMF) from d-fructose in the presence of DMSO", *Biomass*, vol. 13, no. 1, pp. 67–74, 1987. DOI : 10.1016/0144-4565(87)90072-2

NASDAQ, "Ethanol futures", 2017. En ligne : http://www.nasdaq.com/markets/ethanol.aspx

G. G. Nasr, A. J. Yule, et L. Bendig, *Industrial sprays and atomization : design, analysis and applications*. Springer Science & Business Media, 2013.

M. a. Neves, T. Kimura, N. Shimizu, et M. Nakajima, "State of the Art and Future Trends of Bioethanol Production", *Dynamic Biochemistry, Process Biotechnology and Molecular Biology*, vol. 1, no. 1, pp. 1–14, 2007.

J. Nie, J. Xie, et H. Liu, "Efficient aerobic oxidation of 5-hydroxymethylfurfural to 2,5-diformylfuran on supported Ru catalysts", *Journal of Catalysis*, vol. 301, pp. 83–91. DOI : 10.1016/j.jcat.2013.01.007

S.-J. Oh, S.-H. Jung, et J.-S. Kim, "Co-production of furfural and acetic acid from corncob using $ZnCl_2$ through fast pyrolysis in a fluidized bed reactor", *Bioresour. Technol.*, vol. 144, pp. 172–178, sep 2013. DOI : 10.1016/j.biortech.2013.06.077

Y. Önal, S. Schimpf, et P. Claus, "Structure sensitivity and kinetics of D-glucose oxidation to D-gluconic acid over carbon-supported gold catalysts", *Journal of Catalysis*, vol. 223, no. 1, pp. 122–133, 2004. DOI : 10.1016/j.jcat.2004.01.010

C. Orr et J. Dallavalle, *Fine Particle Measurement*. Macmillan, N.Y., 1959.

Y. J. Pagán-Torres, T. Wang, J. M. R. Gallo, B. H. Shanks, et J. A. Dumesic, "Production of 5-hydroxymethylfurfural from glucose using a combination of lewis and brønsted acid catalysts in water in a biphasic reactor with an alkylphenol solvent", *ACS Catalysis*, vol. 2, no. 6, pp. 930–934, 2012. DOI : 10.1021/cs300192z

J. B. Paine, Y. B. Pithawalla, et J. D. Naworal, "Carbohydrate pyrolysis mechanisms from isotopic labeling. part 4. the pyrolysis of d-glucose : The formation of furans", *J. Anal. Appl. Pyrolysis*, vol. 83, no. 1, pp. 37–63, 2008. DOI : 10.1016/j.jaap.2008.05.008

T. Pan, J. Deng, Q. Xu, Y. Zuo, Q. X. Guo, et Y. Fu, “Catalytic conversion of furfural into a 2,5-furandicarboxylic acid-based polyester with total carbon utilization”, *ChemSusChem*, vol. 6, no. 1, pp. 47–50, 2013. DOI : 10.1002/cssc.201200652

T. Pasini, M. Piccinini, M. Blosi, R. Bonelli, S. Albonetti, N. Dimitratos, J. A. Lopez-Sanchez, M. Sankar, Q. He, C. J. Kiely, G. J. Hutchings, et F. Cavani, “Selective oxidation of 5-hydroxymethyl-2-furfural using supported gold–copper nanoparticles”, *Green Chemistry*, vol. 13, no. 8, p. 2091, 2011. DOI : 10.1039/c1gc15355b

R. Patel, D. Wang, C. Zhu, et T. C. Ho, “Effect of injection zone cracking on fluid catalytic cracking”, *AIChE Journal*, vol. 59, no. 4, pp. 1226–1235, 2013. DOI : 10.1002/aic.13902

G. S. Patience et R. E. Bockrath, “Butane oxidation process development in a circulating fluidized bed”, *Applied Catalysis A : General*, vol. 376, pp. 4–12, 2010.

G. S. Patience, *Experimental Methods and Instrumentation for Chemical Engineers*, 2e éd. Amsterdam, Netherlands : Elsevier B.V., 2017.

S. K. Patil et C. R. Lund, “Formation and growth of humins via aldol addition and condensation during acid-catalyzed conversion of 5-hydroxymethylfurfural”, *Energy and Fuels*, vol. 25, no. 10, pp. 4745–4755, 2011. DOI : 10.1021/ef2010157

S. Peleteiro, S. Rivas, J. L. Alonso, V. Santos, et J. C. Parajó, “Furfural production using ionic liquids : A review”, *Bioresour. Technol.*, vol. 202, pp. 181–191, 2016. DOI : 10.1016/j.biortech.2015.12.017

M. H. Penner et E. T. Liaw, “Kinetic consequences of high ratios of substrate to enzyme saccharification systems based on Trichoderma cellulase”, *Enzymatic Conversion of Biomass for Fuels Production*, no. 6, pp. 363–371, 1994.

F. D. Pileidis et M. M. Titirici, “Levulinic Acid Biorefineries : New Challenges for Efficient Utilization of Biomass”, *ChemSusChem*, vol. 9, no. 6, pp. 562–582, 2016. DOI : 10.1002/cssc.201501405

I. Podolean, V. Kuncser, N. Gheorghe, D. Macovei, V. I. Parvulescu, et S. M. Coman, “Ru-based magnetic nanoparticles (MNP) for succinic acid synthesis from levulinic acid”, *Green Chemistry*, vol. 15, no. 11, p. 3077, 2013. DOI : 10.1039/c3gc41120f

F. Portoghese, L. Ferrante, F. Berruti, C. Briens, et E. Chan, “Effect of the injection-nozzle geometry on the interaction between a gas-liquid jet and a gas-solid fluidized bed”, *Chemical*

Engineering and Processing : Process Intensification, vol. 49, no. 6, pp. 605–615, 2010. DOI : 10.1016/j.cep.2010.04.011

B. Potic, S. R. A. Kersten, M. Ye, M. A. Van Der Hoef, J. A. M. Kuipers, et W. P. M. Van Swaaij, "Fluidization with hot compressed water in micro-reactors", *Chemical Engineering Science*, vol. 60, no. 22, pp. 5982–5990, 2005. DOI : 10.1016/j.ces.2005.04.047

X. Qi, M. Watanabe, T. M. Aida, et R. L. Smith Jr., "Efficient one-pot production of 5-hydroxymethylfurfural from inulin in ionic liquids", *Green Chemistry*, vol. 12, no. 10, p. 1855, 2010. DOI : 10.1039/c0gc00141d

X. Qi, H. Guo, L. Li, et R. L. Smith, "Acid-catalyzed dehydration of fructose into 5-hydroxymethylfurfural by cellulose-derived amorphous carbon", *ChemSusChem*, vol. 5, no. 11, pp. 2215–2220, 2012. DOI : 10.1002/cssc.201200363

J. L. Rahikainen, R. Martin-Sampedro, H. Heikkinen, S. Rovio, K. Marjamaa, T. Tamminen, O. J. Rojas, et K. Kruus, "Inhibitory effect of lignin during cellulose bioconversion : The effect of lignin chemistry on non-productive enzyme adsorption", *Bioresource Technology*, vol. 133, pp. 270–278, 2013. DOI : 10.1016/j.biortech.2013.01.075

C. V. Ramana, S. Utsunomiya, R. C. Ewing, C. M. Julien, et U. Becker, "Structural stability and phase transitions in WO_3 thin films", *J. Phys. Chem. B*, vol. 110, no. 21, pp. 10 430–10 435, 2006. DOI : 10.1021/jp056664i

P. V. Rathod et V. H. Jadhav, "Efficient Method for Synthesis of 2,5-Furandicarboxylic Acid from 5-Hydroxymethylfurfural and Fructose Using Pd/CC Catalyst under Aqueous Conditions", *ACS Sustainable Chemistry & Engineering*, vol. 6, p. acssuschemeng.7b03124, 2018. DOI : 10.1021/acssuschemeng.7b03124

M. G. Rigamonti, Y.-X. Song, H. Li, N. Saadatkhah, P. Sauriol, et G. S. Patience, "Influence of atomization conditions on spray drying lithium iron phosphate nanoparticle suspensions, accepted for publication", *Can. J. Chem. Eng.*, 2018.

Y. Román-Leshkov et J. A. Dumesic, "Solvent effects on fructose dehydration to 5-hydroxymethylfurfural in biphasic systems saturated with inorganic salts", *Topics in Catalysis*, vol. 52, no. 3, pp. 297–303, 2009. DOI : 10.1007/s11244-008-9166-0

Y. Román-Leshkov, C. J. Barrett, Z. Y. Liu, et J. A. Dumesic, "Production of dimethylfuran for liquid fuels from biomass-derived carbohydrates", *Nature*, vol. 447, no. 7147, pp. 982–985, 2007. DOI : 10.1038/nature05923

A. A. Rosatella, S. P. Simeonov, R. F. M. Frade, et C. A. M. Afonso, "5-Hydroxymethylfurfural (HMF) as a building block platform : Biological properties, synthesis and synthetic applications", *Green Chemistry*, vol. 13, no. 4, p. 754, 2011. DOI : 10.1039/c0gc00401d

E. Rozhko, S. Solmi, F. Cavani, A. Albini, P. Righi, et D. Ravelli, "Revising the Role of a Dioxirane as an Intermediate in the Uncatalyzed Hydroperoxidation of Cyclohexanone in Water", *Journal of Organic Chemistry*, vol. 80, no. 12, pp. 6425–6431, 2015. DOI : 10.1021/acs.joc.5b00861

S & P Global Platts, "The global proce of ethanol fuel : agriculture price assessments", 2018. En ligne : https://www.platts.com/price-assessments/agriculture/ethanol

N. Saadatkhah, M. G. Rigamonti, D. C. Boffito, H. Li, et G. S. Patience, "Spray dried SiO_2, WO_3/TiO_2, and SiO_2 vanadium pyrophosphate core-shell catalysts", *Powder Technology*, vol. 316, no. Supplement C, pp. 434–440, 2017. DOI : https://doi.org/10.1016/j.powtec.2016.10.056

I. Sádaba, S. Lima, A. A. Valente, et M. López Granados, "Catalytic dehydration of xylose to furfural : Vanadyl pyrophosphate as source of active soluble species", *Carbohydr. Res.*, vol. 346, no. 17, pp. 2785–2791, 2011. DOI : 10.1016/j.carres.2011.10.001

E. Sairanen, R. Karinen, et J. Lehtonen, "Comparison of solid acid-catalyzed and autocatalyzed C5 and C6 sugar dehydration reactions with water as a solvent", *Catalysis Letters*, vol. 144, no. 11, pp. 1839–1850, 2014. DOI : 10.1007/s10562-014-1350-1

Ó. J. Sánchez et C. A. Cardona, "Trends in biotechnological production of fuel ethanol from different feedstocks", *Bioresource Technology*, vol. 99, no. 13, pp. 5270–5295, 2008. DOI : 10.1016/j.biortech.2007.11.013

A. Scott, "Synvina's FDCA plant delayed by two years", *Chemical & Engineering News*, vol. 96, p. 12, jan 2018.

J. Shabanian et J. Chaouki, "Hydrodynamics of a gas-solid fluidized bed with thermally induced interparticle forces", *Chemical Engineering Journal*, vol. 259, pp. 135–152, 2015. DOI : 10.1016/j.cej.2014.07.117

H. Shapouri et M. Salassi, "The economic feasibility of ethanol production from sugar in the united states", *USDA report*, p. 78, 2006. DOI : 10.1016/j.biortech.2007.11.013

D. K. Shen et S. Gu, “Pyrolytic behaviour of cellulose in a fluidized bed reactor”, *Cellulose chemistry and technology*, vol. 44, no. 1-3, pp. 79–87, 2010.

R. V. Shende et J. Levee, “Kinetics of wet oxidation of propionic and 3-hydroxypropionic acids”, *Industrial and Engineering Chemistry Research*, vol. 38, no. 7, pp. 2557–2563, 1999. DOI : 10.1021/ie9900061

J. Shi, Y. Wang, X. Yu, W. Du, et Z. Hou, “Production of 2,5-dimethylfuran from 5-hydroxymethylfurfural over reduced graphene oxides supported Pt catalyst under mild conditions”, *Fuel*, vol. 163, pp. 74–79, 2016. DOI : 10.1016/j.fuel.2015.09.047

K. Shimizu, R. Uozumi, et A. Satsuma, “Enhanced production of hydroxymethylfurfural from fructose with solid acid catalysts by simple water removal methods”, *Catalysis Communications*, vol. 10, no. 14, pp. 1849–1853, 2009. DOI : 10.1016/j.catcom.2009.06.012

Z. Shuping, W. Yulong, Y. Mingde, L. Chun, et T. Junmao, “Pyrolysis characteristics and kinetics of the marine microalgae *Dunaliella tertiolecta* using thermogravimetric analyzer”, *Bioresource Technology*, vol. 101, no. 1, pp. 359–365, 2010. DOI : 10.1016/j.biortech.2009.08.020

K. S. W. Sing, D. H. Everett, R. A. W. Haul, L. Moscou, R. A. Pierotti, J. Roquerol, et T. Siemieniewska, *Pure Applied Chemistry*, vol. 57, p. 603, 1985.

S. Sitthisa et D. E. Resasco, “Hydrodeoxygenation of furfural over supported metal catalysts : A comparative study of cu, pd and ni”, *Catal. Lett.*, vol. 141, no. 6, pp. 784–791, 2011. DOI : 10.1007/s10562-011-0581-7

E. Siva Sankar, V. Mohan, M. Suresh, G. Saidulu, B. David Raju, et K. S. Rama Rao, “Vapor phase esterification of levulinic acid over ZrO_2/SBA-15 catalyst”, *Catalysis Communications*, vol. 75, pp. 1–5, 2016. DOI : 10.1016/j.catcom.2015.10.013

P. A. Son, S. Nishimura, et K. Ebitani, “Synthesis of levulinic acid from fructose using Amberlyst-15 as a solid acid catalyst”, *Reaction Kinetics, Mechanisms and Catalysis*, vol. 106, no. 1, pp. 185–192, 2012. DOI : 10.1007/s11144-012-0429-1

Statista, “Fuel ethanol production worldwide in 2017, by country (in million gallons)”, 2017. En ligne : https://www.statista.com/statistics/281606/ethanol-production-in-selected-countries/

——, “Solid biomass and renewable waste energy capacity in canada from 2007 to

2017 (in megawatts)", 2017. En ligne : https://www.statista.com/statistics/476426/biomass-and-renewable-waste-energy-capacity-in-canada/

D. Sun, Y. Takahashi, Y. Yamada, et S. Sato, "Efficient formation of angelica lactones in a vapor-phase conversion of levulinic acid", *Applied Catalysis A : General*, vol. 526, pp. 62–69, 2016. DOI : 10.1016/j.apcata.2016.07.025

G. Sun, "Influence of particle size distribution on the performance of fluidized bed reactors", *The Canadian Journal of Chemical Engineering*, vol. 69, no. 5, p. 207, 1991. DOI : 10.1002/cjce.5450690512

Y. Sun et J. Cheng, "Hydrolysis of lignocellulosic materials for ethanol production : a review", *Bioresource technology*, vol. 83, no. 1, pp. 1–11, 2002. DOI : 10.1016/S0960-8524(01)00212-7

Á. Szabolcs, M. Molnár, G. Dibó, et L. T. Mika, "Microwave-assisted conversion of carbohydrates to levulinic acid : an essential step in biomass conversion", *Green Chem.*, vol. 15, no. 2, pp. 439–445, 2013. DOI : 10.1039/C2GC36682G

C. Tagusagawa, A. Takagaki, A. Iguchi, K. Takanabe, J. N. Kondo, K. Ebitani, S. Hayashi, T. Tatsumi, et K. Domen, "Highly active mesoporous Nb-W oxide solid-acid catalyst", *Angewandte Chemie - International Edition*, vol. 49, no. 6, pp. 1128–1132, 2010. DOI : 10.1002/anie.200904791

M. J. Taherzadeh, L. Gustafsson, C. Niklasson, et G. Lidén, "Conversion of furfural in aerobic and anaerobic batch fermentation of glucose by *Saccharomyces cerevisiae*", *Journal of Bioscience and Bioengineering*, vol. 87, no. 2, pp. 169–174, 1999. DOI : 10.1016/S1389-1723(99)89007-0

J. Tan, J. Cui, G. Ding, T. Deng, Y. Zhu, et Y.-w. Li, "Efficient aqueous hydrogenation of levulinic acid to γ -valerolactone over a highly active and stable", *Catalysis Science & Technology*, vol. 6, pp. 1469–1475, 2016. DOI : 10.1039/C5CY01374G

J. N. Tan-Soetedjo, H. H. Van De Bovenkamp, R. M. Abdilla, C. B. Rasrendra, J. Van Ginkel, et H. J. Heeres, "Experimental and Kinetic Modeling Studies on the Conversion of Sucrose to Levulinic Acid and 5-Hydroxymethylfurfural Using Sulfuric Acid in Water", *Industrial and Engineering Chemistry Research*, vol. 56, no. 45, pp. 13 228–13 239, 2017. DOI : 10.1021/acs.iecr.7b01611

H. Tang, N. Li, G. Li, W. Wang, A. Wang, Y. Cong, et X. Wang, "Dehydration

of Carbohydrates to 5-Hydroxymethylfurfural over Lignosulfonate-Based Acidic Resin", *ACS Sustainable Chemistry and Engineering*, vol. 6, no. 4, pp. 5645–5652, 2018. DOI : 10.1021/acssuschemeng.8b00757

F. Tao, H. Song, et L. Chou, "Efficient process for the conversion of xylose to furfural with acidic ionic liquid", *Can. J. Chem.*, vol. 89, no. 1, pp. 83–87, 2011. DOI : 10.1139/V10-153

The Royal Society, "Sustainable biofuels : prospects and challenges", *Sustainable biofuels*, no. January, pp. 1–79, 2008. DOI : ISBN 978 0 85403 662 2

K. N. Theologos et N. C. Markatos, "Advanced Modeling of Fluid Catalytic Cracking Riser type Reactors", *AIChE Journal*, vol. 39, no. 6, p. 1007, 1993.

A. Tube, S. Chamber, et F. C. Assembly, "Standard Test Method for Determination of Attrition of FCC Catalysts by Air Jets 1", ASTM, Rapp. tech., 2013. DOI : 10.1520/D5757-11.2

T. Tuercke, S. Panic, et S. Loebbecke, "Microreactor process for the optimized synthesis of 5-hydroxymethylfurfural : A promising building block obtained by catalytic dehydration of fructose", *Chemical Engineering and Technology*, vol. 32, no. 11, pp. 1815–1822, 2009. DOI : 10.1002/ceat.200900427

J. Tuteja, H. Choudhary, S. Nishimura, et K. Ebitani, "Direct synthesis of 1,6-hexanediol from HMF over a heterogeneous Pd/ZrP catalyst using formic acid as hydrogen source", *ChemSusChem*, vol. 7, no. 1, pp. 96–100, 2014. DOI : 10.1002/cssc.201300832

P. P. Upare, J. M. Lee, Y. K. Hwang, D. W. Hwang, J. H. Lee, S. B. Halligudi, J. S. Hwang, et J. S. Chang, "Direct hydrocyclization of biomass-derived levulinic acid to 2-methyltetrahydrofuran over nanocomposite copper/silica catalysts", *ChemSusChem*, vol. 4, no. 12, pp. 1749–1752, 2011. DOI : 10.1002/cssc.201100380

US Department of Agiculture, "Sugar and sweeteners yearbook tables", 2016. En ligne : https://www.ers.usda.gov/data-products/sugar-and-sweeteners-yearbook-tables.aspx

USP Technologies, "Permanganate Titration", 2018. En ligne : www.h2o2.com

F. Van Der Klis, D. S. Van ES, et J. Van Haveren, "Succinic acid from biomass", pp. 2–3, apr 2012, uS Patent # WO2012044168 A1.

D. R. Vardon, M. A. Franden, C. W. Johnson, E. M. Karp, M. T. Guarnieri, J. G. Linger, M. J. Salm, T. J. Strathmann, et G. T. Beckham, "Adipic acid production from lignin",

Energy Environ. Sci., vol. 8, no. 2, pp. 617–628, 2015. DOI : 10.1039/C4EE03230F

D. R. Vardon, A. E. Settle, V. Vorotnikov, M. J. Menart, T. R. Eaton, K. A. Unocic, K. X. Steirer, K. N. Wood, N. S. Cleveland, K. E. Moyer, W. E. Michener, et G. T. Beckham, "Ru-Sn / AC for the Aqueous-Phase Reduction of Succinic Acid to 1 , 4 - Butanediol under Continuous Process Conditions", 2017. DOI : 10.1021/acscatal.7b02015

S. V. Vassilev, D. Baxter, L. K. Andersen, et C. G. Vassileva, "An overview of the chemical composition of biomass", *Fuel*, vol. 89, no. 5, pp. 913–933, 2010. DOI : 10.1016/j.fuel.2009.10.022

S. V. Vassilev, D. Baxter, L. K. Andersen, C. G. Vassileva, et T. J. Morgan, "An overview of the organic and inorganic phase composition of biomass", *Fuel*, vol. 94, pp. 1—33, 2012. DOI : 10.1016/j.fuel.2011.09.030

M. Ventura, F. Lobefaro, D. Elvira, D. Monica, N. Francesco, et D. Angela, "Selective Aerobic Oxidation of 5-Hydroxymethylfurfural to 2,5-Diformylfuran or 2-Formyl-5-furancarboxylic Acid in Water by using MgO · CeO Mixed Oxides as Catalysts", *ChemSusChem*, pp. 1305–1315, 2018. DOI : 10.1002/cssc.201800334

P. Verdeguer, N. Merat, L. Rigal, et A. Gaset, "Optimization of experimental conditions for the catalytic oxidation of furfural to furoic acid", *J. Chem. Technol. Biotechnol.*, vol. 61, no. 2, pp. 97–102, 1994. DOI : 10.1002/jctb.280610203

A. Victor, I. N. Pulidindi, et A. Gedanken, "Levulinic acid production from Cicer arietinum, cotton, Pinus radiata and sugarcane bagasse", *RSC Adv.*, vol. 4, no. 84, pp. 44 706–44 711, 2014. DOI : 10.1039/C4RA06246A

M. von Sivers et G. Zacchi, "A techno-economical comparison of three processes for the production of ethanol from pine", *Bioresource Technology*, vol. 51, no. 1, pp. 43–52, 1995. DOI : 10.1016/0960-8524(94)00094-H

X. Wan, C. Zhou, J. Chen, W. Deng, Q. Zhang, Y. Yang, et Y. Wang, "Base-free aerobic oxidation of 5-hydroxymethyl-furfural to 2,5-furandicarboxylic acid in water catalyzed by functionalized carbon nanotube-supported au-pd alloy nanoparticles", *ACS Catalysis*, vol. 4, no. 7, pp. 2175–2185, 2014. DOI : 10.1021/cs5003096

F. Wang et Z. Zhang, "Cs-substituted tungstophosphate-supported ruthenium nanoparticles : An effective catalyst for the aerobic oxidation of 5-hydroxymethylfurfural into 5-

hydroxymethyl-2-furancarboxylic acid", *Journal of the Taiwan Institute of Chemical Engineers*, vol. 70, pp. 1–6, 2017. DOI : 10.1016/j.jtice.2016.10.003

K. F. Wang, C. L. Liu, K. Y. Sui, C. Guo, et C. Z. Liu, "Efficient Catalytic Oxidation of 5-Hydroxymethylfurfural to 2,5-Furandicarboxylic Acid by Magnetic Laccase Catalyst", *ChemBioChem*, vol. 19, no. 7, pp. 654–659, 2018. DOI : 10.1002/cbic.201800008

Y. Wang, K. Yu, W. Si, Y. Feng, L.-l. Lou, et S. Liu, "Basicity-tuned hydrotalcite-supported pd catalysts for aerobic oxidation of 5-hydroxymethyl-2-furfural under mild conditions", *ACS Sustainable Chemistry & Engineering*, 2016. DOI : 10.1021/acssuschemeng.6b00965

Y. Wang, F. Vogelgsang, et Y. Román-Leshkov, "Acid-catalyzed oxidation of levulinate derivatives to succinates under mild conditions", *ChemCatChem*, vol. 7, no. 6, pp. 916–920, 2015. DOI : 10.1002/cctc.201403014

F. Weiss, Pierre-Benire, et A. Isard, "Process of recovering tungstic acid catalyst", 1966.

T. Werpy et G. Petersen, "Top value added chemicals from biomass volume i — results of screening for potential candidates from sugars and synthesis gas top value added chemicals from biomass volume i : Results of screening for potential candidates", p. Medium : ED ; Size : 76 pp. pages, 2004. DOI : 10.2172/15008859

R. Wooley, M. Ruth, J. Sheehan, K. Ibsen, H. Majdeski, et A. Galvez, "Lignocellulosic Biomass to Ethanol Process Design and Economics Utilizing Co-Current Dilute Acid Prehydrolysis and Enzymatic Hydrolysis Current and Futuristic Scenarios", 1999. DOI : 10.2172/12150

L. Wu, S. Dutta, et M. Mascal, "Efficient, chemical-catalytic approach to the production of 3-hydroxypropanoic acid by oxidation of biomass-derived levulinic acid with hydrogen peroxide", *ChemSusChem*, vol. 8, no. 7, pp. 1167–1169, 2015. DOI : 10.1002/cssc.201500025

C. E. Wyman et B. Yang, "Cellulosic biomass could help* meet California's transportation fuel needs", *California Agriculture*, vol. 63, no. 4, pp. 185–190, 2009. DOI : 10.3733/ca.v063n04p185

F. Xia, Z. Du, J. Liu, Y. Ma, et J. Xu, "Catalytic oxidative C–C bond cleavage route of levulinic acid and methyl levulinate", *RSC Adv.*, vol. 6, no. 76, pp. 72 744–72 749, 2016. DOI : 10.1039/C6RA16149A

H. Xie, Z. K. Zhao, et Q. Wang, "Catalytic conversion of inulin and fructose into 5-hydroxymethylfurfural by lignosulfonic acid in ionic liquids", *ChemSusChem*, vol. 5, no. 5,

pp. 901–905, 2012. DOI : 10.1002/cssc.201100588

A. Yaghmur, A. Aserin, et N. Garti, “Furfural-cysteine model reaction in food grade nonionic oil/water microemulsions for selective flavor formation”, *J. Agric. Food. Chem.*, vol. 50, no. 10, pp. 2878–2883, 2002. DOI : 10.1021/jf0111581

D. Yan, G. Wang, K. Gao, X. Lu, J. Xin, et S. Zhang, “One-Pot Synthesis of 2,5-Furandicarboxylic Acid from Fructose in Ionic Liquids”, *Industrial and Engineering Chemistry Research*, vol. 57, no. 6, pp. 1851–1858, 2018. DOI : 10.1021/acs.iecr.7b04947

Z. Yang, W. Qi, R. Su, et Z. He, “Selective Synthesis of 2,5-Diformylfuran and 2,5-Furandicarboxylic Acid from 5-Hydroxymethylfurfural and Fructose Catalyzed by Magnetically Separable Catalysts”, *Energy & Fuels*, p. acs.energyfuels.6b02012, 2016. DOI : 10.1021/acs.energyfuels.6b02012

G. Yi, S. P. Teong, et Y. Zhang, “The Direct Conversion of Sugars into 2,5-Furandicarboxylic Acid in a Triphasic System”, *ChemSusChem*, vol. 8, no. 7, pp. 1151–1155, 2015. DOI : 10.1002/cssc.201500118

——, “Base-free conversion of 5-hydroxymethylfurfural to 2,5-furandicarboxylic acid over a Ru/C catalyst”, *Green Chem.*, vol. 18, no. 4, pp. 979–983, 2016. DOI : 10.1039/C5GC01584G

X. Ying Hao, W. Zhou, J.-W. Wang, Y.-Q. Zhang, et S. Liu, “A Novel Catalyst for the Selective Hydrogenation of Furfural to Furfuryl Alcohol”, *Chemistry Letters*, vol. 34, no. 7, pp. 1000–1001, 2005. DOI : 10.1246/cl.2005.1000

J. Yu, J. Yue, Z. Liu, L. Dong, G. Xu, J. Zhu, Z. Duan, et L. Sun, “Kinetics and mechanism of solid reactions in a micro fluidized bed reactor”, *AIChE Journal*, vol. 56, no. 11, pp. 2905–2912, 2010. DOI : 10.1002/aic.12205

J. Yu, C. Yao, X. Zeng, S. Geng, L. Dong, Y. Wang, S. Gao, et G. Xu, “Biomass pyrolysis in a micro-fluidized bed reactor : Characterization and kinetics”, *Chemical Engineering Journal*, vol. 168, no. 2, pp. 839–847, 2011. DOI : 10.1016/j.cej.2011.01.097

J. Yu et P. E. Savage, “Decomposition of formic acid under hydrothermal conditions”, *Ind. Eng. Chem. Res.*, vol. 37, no. 1, pp. 2–10, 1998. DOI : 10.1021/ie970182e

H. Yuan, J. Li, H. dong Shin, G. Du, J. Chen, Z. Shi, et L. Liu, “Improved production of 2,5-furandicarboxylic acid by overexpression of 5-hydroxymethylfurfural oxidase and 5-hydroxymethylfurfural/furfural *oxidoreductase* in *Raoultella ornithinolytica*

BF60", *Bioresource Technology*, vol. 247, no. August 2017, pp. 1184–1188, 2018. DOI : 10.1016/j.biortech.2017.08.166

J. G. Zeikus, M. K. Jain, et P. Elankovan, "Biotechnology of succinic acid production and markets for derived industrial products", *Applied Microbiology and Biotechnology*, vol. 51, no. 5, pp. 545–552, 1999. DOI : 10.1007/s002530051431

K. J. Zeitsch, "Furfural processes", dans *the chemistry and technology of furfural and its many by-products*, série Sugar Series. Elsevier, 2000, vol. 13, pp. 36 – 74.

L. Zhang, G. Xi, Z. Chen, D. Jiang, H. Yu, et X. Wang, "Highly selective conversion of glucose into furfural over modified zeolites", *Chemical Engineering Journal*, vol. 307, pp. 868–876, 2017. DOI : 10.1016/j.cej.2016.09.001

Z. Zhang, B. Liu, K. Lv, J. Sun, et K. Deng, "Aerobic oxidation of biomass derived 5-hydroxymethylfurfural into 5-hydroxymethyl-2-furancarboxylic acid catalyzed by a montmorillonite K-10 clay immobilized molybdenum acetylacetonate complex", *Green Chemistry*, vol. 16, no. 5, p. 2762, 2014. DOI : 10.1039/c4gc00062e

Z. Zhang, J. Zhen, B. Liu, K. Lv, et K. Deng, "Selective aerobic oxidation of the biomass-derived precursor 5-hydroxymethylfurfural to 2,5-furandicarboxylic acid under mild conditions over a magnetic palladium nanocatalyst", *Green Chem.*, vol. 17, no. 2, pp. 1308–1317, 2015. DOI : 10.1039/C4GC01833H

H. Zhao, J. E. Holladay, H. Brown, et Z. C. Zhang, "Metal chlorides in ionic liquid solvents convert sugars to 5-hydroxymethylfurfural", *Science*, vol. 316, no. 5831, pp. 1597–1600, 2007. DOI : 10.1126/science.1141199

J. Zhao, A. Jayakumar, Z. T. Hu, Y. Yan, Y. Yang, et J. M. Lee, "MoO3-Containing Protonated Nitrogen Doped Carbon as a Bifunctional Catalyst for One-Step Synthesis of 2,5-Diformylfuran from Fructose", *ACS Sustainable Chemistry and Engineering*, vol. 6, no. 1, pp. 284–291, 2018. DOI : 10.1021/acssuschemeng.7b02408

J. Zhao, A. Jayakumar, et J. M. Lee, "Bifunctional Sulfonated MoO_3-ZrO_2 Binary Oxide Catalysts for the One-Step Synthesis of 2,5-Diformylfuran from Fructose", *ACS Sustainable Chemistry and Engineering*, vol. 6, no. 3, pp. 2976–2982, 2018. DOI : 10.1021/acssuschemeng.7b02671

H. Y. Zheng, Y. L. Zhu, B. T. Teng, Z. Q. Bai, C. H. Zhang, H. W. Xiang, et Y. W. Li, "Towards understanding the reaction pathway in vapour phase hydrogenation of furfural

to 2-methylfuran", *J. Mol. Catal. A : Chem.*, vol. 246, no. 1-2, pp. 18–23, 2006. DOI : 10.1016/j.molcata.2005.10.003

C. Zhou, W. Deng, X. Wan, Q. Zhang, Y. Yang, et Y. Wang, "Functionalized Carbon Nanotubes for Biomass Conversion : The Base-Free Aerobic Oxidation of 5-Hydroxymethylfurfural to 2,5-Furandicarboxylic Acid over Platinum Supported on a Carbon Nanotube Catalyst", *ChemCatChem*, vol. 7, no. 18, pp. 2853–2863, 2015. DOI : 10.1002/cctc.201500352

X. Zuo, P. Venkitasubramanian, D. H. Busch, et B. Subramaniam, "Optimization of Co/Mn/Br-catalyzed oxidation of 5-hydroxymethylfurfural to enhance 2,5-furandicarboxylic acid yield and minimize substrate burning", *ACS Sustain. Chem. Eng.*, vol. 4, no. 7, pp. 3659–3668, 2016. DOI : 10.1021/acssuschemeng.6b00174

ANNEX A INVENTION DISCLOSURE DIV474

ÉCOLE POLYTECHNIQUE

B.R.C.D.T.
Bureau de la recherche et
Centre de développement
Technologique

DÉCLARATION D'INVENTION

DIV – 747

A L'USAGE DU BRCDT	
CTT : AMB	VAL :
Chercheur contact : G PATIENCE	
1er contact : 2016	
1ère version :	
Signatures : CHERCHEURS	
POLY	
UNIVALOR	

La présente déclaration d'invention est faite au Bureau de la recherche et Centre de développement technologique (BRCDT), conformément à la *Politique de propriété intellectuelle technologique* de l'École Polytechnique de Montréal (la "Politique") et vise les résultats de travaux de recherche réalisés par un ou des *chercheurs* liés à l'École Polytechnique de Montréal, tels que définis par la Politique et désignés ci-après comme les "Inventeurs" et/ou les "auteurs", qui estiment que ces résultats constituent la mise en œuvre innovatrice de technologies, connaissances ou savoir faire existants ou connus, ou la création de technologies, de produits, de savoir-faire ou de procédés nouveaux ou d'autres innovations technologiques ("l'Invention").

Section A. Titre de l'Invention et mots clés (en anglais et en français)

Oxidation of C5 and C6 sugar feedstocks to carboxylic acids, ethers and ketones
Keywords : glucose/fructose conversion, bifunctional catalyst, oxidation, fluidized bed reactor, reaction kinetics, ethers, organic acids, ketones, gas-solids hydrodynamics

Oxydation de matières premières de sucre C5 et C6 en acides carboxyliques, éther et cétones

Mots-clés : conversion de glucose / fructose, catalyseur bifonctionnel, oxydation, réacteur à lit fluidisé, cinétique de la réaction, éther, des acides organiques, cétones, solides-gaz hydrodynamiques

Section B. Description sommaire de l'Invention

Voir en Annexe A ci-jointe la description détaillée de l'Invention.

Biomass is organic matter that can be converted to fuel or energy sources. It is inexpensive, renewable and a potential substitute for fossil fuels. Oxidation of C5 and C6 sugar feedstocks to specialty chemicals (e.g. 2,5 – furan dicarboxylic acid, cyclopentenone, levulinic acid, glucaric acid, adipic acid and γ-valero lactone) is a new promising pathway with a huge potential market value. Some examples are: 2,5 – FDCA (recently applied to produce new polymers able to replace PET), adipic acid (building block for the synthesis of nylon), levulinic acid (cosmetic and medical industries) and γ-valero lactone (potential fuel and green solvent).

Gas-solid heterogeneous catalysis may achieve value-added chemicals reducing the number of process steps and the total cost. Liquid-solid heterogeneous catalysts have several drawbacks: low mass transfer rates, low temperatures thus slow kinetics, final purity may be lower, which increase separation costs, and recovering the catalyst is often difficult. These problems may be solved operating in the gas-phase with a liquid aerosol. A suitable technology is a gas-phase fluidized bed reactor, in which the aerosol is sprayed into the catalytic bed. Its high heat transfer rates reduce the degradation or the caramelization of the sugars. It is instantaneously vaporized and the feed reacts with the catalyst to form value added specialty chemicals or fuels/additives.

The main problems with high temperatures and sugars are the thermal degradation and the caramelization. Our setup is composed by a fluidized bed reactor, loaded with the catalyst on the grid plate, in which oxygen is introduced as reactant. Through a nozzle the sugar solution is injected in the catalytic bed. A carrier gas improves the spray atomization by reducing the droplet size and increase the uniformity. High temperatures vaporize the feed which reacts instantaneously with the catalyst, reducing the degradation or the loss of the reagent.

Based on our preliminary tests, for the first time, we report the oxidation of C5 and C6 sugar feedstocks in the gas-phase to C6 carboxylic acids, ethers and ketones. We operated at ambient pressure and with temperature in the range of 300 °C - 400 °C, using oxidizing catalysts e.g. Pt / WO_3 / Al_2O_3 and Mo/V/TiO_2.

The thrust of this research program will be to develop the process conditions to optimize the production of specialty chemicals and eventually to test new catalysts for other applications.

Section C. Type d'Invention

Logiciel ☐ Appareil ☐ Produit ☐ Procédé ☒ Méthode ☐

Autre (décrire) _____

Section D : Publications

L'Invention a fait ou fera l'objet des publications (sous forme d'articles scientifiques, thèses, mémoires, présentations, cours, conférences, ou toute autre forme de communication au public) et divulgations suivantes, aux dates indiquées.

- *Aucune*
-
-
-
-

Une bibliographie et liste complémentaire des autres divulgations, s'il en est, et copie des publications sont jointes en Annexe D de la présente déclaration, si nécessaire.

Section E1 : Inventeur(s)

*Le terme «**Inventeur**» se définit comme étant une personne qui a eu un apport inventif à la conception de la technologie telle que décrite ci-dessous. Pour plus de clarté, un «**Inventeur**» doit avoir contribué à la mise en œuvre de l'idée à la base de cette déclaration d'invention sous forme définie et pratique. Une personne ayant contribué à l'élaboration de la Technologie uniquement par le biais de conseils, de suggestions, ou de support financier, ne peut être considérée comme Inventeur.*
***L'inventeur** doit inscrire son **adresse personnelle** à la date la plus récente, soit à la date de signature du présent formulaire.*
***Le nom et l'adresse de **l'employeur** inscrits ci-dessous sont ceux définis au moment de la réalisation des travaux de recherche.*

				APPORT INVENTIF (TOTAL 100%)
Nom :	*PATIENCE*	Prénom :	*GREGORY*	*50*
Adresse résidence* :	*107 Vivian Av, Town of Mount Royal, H3P 1N8, Montréal, QC, Canada*			
Citoyenneté :	*Canadienne*	Tél (rés) :	*514 735-3675*	
Employeur**:	*Polytechnique Montréal, C.P. 6079, Station «Centre-Ville», Montréal, QC, H3C 3A7*			
Département/Groupe de recherche :	*Département de génie chimique*			
Courriel	*gregory-s.patience@polymtl.ca*	Position :	*Professeur Agrégé*	
Tél (bur) :	*514 340-4711 (3439)*	Fax :	*514 340-4159*	

Nom :	*CARNEVALI*	Prénom :	*DAVIDE*	*50*
Adresse résidence* :	*4250, Apt - 14, Avenue Marcil, H4A 2Z6, Montréal, QC, Canada*			
Citoyenneté :	*Italian*	Tél (rés) :	*514 9951072*	
Employeur**:	*Polytechnique Montréal, C.P. 6079, Station «Centre-Ville», Montréal, QC, H3C 3A7*			
Département/Groupe de recherche :	*Département de génie chimique*			
Courriel	davide.carnevali@polymtl.ca	Position :	*étudiant au doctorat (PhD)*	
Tél (bur) :	*514 340-4711 (3129)*	Fax :	*514 340-4711 (3129)*	

Nom :		Prénom :		
Adresse résidence* :				
Citoyenneté :		Tél (rés) :		
Employeur**:				
Département/Groupe de recherche :				
Courriel		Position :		
Tél (bur) :		Fax :		

Nom :		Prénom :		
Adresse résidence* :				
Citoyenneté :		Tél (rés) :		
Employeur**:				
Département/Groupe de recherche :				
Courriel		Position :		
Tél (bur) :		Fax :		

Nom :		Prénom :		
Adresse résidence* :				
Citoyenneté :		Tél (rés) :		
Employeur**:				
Département/Groupe de recherche :				
Courriel		Position :		
Tél (bur) :		Fax :		

Section E2 : Droits d'auteur (pour les logiciels uniquement)

Le terme «Auteur» s'applique à tout chercheur ayant participé à l'écriture du code du logiciel tel que décrit dans la présente déclaration d'invention.
Un Auteur peut également être Inventeur et/ou Collaborateur.
Les % inscrits à la présente rubrique ne s'appliquent qu'aux droits d'auteur et excluent les droits d'Inventeur.
***L'Auteur** doit inscrire son **adresse personnelle** à la date la plus récente, soit à la signature du présent formulaire.*
***Le nom et l'adresse de **l'employeur** inscrits ci-dessous sont ceux au moment de la réalisation des travaux de recherche.*

DROITS D'AUTEUR (TOTAL 100%)

Nom :		Prénom :		
Adresse résidence* :				
Citoyenneté :		Tél (rés) :		
Employeur**:				
Département/Groupe de recherche :				
Courriel		Position :		
Tél (bur) :		Fax :		

Nom :		Prénom :		
Adresse résidence* :				
Citoyenneté :		Tél (rés) :		
Employeur**:				
Département/Groupe de recherche :				
Courriel		Position :		
Tél (bur) :		Fax :		

Nom :		Prénom :		
Adresse résidence* :				
Citoyenneté :		Tél (rés) :		
Employeur**:				
Département/Groupe de recherche :				
Courriel		Position :		
Tél (bur) :		Fax :		

Nom :		Prénom :		
Adresse résidence* :				
Citoyenneté :		Tél (rés) :		
Employeur**:				
Département/Groupe de recherche :				
Courriel		Position :		
Tél (bur) :		Fax :		

Nom :		Prénom :		
Adresse résidence* :				
Citoyenneté :		Tél (rés) :		
Employeur**:				
Département/Groupe de recherche :				
Courriel		Position :		
Tél (bur) :		Fax :		

Section E3 : Autres collaborateurs

*Le terme «**Collaborateur**» se définit comme étant une personne qui a contribué à valider ou tester, ou encore qui a tout simplement concrétisé l'idée d'un Inventeur de façon matérielle en suivant les instructions de ce dernier.*
***Le Collaborateur** doit inscrire son **adresse personnelle** à la date la plus récente, soit au moment où la déclaration d'invention est déposée au BRCDT.*
***Le nom et l'adresse de **l'employeur** inscrits ci-dessous sont ceux au moment de la réalisation des travaux de recherche.*

Nom :		Prénom :		Courriel :	
Adresse résidence* :					
Employeur**:					
Département/Groupe de recherche :					
Tél (bur) :		Fax :		Position :	
Détails de la collaboration :					

Nom :		Prénom :		Courriel :	
Adresse résidence* :					
Employeur**:					
Département/Groupe de recherche :					
Tél (bur) :		Fax :		Position :	
Détails de la collaboration :					

Nom :		Prénom :		Courriel :	
Adresse résidence* :					
Employeur**:					
Département/Groupe de recherche :					
Tél (bur) :		Fax :		Position :	
Détails de la collaboration :					

Nom :		Prénom :		Courriel :	
Adresse résidence* :					
Employeur**:					
Département/Groupe de recherche :					
Tél (bur) :		Fax :		Position :	
Détails de la collaboration :					

Section F : Subventions

Section F-1 : MODES DE FINANCEMENT :

Liste des subventions, contrats, et autres modes de financement ayant permis, dès le début, la création de l'Invention (dates, montants, commanditaires)

Le financement de cette recherche provient des fonds de recherche de professeur Gregory Patience.

Section F-2 : PROPRIÉTÉ INTELLECTUELLE :

Droit de Polytechnique et des tierces parties sur la propriété intellectuelle lié à l'Invention :

SECTION F-3 : CONTRATS :

Accords d'exploitation, de développement et autres contrats existants liés à l'Invention :

Section G : Brevets

L'Invention a fait ou fera l'objet des démarches suivantes relativement à sa brevetabilité :

Type de demande		Pays		Date		# Appl.	
Demandeur		Propriétaire					
Type de demande		Pays		Date		# Appl.	
Demandeur		Propriétaire					
Type de demande		Pays		Date		# Appl.	
Demandeur		Propriétaire					

Les Inventeurs et/ou Auteurs soussignés déclarent et garantissent qu'ils sont les seuls créateurs, inventeurs ou auteurs à l'origine de l'Invention et que l'information fournie dans le cadre de la présente divulgation, y compris dans l'annexe A et dans les pièces qui y sont jointes, est vraie, précise et complète, et qu'elle fait état de toute l'information pertinente relative à l'Invention.

Les Inventeurs et/ou Auteurs soussignés consentent par les présentes à ce que leurs noms et le titre de l'Invention puissent être diffusés publiquement par Polytechnique Montréal.

EN FOI DE QUOI, les Inventeurs et/ou Auteurs ont signé la présente divulgation, aux dates et lieux indiqués ci-dessous.

Nom : *Gregory S. Patience* Signé à *Montréal* le	Nom : *Davide Carnevali* Signé à *Montréal* le
Nom : Signé à le	Nom : Signé à le
Nom : Signé à le	Nom : Signé à le

ANNEXE A

Description détaillée de l'Invention

Comprenant notamment les informations suivantes:

1. Description sommaire de l'Invention (environ 5 lignes)

   For the first time we report the gas-phase oxidation of C5 and C6 sugars to C6 carboxylic acids, ethers and ketones over $Pt/WO_3/Al_2O_3$ and $Mo/V/TiO_2$, at ambient pressure and temperatures in the range of 300˚C – 400 ˚C.

   An aqueous solution of C5 or C6 sugars is injected into a fluidized bed reactor, operating at high temperature and ambient pressure. The feed is atomized with a carrier gas through a nozzle to obtain an aerosol in the catalytic bed. The small droplets instantaneously vaporize and the feed reacts with the catalyst to produce value-added chemicals (e.g. 2,5 – FDCA, furfural , γ - valero lactone and cyclopentenone). The catalytic bed may be fluidized by inert gases or air, and by-products such as hydrogen, carbon oxides and water are detected.

   This technology relies on the ability to vaporize sugars and to react instantaneously with catalysts, minimizing the thermal decomposition or the caramelization, reducing the production of humins and undesirable by-products.

2. Contexte et définition du problème

   Biomass, and more specific carbohydrates feedstocks, are potential raw materials for the production of specialty chemicals and fuels. Generally, reactions occur in the liquid phase and mainly in multiphasic reactors, using both homogeneous and heterogeneous catalysts. Those technologies led to high-cost processes, due to multiple steps reactions, use of particular solvents and products separation.

   Here, for the first time, we report the gas-phase oxidation of C5 and C6 sugar feedstocks to value-added C6 and C5 molecules, including carboxylic acids, ketones and esters, producing an aerosol of the liquid feed in a designed catalytic bed, operating in a high temperature and an ambient pressure fluidized bed reactor.

3. État actuel des connaissances

   We have as of yet found no references related to gas phase, oxidation of C5 and C6 sugar feedstocks to C6 molecules in a fluidized bed at ambient pressure or the like. Liquid phase reactions, in a single or a multiphase reactor, are common but no references have been found citing gas phase. In our previous patent applications, we claimed an oxidation process that partially cracked the sugars to make carboxylic acids and we also claimed a hydrogenation process to make molecules by injecting sugars with hydrogen in a fluidized bed.

4. Description détaillée de l'Invention (aspects importants, éléments nouveaux et originaux, etc …)

   This innovation is related to the gas phase heterogeneous catalytic oxidation of C5 and C6 feedstocks (in particular glucose, fructose and xylose) in a fluidized bed reactor. This technology is designed to operate at high temperatures and ambient pressure, using selected catalysts e.g. $Pt/WO_3/Al_2O_3$ or $Mo/V/TiO_2$ to produce selectively a variety of chemical classes (carboxylic acids, ethers and ketones).

   We have demonstrated the feasibility of the process by performing preliminary experiments in a micro fluidized bed reactor (1.5 cm ID). The catalyst is added on the grid plate and fluidized with a mixture of Ar and O_2. The flowrates are set by Bronkhorst mass flow controllers (MFC). A furnace maintains the reactor at the desired temperature. An HPLC pump injects the aqueous sugar solution through a nozzle, from the bottom of the reactor, directly inside the catalytic bed. Co-feeding Ar increases and improves the quality of the aerosol. Atomization of the feed is fundamental, because inhomogeneity or high sized of the droplets agglomerate the catalysts, blocking the injector. Thermocouples monitored the catalytic bed and the exit temperatures. The exit line is heated in order to avoid the condensation of the products. A quench, directly connected to a recirculation pump, trap all the condensable products. An online mass spectroscopy (MS) measures the non-condensable products (CO, CO_2, Ar and H_2O). The products trapped in the quench are analyzed offline by a high performance liquid chromatography (HPLC) and gas chromatography – mass spectroscopy (GC-MS). Liquid chromatography – mass spectroscopy (LC-MS) of the quench were also carried out to minor products and validate the products.

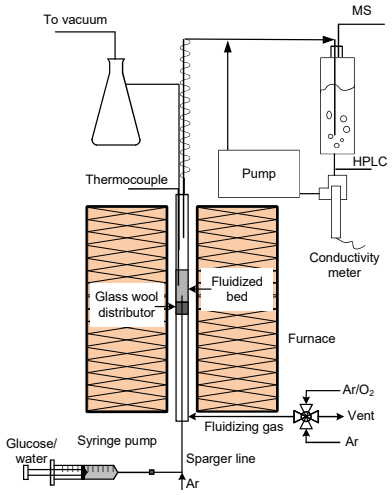

5. Date et lieux de conception et de première divulgation publique

   The idea has not been published. We first had the idea before August 5, 2016 at Polytechnique Montreal.

6. Avantages et limites de l'Invention

   Vaporizing and reacting carbohydrates has the following advantages:

   (1) Higher through put rates – higher reaction rates
   (2) Lower catalyst inventory
   (3) Smaller reaction vessels
   (4) Higher selectivities
   (5) Lower yield losses
   (6) Lower number of unit operations
   (7) Superior economics
   (8) New classes of compounds
   (9) Ability to react pentose sugars directly
   (10) Reduces the number of process steps

   Limitations:

   (1) Currently yields need to be improved
   (2) Contacting liquid with the solids can form agglomerates if the solids are hydrophilic
   (3) Vaporizing the entire liquid solution increases operational costs
   (4) High temperature of the injector causes blocking
   (5) High sugar concentrations are preferred to minimize cost to vaporize the feed gas
   (6) Higher selective catalyst may be required for increasing the selectivity of the desired products

7. État de développement de l'Invention (tests, prototypes, démonstrations, photos et enregistrements, travaux terminés, en cours et prévus, améliorations, etc… dates et lieux s'y rapportant)

   Here are presented the preliminary results obtained starting from glucose and fructose and a dehydrating/oxidizing catalyst.

Feedstock	Catalyst	Reagents	Products
Glucose	VPP	Oxygen	Maleic anhydride, Acrylic acid, Succinic acid
Glucose	H - ZSM5	Oxygen	Maleic anhydride, Acrylic acid, Levulinic acid
Glucose	WO_3/TiO_2	Oxygen	Maleic anhydride, Acrylic acid, Levulinic acid
Glucose	2 % Pt / 20 % WO_3 / TiO_2	Oxygen, Hydrogen	Glucaric acid, 2,5 – Furan dicarboxylic acid
Glucose	2 % Pt / 20% WO_3 / H - ZSM-5	Oxygen, Hydrogen	Gluconic acid, Adipic acid
Glucose	2 % Pt / H - ZSM-5	Oxygen, Hydrogen	Gluconic acid, Adipic acid
Glucose	2 % Pt / 30 % WO_3 / Al_2O_3	Oxygen	Cyclopentenone, Methylfurfural, Furfural
Fructose	2 % Pt / 30 % WO_3 / Al_2O_3	Oxygen	Cyclopentenone, Methylfurfural, Furfural

Demonstration of the products obtained from the reactions:

- HPLC analysis of the oxidation of glucose with VPP

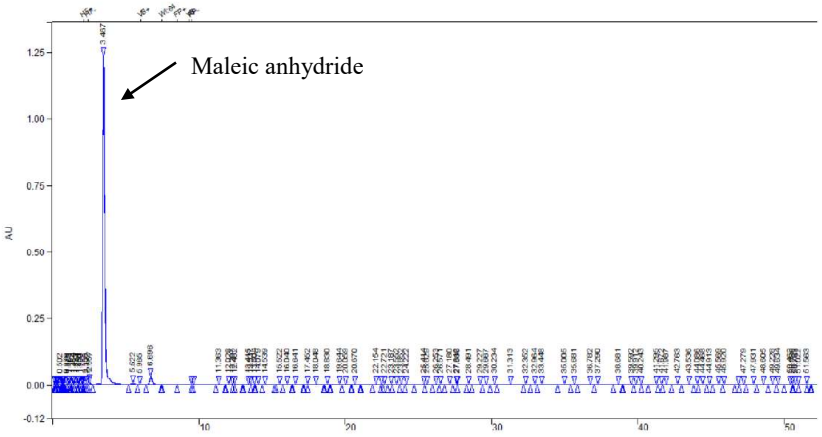

- HPLC analysis of the final products after 60 minutes of the reaction of glucose and oxygen with $Pt_{2\%}$ / $WO_{3\ 30\%}$ / Al_2O_3 at different conditions:

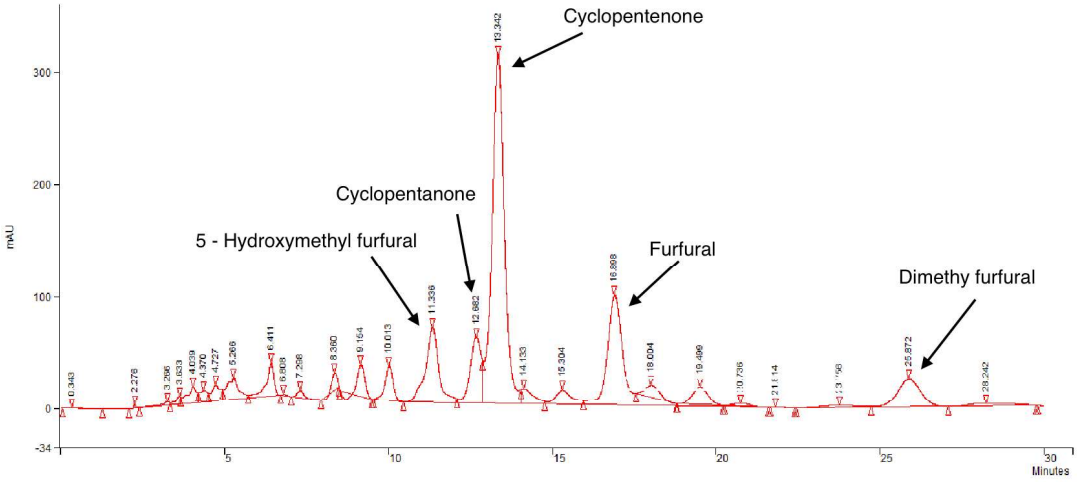
Cyclopentenone
Cyclopentanone
5 - Hydroxymethyl furfural
Furfural
Dimethy furfural
mAU
Minutes

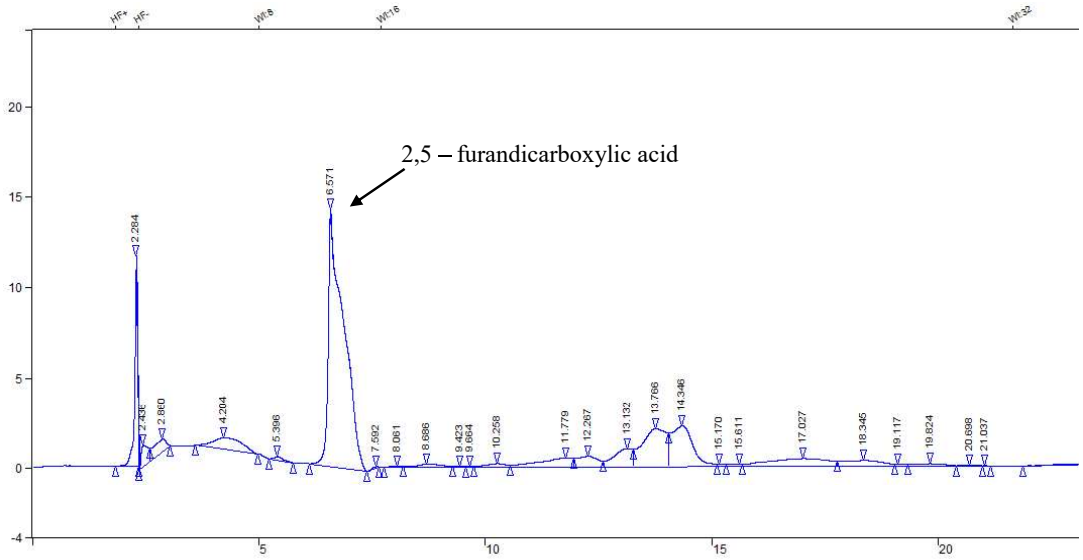
2,5 – furandicarboxylic acid

GC-MS analysis of the sample of fructose with $Pt_{2\%}$ / $WO_{3\ 30\%}$ / Al_2O_3

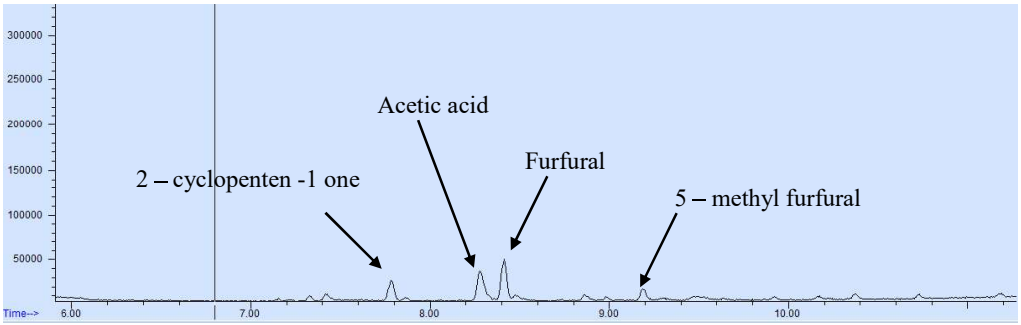

Conclusion

For the first time we present a technology able to convert C5 and C6 sugars to carboxylic acids, ethers and ketones in the gas-phase, using a continuous fluidized bed reactor. Preliminary results confirm the synthesis of the desired products.

8. Référence(s) citée(s)

ANNEXE B

Données relatives à la commercialisation de l'Invention

Pouvant comprendre notamment les informations suivantes:

1. Application(s) commerciale(s) possible(s).
   Biomass conversion
   Polymer industry
   Biofuels

2. Bénéfices commerciaux possibles.
   Relatively low cost production of biobased monomer and biofuels

3. Démarches de commercialisation entreprises (incluant les contacts établis).
   No conflict of interest with any industry.

4. Coordonnées de tiers présentement ou probablement intéressés à commercialiser l'Invention.

5. Recommandations et suggestions quant à l'exploitation commerciale de l'Invention.
   File a patent immediately then apply for additional funding (INNOV, for example) to explore different reactions including yields.
   Then approach third party to participate in the commercialization.

ANNEXE C

ENTENTE DE CONFIDENTIALITÉ RELATIVE À LA DÉCLARATION D'INVENTION

EN CONSIDÉRATION de la présente déclaration d'invention faite ce jour par:

UNTEL,
UNTEL, et
UNTEL

(ci-après appelés les «Inventeurs» et/ou «Auteurs»),

et se rapportant aux travaux et développements faits par eux-mêmes concernant le projet désigné sous le nom de « **Oxidation of C5 and C6 sugar feedstocks to carboxylic acids, ethers and ketones**» (ci-après appelé « l'Invention »), **la corporation de Polytechnique Montréal** (« POLYTECHNIQUE ») et **POLYVALOR, société en commandite**, représentée aux présentes par son commandité **Univalor inc.** (« UNIVALOR ») sont autorisées à examiner ou à faire examiner toute information pertinente à l'Invention tel qu'entendu entre les parties.

Les Inventeurs et/ou Auteurs s'engagent à transmettre à POLYTECHNIQUE et à UNIVALOR toute information relative à l'Invention pertinente et utile à son évaluation et sa valorisation, et toute information relative à l'Invention que pourra requérir POLYTECHNIQUE ou UNIVALOR de temps à autre.

Les Inventeurs et/ou Auteurs s'engagent, pour une période maximale de deux ans, à maintenir confidentielle et à ne pas divulguer à des tiers, par quelque moyen que ce soit, en partie ou en totalité, l'information ainsi communiquée à POLYTECHNIQUE et UNIVALOR ou toute autre information relative à l'Invention, sans l'autorisation préalable expresse et par écrit de POLYTECHNIQUE.

Par ailleurs, POLYTECHNIQUE et UNIVALOR s'engagent, pour une période d'évaluation d'au maximum deux (2) ans, à utiliser l'information reçue et relative à l'Invention uniquement dans le but d'évaluer l'Invention et d'effectuer des démarches de valorisation de cette Invention en accord avec les Inventeurs.

Cette information ne sera utilisée ni par POLYTECHNIQUE, ni par UNIVALOR, ni par les Inventeurs et/ou Auteurs d'une manière quelconque qui pourrait affecter négativement l'exploitation commerciale de l'Invention ou les droits et intérêts de UNIVALOR, ses successeurs ou ayants droits, de POLYTECHNIQUE, et des Inventeurs et/ou Auteurs ou d'un tiers ayant des droits ou intérêts dans ou sur cette information.

Les obligations de confidentialité et de non-utilisation imposées à POLYTECHNIQUE et UNIVALOR ci-haut mentionnées ne s'appliqueront pas à toute information qui:

(a) au moment de ladite divulgation à POLYTECHNIQUE et UNIVALOR par les Inventeurs est, ou après la divulgation tombe, dans le domaine public par publication, ou autrement sans la faute de POLYTECHNIQUE ou de UNIVALOR de l'une ou l'autre des parties ou sans un manquement à leurs obligations de confidentialité;

(b) était en possession ou était déjà connue de POLYTECHNIQUE et de UNIVALOR avant de leur avoir été divulguée ou transmise par les Inventeurs;

(c) a été reçue par POLYTECHNIQUE ou UNIVALOR d'une tierce partie qui n'avait pas acquis cette information directement des Inventeurs.

EN FOI DE QUOI, les Inventeurs et/ou Auteurs ont signé la présente divulgation, aux dates et lieux indiqués ci-dessous.

Nom : *Gregory S. Patience*
Signé à *Montréal* le

Nom : *Davide Carnevali*
Signé à *Montréal* le

Nom :
Signé à le

Nom :
Signé à le

Nom :
Signé à le

Nom :
Signé à le

LA CORPORATION DE L'ÉCOLE POLYTECHNIQUE

Signé à *Montréal* le

Par *Augustin BRAIS*
Directeur (BRCDT)
Dûment autorisé

Agissant par son commandité Gestion Univalor, s.e.c., elle-même agissant par son commandité Univalor inc.

Signé à *Montréal* le

Par *Marc LEROUX*
Président-directeur général
Dûment autorisé

POLYVALOR, SOCIÉTÉ EN COMMANDITE

ANNEX B ELECTRONIC SUPPLEMENTARY INFORMATION ARTICLE 3

Electronic supplementary information

Levulinic acid upgrade to succinic acid with hydrogen peroxide

Davide Carnevali[a,b], Marco G. Rigamonti[a], Tommaso Tabanelli[b], Gregory S. Patience[a], Fabrizio Cavani[b, *]

[a]Polytechnique Montreal, Chemical Engineering department, 2900 Edouard Montpetit Blvd, Montreal, H31 1J4, QC, Canada

[b]Dipartimento di Chimica Industriale "Toso Montanari", Alma Mater Studiorum Universitá di Bologna, Viale del Risorgimento, 4, 40136, Bologna, Italy

Catalyst characterisation

Powder X-ray diffraction analyses (XRD).

XRD powder patterns of the catalysts were recorded with Ni-filtered Cu Kα radiation (λ = 1.54178 Å) on a Philips X'Pert vertical diffractometer equipped with a pulse height analyser and a secondary curved graphite-crystal monochromator.

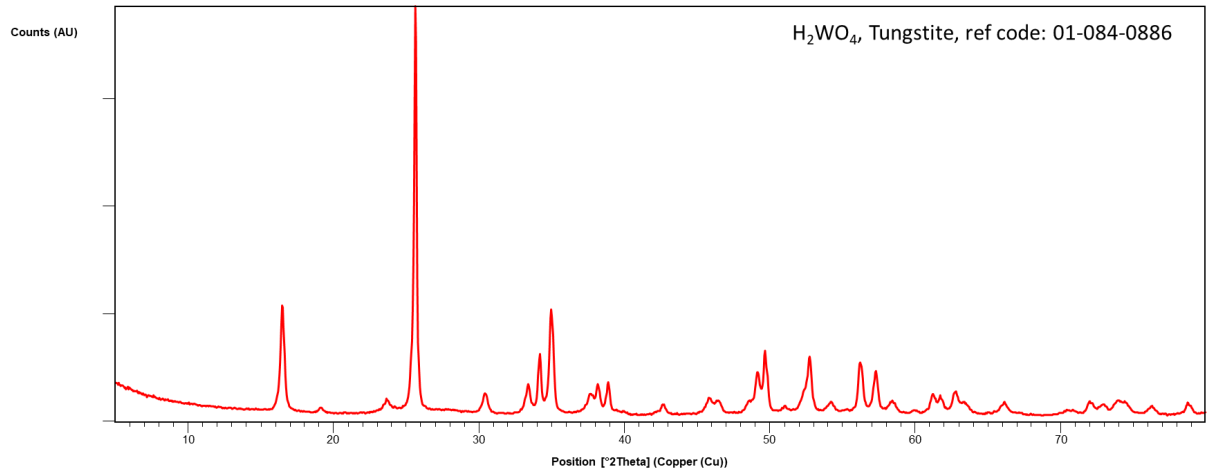

BET specific surface area.

The BET surface area of catalysts was determined by means of N_2 absorption–desorption at liquid N_2 temperature, using a Sorpty 1750 Fison instrument. 0.3 g of the sample was used for the measurement, and the sample was outgassed at 150°C before N_2 absorption.

H_2WO_4 SSA: 12 m^2/g

Table S1: Results obtained recycling the catalyst. Reaction conditions: T 90 °C, LEV:H_2WO_4 molar ratio 10 and H_2O_2:LEV ratio 5. LEV: levulinic acid; succ: succinic acid; acet: acetic acid; mal: malonic acid; oxal: oxalic acid; form: formic acid; AL: α-angelica lactone; HPA: 3-hydroxypropionic acid; gly+glyox: glycolic acid and glyoxylic acid; prop: propionic acid.

Catalytic cycle n°	H_2O_2*	H_2WO_4**	Time, h	Conv, %	S_{succ}, %	S_{acet}, %	S_{mal}, %	S_{oxal}, %	S_{form}, %	S_{AL}, %	S_{HPA}, %	$S_{gly+glyox}$, %	S_{prop}, %
Entry 25 Table 3	5	10	1	43	58	12	5	4	2	4	1	1	2
1	5	10	1	42	56	12	5	4	2	4	1	0	0
2	5	10	1	38	54	10	8	3	2	3	1	0	0
3	5	10	1	40	58	10	8	4	3	6	1	0	0